NOTICE

The quality of this microform is heavily dependent upon the quality of the original thesis submitted for microfilming. Every effort has been made to ensure the highest quality of reproduction possible.

If pages are missing, contact the university which granted the degree.

Some pages may have indistinct print especially if the original pages were typed with a poor typewriter ribbon or if the university sent us an inferior photocopy.

Previously copyrighted materials (journal articles, published tests, etc.) are not filmed.

Reproduction in full or in part of this microform is governed by the Canadian Copyright Act, R S.C. 1970, c. C-30.

AVIS

La qualité de cette microforme dépend grandement de la qualité de la thèse soumise au microfilmage. Nous avons tout fait pour assurer une qualité supérieure de reproduction.

S'il manque des pages, veuillez communiquer avec l'université qui a conféré le grade.

La qualité d'impression de certaines pages peut laisser à désirer, surtout si les pages originales ont été dactylographiées à l'aide d'un ruban usé ou si l'université nous a fait parvenir une photocopie de qualité inférieure.

Les documents qui font déjà l'objet d'un droit d'auteur (articles de revue, tests publiés, etc.) ne sont pas microfilmés.

La reproduction, même partielle, de cette microforme est soumise à la Loi canadienne sur le droit d'auteur, SRC 1970, c. C-30.

Canada

Performance of Various Line Coding Formats on Optical Fiber Link

Krishna P. Aribindi

A Thesis

in

The Department

of

Electrical & Computer Engineering

Presented in Partial Fulfillment of the Requirements
for the Degree of Master of Engineering at
Concordia University
Montreal, Quebec, Canada

May, 1988

ISBN 0-315-44818-0

ABSTRACT

Performance of Various Line Coding Formats on Optical Fiber Link

Krishna P. Aribindi

Line coding is one of the important aspects of an optical communication systems. Choice of an appropriate line code will determine such factors as probability of error, bandwidth, and power on an optical link. The popular line coding schemes for an optical communication systems are RZ, NRZ, Manchester, and Miller. The performance of these line codes on optical fiber link is investigated. The performance of an optical communication system is dependent on the noise introduced by the front end of the system, specifically, photodetector, preamplifier and main amplifier. There are two types of noises present at the front end of the system thermal noise and shot noise, which are modeled as Gaussian and Poisson distributions respectively . However, only one of these types of noises dominates depending on the optical power transmitted. The performance of various line codes are investigated under the influence of these noises. In both of these environments an optimum receiver is assumed to guarantee a minimum probability of error. The equations for probability of error for different line coding formats under the influence of thermal as well as shot noise are derived. A practical design method of an optical communication system is also described.

ACKNOWLEDGMENTS

I would like to express my heartfelt gratitude to my thesis supervisors Dr. Tho Le-Ngoc, Dr. J.F. Hayes and Dr. Elhakeem for their constant guidance throughout this research, and for their suggestions and constructive criticism during the preparation of the thesis.

I would also like to express my deep appreciation to Dr. MacGregor of RCA Inc., for his interest and financial support.

I would also like to thank RCA Inc., engineers for providing necessary components and for their helpful suggestions.

Last but not least I would like to thank all my friends at Concordia University for their encouragement and support throughout my studies.

To my parents

Table of Contents

LIST OF FIGURES

LIST OF TABLES

LIST OF SYMBOLS

A	: Amplifier gain
a	: Core radius
B	: Receivers bandwidth
c	: Velocity of light
D	: Dispersion factor
D_o	: Decision voltage
E_o	: Signal energy
f	: Frequency of radiation
G	: Random gain factor in APD's
h_p	: Pulse shaping function
h	: Planck's constant
i_{th}	: Thermal noise current
$\bar{i}_{sh}$	: Average signal current
K_B	: Boltzmann constant
N	: Number of modes
P_E	: Probability of error
P_i	: Incident power on photodiode
P_{sh}	: Shot noise power
R_l	: Load resistor
R	: Reflectance
R_o	: Responsivity

S_I : PSD of amplifiers input noise current

S_E : PSD of amplifiers noise voltage source

T_f : Solidifying temperature

V_g : Group velocity

$V_E(t)$: Noise due to amplifiers noise voltage source

$V_s(t)$: Shot noise current source

$V_R(t)$: Thermal noise current source

α_{scat} : Rayleigh type scattering

β_T : Isothermal compressibility

β : Propagation constant

λ : Free space wavelength

τ_{mat} : Material dispersion

τ_{wg} : Waveguide dispersion

τ_{mod} : Intermodal dispersion

τ_g : Group delay

η : Quantum efficiency

θ_i : Angle of incidence

θ_r : Angle of reflection

θ_t : Angle of refraction

ψ : Reflection coefficient

ψ_s : Perpendicular polarization

ψ_p : Parallel polarization

CHAPTER 1

INTRODUCTION

The purpose of a communication system is to transfer information from the source to the destination. The essential blocks of a communication system are shown in Fig. 1.1.

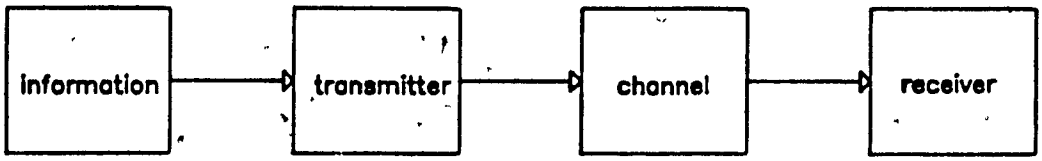

Figure 1.1 Typical block diagram of a communication system.

The communication system consists of an information source such as voice, video or data from a computer etc., the transmitter modulates the information so as to make it suitable for transmission. The channel is the medium which couples the source to the destination. The channel could be either guided transmission such as wire, waveguide, optical fiber or it can be unguided channel such as space channel. As the signal propagates along the channel, the signal gets distorted and attenuated. The purpose of the receiver is to detect the transmitted signal with a least possible error.

1.1 Communication Systems and its Evolution

Several forms of communication systems have appeared over the years. The main objective behind each communication system is to improve the estimation of the transmitted signal with least possible error, or to increase the data rate so that more information could be sent or to increase the distance between repeaters.

Before 19th century, many of the communication systems were of low data rate and the popular means of communication was optical or acoustical means, such as signal lamps or horns [1]. Optical carrier or light for communication has been known for many centuries. One of the earliest known transmission using optical signal was the use of fire signal by the Greeks in the eighteenth century B.C. [1]. However, the speed of communication was limited, since the human eye was used as a receiver and also the sender and the receiver must always be in line of sight of transmission. This type of transmission is heavily dependent on the atmospheric effects such as rain and fog. Consequently, the transmission was unsuitable for reliable communication.

With the advent of telegraph by Morse in 1838 we entered the age of electronic communication [1]. The first commercial telegraph service using wires was established in 1844 and many installations were developed in the following years throughout the world [1]. This type of transmission using cables as the medium of transmission was the only communication until the discovery of long wavelength electromagnetic radiation by Heinrich Hertz in 1887. The first implementation of this idea was demonstrated by Marconi in 1895 [1].

In the following years, the large portion of the electromagnetic spectrum was utilized for conveying the information. The information to be conveyed is usually modulated on a high frequency carrier for transmission through the channel. At the receiver the carrier is filtered out to recover the message. It is well known that the amount of information that can be transmitted is proportional to the frequency range over which the carrier operates. By increasing the carrier frequency, it is possible to increase the information carrying capacity. Thus, the obvious trend in communication systems is to use carriers of higher frequencies, consequently, increasing the information carrying capacity. This process led to the invention of most important communication systems such as T.V. and Radar.

The electromagnetic spectrum shown in Fig. 1.2, indicates the frequencies occupied by the electronic communication and optical communication. A significant development occurred in 1880 when Alexander Graham Bell invented a light communication system, the photophone. He used sunlight modulated by a diaphragm to transmit speech to a receiver over 200 meters away [2].

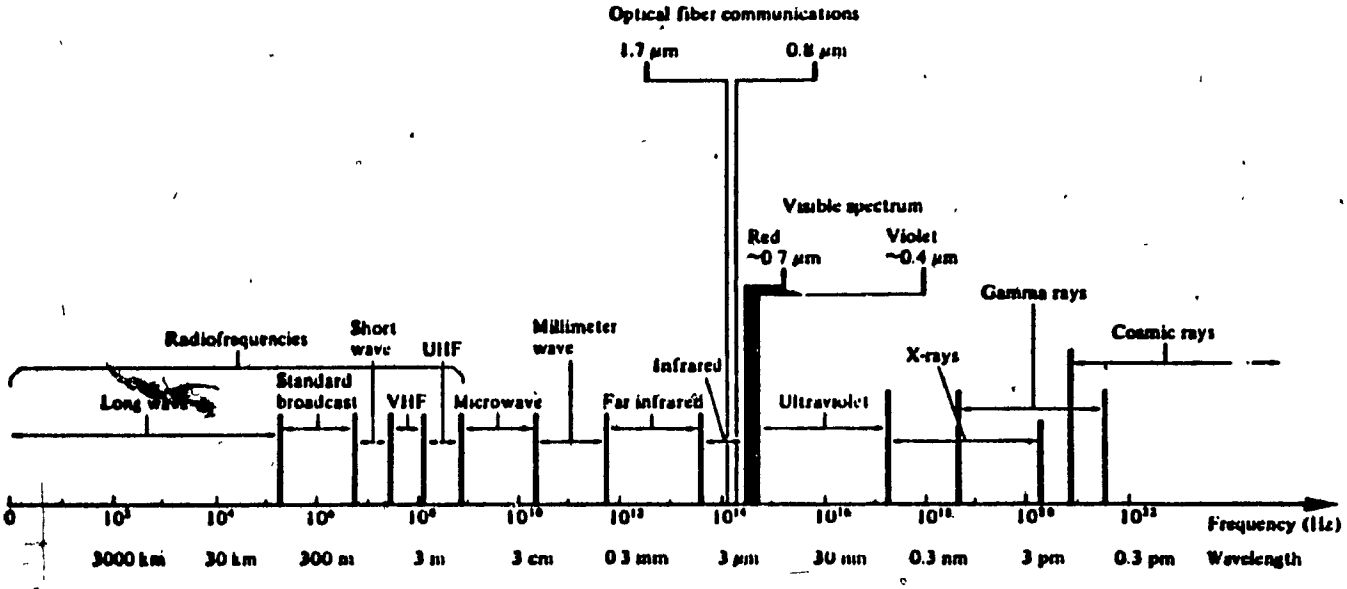

Figure 1.2 Electromagnetic spectrum [2].

All the systems illustrated above have severe limitations in terms of distance and information carrying capacity. This is mainly due to lack of appropriate light sources and the transmission is limited by line of sight and the light signals are severely deteriorated due to atmospheric conditions such as rain, fog, etc [2].

The invention of laser source in 1960, the interest in optical communications has been renewed. This device provided a coherent light source of optic radiation. Due to the narrow line width of the laser beam the free space communication was easily accomplished. However, the previously mentioned constraints such as rain,

fog, clear atmosphere, and line of sight path between transmitter and receiver still remained a major obstacle. As a result, the free space communication is restricted to short distance applications. Although the free space communication with laser is proved to be severely limited in application a great amount of research has been done to improve the reliability of communication by guiding light energy and thus overcome the limitations imposed by the atmosphere.

The idea of propagation of light energy through optical fiber fabricated from silica or glass was proposed by Kao and Hocklam in 1966 [2]. Initially the fibers extracted from glass were of low quality, consequently very high attenuation and were therefore not comparable with the existing co-axial cables that were to be replaced eventually. However, with in a span of 10 years since the proposal was made the low loss fibers ($\approx$ 0.2 dB/km) were developed and fiber optic communication system became pragmatic [2].

1.2 The Advantages of Optical Fiber Systems

There are several advantages of optical fiber systems compared to existing channels such as free space, copper cable, co-axial cable and twisted pair [3,4] :

(i) Since the optical frequencies are on the order of $10^{13} - 10^{14}$ Hz as compared to radio frequencies ($10^{6} - 10^{8}$ Hz), the available bandwidth is approximately 10^{6} times greater then radio frequencies, which is approximately equal to 10 million T.V. channels.

(ii) The fiber is very small in size, diameter and weight. It is slightly thicker than a human hair, consequently, very large numbers of fibers can be packaged in a bundle.

(iii) The quality fibers known to have lower attenuation as compared to twisted pair or co-axial cable. As a result, the number of repeaters required are minimized. The attenuation in fibers is not frequency dependent as opposed

to that of wire.

(iv) Fibers are safe from short circuit protection, because of the nature of the dielectric as opposed to metallic wires.

(v) Fiber optic cables are immune to electromagnetic interference. Also, fiber to fiber crosstalk is minimal. The corrosion due to water or chemicals is less prominent for glass than for copper.

(vi) The prime ingredient in optical fibers is the silica which is inexpensive and abundant in nature, consequently, the optical fiber costs are continuing to decline. However, the associated components of the fiber optic systems such as sources and detectors are relatively expensive compared to wired systems but as time progresses the manufacturing techniques will be improved leading to lower manufacturing costs. Consequently the fiber optic communication systems will be viable option to present day electronic communication.

Although there are many advantages for using optical medium as the channel for transmission of information, there are some difficulties with the present technology especially in the area of optical connectors and and splicing (connection between fibers). Optical connectors are difficult to install and are very expensive. The reason being the two fibers must be precisely aligned for proper coupling of the light energy. Optical system designers would like to see the connector loss to be less than one dB. However, this may increase the system cost. Inexpensive plastic connectors are available with typical losses of 2 dB or less, for many applications this loss is tolerable and can be incorporated in the system design without much difficulty [4].

1.3 Scope of the Thesis and Research Contributions

In digital communications, there are three fundamental types of coding are used to improve the overall performance of the system. They are source coding, channel coding and *line coding*. Source coding is used to reduce the redundancy in the transmitting source, channel coding is used to ensure reliable transmission over noisy channels. The other important type of coding is the *line coding*, the purpose of which is to improve the efficiency of the transmission facility in terms of bandwidth (spectrum) and transmitted power. In an optical fiber communications line coding is not only used to improve the performance of the communication system, but also to ensure successful transmission of the data itself. There is a possibility that when transmitting a signal through an optical channel employing an uncoded data stream the signal received is so distorted that it is unintelligible. The requirement of coding in an optical channel is as important as modulation of data with a carrier over conventional facilities.

Although there are many types of line codes used in digital communication the popular line codes in optical transmission systems are RZ, NRZ, Manchester and Miller. In this thesis, these formats are considered for transmission of optical energy and an optimum receiver (a receiver which yields a minimum probability of error) is used to detect different line codes.

Following this introductory chapter, Chapter 2 illustrates the propagation of light energy on optical medium and transmission characteristics of optical channel. In Chapter 3 the fundamentals of light sources such as LED and Laser are studied, this chapter also discusses the motivation to opt for a certain line code and properties of line codes.

In Chapter 4 a typical optical fiber receiver is considered and analysis is carried out to determine the minimum required optical power to achieve a desired

Bit Error Rate (BER).

In Chapter 5 an optimum receiver is considered to detect various line codes such as RZ, NRZ, Manchester and Miller in Gaussian as well as Poisson regime, and probability of error expressions are derived for various line codes. In deriving these expressions the noise encountered at the front end of the system is first modeled as a Gaussian process and then this approximation is compared against shot noise which is modeled as a Poisson process.

Chapter 6, contains the conclusion and suggestions for further studies. Appendix-1, contains derivation of probability of error for binary signaling schemes.

CHAPTER 2

TRANSMISSION CHARACTERISTICS OF OPTICAL FIBERS

2.1 Introduction

This chapter deals with principle of propagation of optical signals through the optical medium and transmission characteristics of optical fibers. In order to examine the principle of propagation of light energy we need to deal with one of the classical fields of Physics known as *Optics,* which forms a basis for optical communications.

2.2 Geometrical Optics

The principle of transmission of optical energy in a fiber can be fully analyzed by application of Maxwell's Equations for electromagnetic fields. However, this approach is complex and can be adequately dealt by considering the light energy as a ray. The theory based on this approach is termed as *Geometrical Optics* [5]. These rays obey some simple rules.

(a) In vacuum, rays travel at a velocity, $c = 3 \times 10^8$ m/sec. In any other medium, rays travel at a speed given by the relation, $v = c/n$ where

n : is the refractive index of the medium

c : is the velocity of light in vacuum.

(b) Rays travel in straight paths unless deflected by some change in the medium.

(c) When a light ray hits a boundary between the media, a ray reflects at an angle equal to the angle of incidence i.e.

$$\theta_i = \theta_r$$

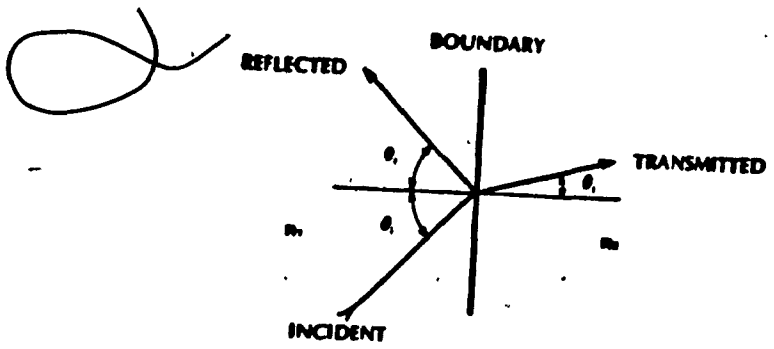

Figure 2.1 Various angles at boundary.

where

θ_i : is the angle of incidence

θ_r : is the angle of reflection

θ_t : is the refracted angle

(d) If a light ray crosses the boundary, the angle of refraction is given by Snell's law

$$\frac{\sin \theta_t}{\sin \theta_i} = \frac{n_1}{n_2} \tag{2.1}$$

2.3 Total Internal Reflection

If a light ray is incident at a boundary in which medium 1 has high refractive index than medium 2, as the angle of incidence θ_i is increased, a situation is attained at which the reflected ray points along the surface, the value of reflected angle at which this occurs is 90^o. For angles of incidence larger than this critical angle θ_c there is no refracted ray, this situation gives rise to a phenomena called *total internal reflection.*

The critical angle is obtained by substituting $\theta_t = 90^o$ in the Snell's law

$$n_1 \sin \theta_c = n_2 \sin 90^o \tag{2.2}$$

$$n_1 \sin \theta_c = n_2 \tag{2.3}$$

$$\sin \theta_c = \frac{n_2}{n_1} \tag{2.4}$$

Total internal reflection occurs when the angle of incidence is equal to or greater than critical angle. This is the primary concept in transmitting light energy in fiber optic medium.

2.4 Principle of Propagation of Light Energy in Optical Fibers

The transmission of optical signal via optical fibers was first proposed by Kao and Hocklam [2] in 1966. At the beginning, the losses or attenuation in fibers were in excess of 1000 dB/km. However, they realized that this high loss is mostly due to the impurities in the glass. This led to great amount of research to reduce the attenuation by purification of the materials. As a result, the glass refining techniques were improved giving fibers with losses around 0.2 dB/km [3].

Various types of fibers are commercially available depending on the application. The widely used fiber consists of a core and a cladding as shown in Fig. 2.2.

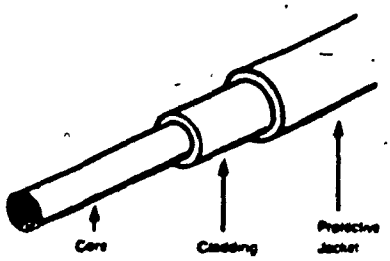

Figure 2.2 Fiber construction.

This type of fiber is known as step index fiber. It is constructed in such a way, the refractive index of the core is larger than refractive index of the cladding. Fig. 2.3, depicts the propagation mechanism of light energy in the fiber.

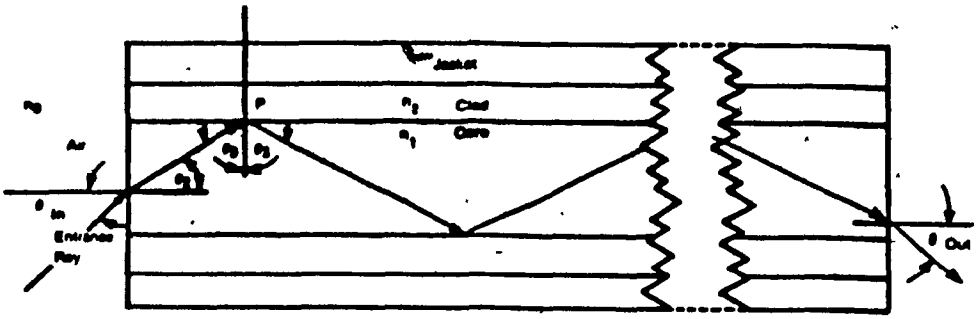

Figure 2.3 Propagation mechanism of light energy within the fiber.

The optical signal will propagate along the fiber by multiple internal reflections, provided that the angle of incidence on the core-cladding boundary θ_i is greater than the critical angle, the critical angle is obtained by substituting $\theta_t = 90^o$ in the Snell's law, we obtain,

$$\sin \theta_c = \frac{n_2}{n_1} . \tag{2.5}$$

2.5 Numerical Aperture (NA)

A number which defines the light gathering power of a fiber. The NA is equal to the sine of the maximum acceptance angle. It can be derived as follows:

Applying Snell's law at the ray entrance of Fig. 2.3, we have,

$$\begin{aligned} n_o \sin \theta_{in} &= n_1 \sin \theta_1 \\ &= n_1 \sin (\pi/2 - \theta_i) \\ &= n_1 \cos \theta_i \end{aligned} \tag{2.6}$$

If θ_{in} is increased sufficiently, θ_i will drop below the critical angle and the ray will not propagate down the fiber. The largest angle is when θ_{in} is equal to the critical angle θ_c. At this angle $\sin \theta_c = \frac{n_2}{n_1}$

$$\cos \theta_c = \sqrt{1 - \sin^2 \theta_c} = \frac{\sqrt{n_1^2 - n_2^2}}{n_1} \tag{2.7}$$

Substituting this value for $\cos\theta_i$ into Eq. (2.6) NA can be written as,

$$NA = n_0 \sin\theta_{in} = \sqrt{n_1^2 - n_2^2} \tag{2.8}$$

$$NA = \sin\theta_{in} = \sqrt{n_1^2 - n_2^2} \tag{2.9}$$

where n_0 is the refractive index of the air (=1).

A ray incident at an angle beyond that obtained for $\sin\theta_{in}$, will not propagate along the fiber. NA is the one of the important design criteria of the optical wave guide.

2.6 Reflection at a Plane Boundary

The reflection at a core-clad boundary, and air-to-glass boundary where optical signal is coupled from source to fiber and from fiber to fiber must be taken into account in order to evaluate the total power system budget. These reflections occur in the situations depicted in Fig. 2.4.

Figure 2.4 Sources of reflection at various interfaces.

The amount of reflection can be determined from the knowledge of refractive indices. This is termed as reflection co-efficient ψ. This is defined as the ratio of reflected electric field intensity to the incident electric field intensity, and is given by [5],

$$\psi = (n_1 - n_2) / (n_1 + n_2) \tag{2.10}$$

where

n_1 : is the refractive index in the incident region

n_2 : is the refractive index in the transmitted region

The reflectance is defined as the ratio of the reflected beam intensity to the incident beam intensity and is given by [5]

$$R = \psi^2 \tag{2.11}$$

The amount of reflection depends on the angle of incidence. If the electric field is polarized perpendicular to the plane of incidence it is termed as S polarization and is given by [5]

$$\psi_s = \frac{n_1 \cos\theta_i - \sqrt{n_2^2 - n_1^2 \sin^2\theta_i}}{n_1 \cos\theta_i + \sqrt{n_2^2 - n_1^2 \sin^2\theta_i}} \tag{2.12}$$

and if the electric field is polarized parallel to the plane of incidence it is termed as parallel polarization and is given by [5]

$$\psi_p = \frac{-n_2^2 \cos\theta_i + n_1\sqrt{n_2^2 - n_1^2 \sin^2\theta_i}}{n_2^2 \cos\theta_i + n_1\sqrt{n_2^2 - n_1^2 \sin^2\theta_i}} \tag{2.13}$$

the corresponding reflectance is given by

$$R = |\psi_p|^2 \text{ or } |\psi_s|^2 \tag{2.14}$$

2.7 Modes in Optical Fiber

When an optical signal is launched into the fiber from the source, all ray's having angles between 90° and critical angle are allowed to propagate, all the other rays exceeding critical angle are evanescent waves i.e., the waves are severely attenuated as they propagate along the fiber. The allowed direction corresponds to the modes of the optical waveguide.

There are two principal types of fiber that are used in optical fiber communications. Step index fibers and graded index fibers. These fibers are fabricated by varying the material composition of the core[1]. In the case of step index fiber the

refractive index of the core is uniform throughout the fiber except at the core-cladding boundary. At the boundary the refractive index undergoes an abrupt change (or step). Where as in graded index fiber the core refractive index varies as a function of the radial distance from the center of the fiber[1]. Step index and graded index fibers can be further classified into (i) single-mode (ii) multimode fibers

(i) Single-mode :

In a single-mode fiber, only one mode is allowed to propagate. The advantage of single-mode propagation is low dispersion of the transmitted pulse [5]. Single-mode fibers are preferred to multimode fibers for high bandwidth and long distance applications and also these fibers do not suffer from intermodal dispersion.

(ii) Multimode :

Multimode fibers allow the propagation of optical energy in many modes as shown in Fig. 2.5

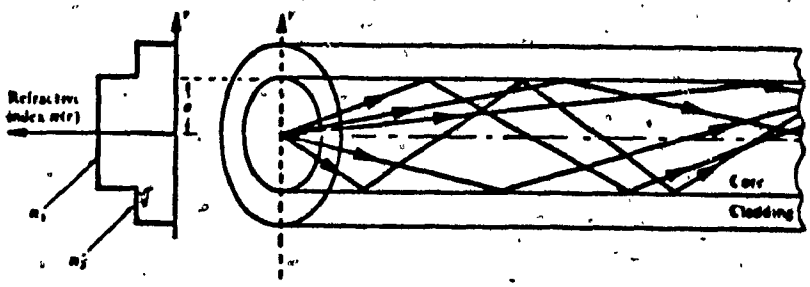

Figure 2.5 Multimode fiber.

The number of modes a fiber can support depends on the physical parameters of the fiber and frequency of the signal to be transmitted. The relation between the number of modes a fiber can support and physical parameters of the optical wave guide. They are related by Eq. (2.15) [5].

$$N = \frac{2\pi^2 a^2}{\lambda^2}(n_1^2 - n_2^2) \qquad (2.15)$$

Where

N : is the number of modes

a : is the core radius

λ : is the free space wavelength

Multimode fibers are preferred to single-mode fibers for low bandwidth and low transmission distances such as local loops in telephony, local area networks etc. Since multimode fibers have larger core diameter than single-mode fibers it is easier to launch optical power from an LED into a multimode fiber than a single-mode fiber. The single-mode fibers are almost always excited with Laser diodes because of their narrow core diameter.

A major disadvantage of multimode fibers is that they suffer from intermodal dispersion. As a result, they are applicable to low bandwidth applications. The dispersion introduces pulse spreading. This effect can be minimized by using graded index fibers [5].

2.8 Transmission Characteristics of Optical Fibers

In this section the transmission characteristics of the optical medium are examined. These characteristics play an important role in determining the maximum limitation on the information carrying capacity of the channel.

The two important characteristics of an optical fiber are *attenuation* and *dispersion*. They are discussed in the following sections.

2.9 Attenuation

Attenuation is one of the fundamental characteristics of any transmission medium such as free space, coaxial cable, and optical fibers etc. This property must be examined carefully since it determines the required transmitted power and repeater spacing between transmitter and receiver. Also, the amount of

attenuation a signal experiences while propagating along the medium play a dominant role in determining system power budget.

There are two types of materials used for fabrication of optical fibers: plastics and glass. The requirements for optical fibers are [1]

(a) Low loss.

(b) Ability to make long, thin flexible fibers from the materials.

(c) Availability of compatible materials to process slightly different refractive indices: this implies light signal propagates by internal reflection.

The fundamental losses (attenuation) are due to *absorption, scattering* and *radiative* losses of the optical energy [1]. These losses are discussed in detail in the following sections.

2.9.1 Absorption

Absorption is due to three mechanisms [1,3] .

(a) Atomic defects in the glass material.

(b) Impurities in the glass material (extrinsic absorption)

(c) Glass material itself (intrinsic absorption)

The atomic defects are due to imperfections in the atomic structure of the fiber material such as missing molecules, or oxygen defects in the glass structure [1,3]. The losses due to atomic defects are usually negligible compared to extrinsic and intrinsic absorptions [1,3].

The extrinsic absorption is mainly due to transition metal ions such as iron, chromium, cobalt, and copper and also due to OH (water) ions. The transition metal impurities which are present in the basic material used for fabrication of the fiber absorb strongly in the region of interest. These impurities range between

1 to 10 ppb (parts per billion) incurring losses between 1 to 10 dB/km [1,3].

The loss due to transition metals occurs because of incompletely filled subshells in the inner electronic structure of the atom [1,3]. Absorption of light imparts some energy to electrons, consequently, the electrons occupy the higher level subshells momentarily, eventually electrons return to the original subshell giving off energy whose frequency of light falls in the region of interest for fiber optic communications [1,3]. Another important loss is due to the presence of OH ion impurities. The loss is due to vibration of atoms due to thermal motion. The resonant frequency is at wavelength of 2.73 μ m (which is not of interest to fiber optic communications) [5]. However, the overtones fall in the range of interest. The significant contribution due to OH occurs at 1.37, 1.23, and 0.95 μ m, when OH ions are embedded in a silica fiber [5]. Water impurity concentrations must be maintained at less than few parts per billion if the attenuation to be less than 20 dB/km [1,3]. Special precautions must be adopted during the fabrication of glass to ensure low loss due to OH impurity.

Intrinsic absorption is associated with the basic ingredient of the fiber material itself such as pure silicon dioxide (SiO_2). This loss is most significant in the short wavelength ultraviolet portion of the electromagnetic spectrum [5]. This loss is due to pronounced electronic and transition bands in the ultraviolet region and a significant loss occurs as the visible region is approached [5].

The intrinsic absorption peaks also occur in the infrared region. The peaks are more pronounced between 7 and 12 μ m for typical glass compositions, which is beyond the region of interest. The loss in the infrared region due to vibrations of chemical bonds such as the SiO_2 bond. This occurs when the thermal energy interacts with a SiO_2 bond, consequently the atoms move, as a result, SiO_2 bond is constantly moving stretching and contracting [5]. This vibration has a resonant

frequency in the infrared region. This contributes a minute loss at the upper limit of fiber optic communication range, 1.6 μ m [5]. As a result, the silica fibers are prohibited to use beyond this range.

2.9.2 Scattering

Scattering losses in glass are due to microscopic variations in the material density, structural inhomogeneities or defects occurring during fiber construction [5]. During manufacture of the fiber, the glass is in molten state (liquid), due to heat the molecules move randomly through the material. As the material cools, the molecular motion would not exist. In solid state, the molecular locations are frozen within the glass material. Consequently, the density is varied [1]. In addition to this, the glass is made of several oxides such as SiO_2 , GeO_2 and P_2O_2 , which results in compositional fluctuations [5]. These two effects contribute to the variation of the refractive index within the glass. The variation in refractive index causes Rayleigh-type scattering of the light. This loss is modeled by Eq. (2.16) [1].

$$\alpha_{scat} = \frac{8\pi}{3\lambda^4}(n^2 - 1)^2 K T_F \beta_T \qquad (2.16)$$

Where

n : is the refractive index

K : is the Boltzman's constant

β_T : is the isothermal compressibility of the material

T_f } is the temperature at which the density fluctuations are frozen into the glass as it solidifies

As can be noted from Eq. (2.16) Rayleigh scattering is inversely varies with λ^4, it decreases at a rapid rate with increasing wavelength (λ). For wavelengths below $1\mu m$, it is the most pronounced loss mechanism in a fiber and exhibits downward trend with increasing wavelength as shown in Fig. 2.6. At wavelengths beyond 1μm, infrared absorption tend to accelerate optical signal attenuation.

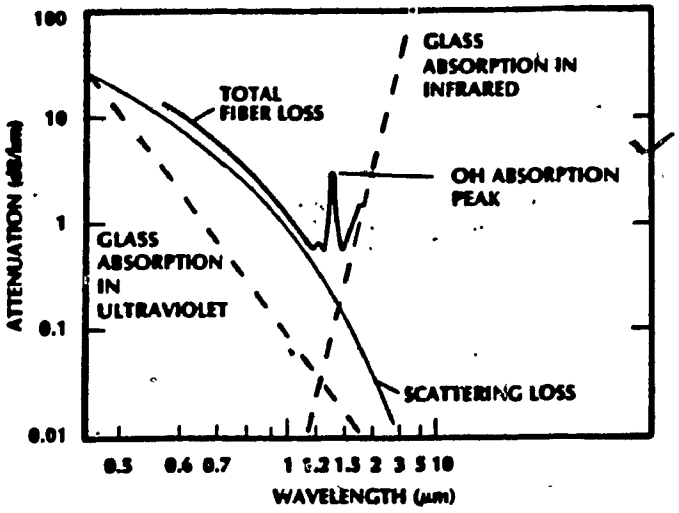

Figure 2.6 Attenuation as a function of wavelength in an optical fiber [5].

2.9.3 Radiative Losses

These losses occur when the optical fiber undergoes a bend. This causes attenuation. The fibers are subject to two types bends, macroscopic and microscopic [5].

Macroscopic bend is due to bends having radii that are larger than the fiber diameter. This occurs when the fiber is wound on a spool or pulling it around a corner [1].

The microscopic bend is due to bend of the fiber axis, this occurs when fibers are incorporated into cables [1]. The stresses due to cabling process cause bends along the fiber axis (microscopic) which appear randomly along the fiber. The microbends causes repetitive coupling of light energy between the guided modes

in the fiber [5].

One way to minimize this loss is by having a protective jacket over the fiber as shown in Fig. 2.7. When external forces act on jacket, the jacket may be deformed but the fiber may stay relatively undeformed [5].

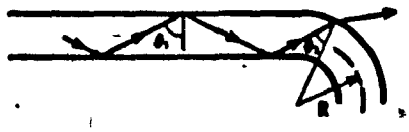

Figure 2.7 Radiation at a bend

Radiation at a bend can be illustrated by considering wave nature of light. At a bend, the light at the outside of the bend must travel at a much faster rate than the the light on the inside of the curve. The smaller the bend radius, the faster the light on the outside must move to keep up with the light inside. As a result, the necessary speed may exceed the velocity of light, consequently the light radiates away.

2.10 Dispersion

If a light pulse is launched into an optical fiber, at the receiving end the pulse appears wider, this is due to dispersive nature of the fiber material i.e., refractive index profile of the medium varies as a function of wavelength. As a result, different wavelengths in the spectrum of the source travel at different velocities thus causing the pulse to spread. The dispersion usually specified in units of ps/nm-km (pico second/nanometer-kilometer).

The most important consequence of dispersion is the limitation of *information carrying capacity* of the optical channel. As the light travels along the fiber the pulse will broaden as depicted in the Fig. 2.8. Eventually, this pulse broadening will cause adjacent pulses to overlap. The resulting interference between symbols is called Inter Symbol Interference (ISI). Consequently, a point will be

reached where the receiver will be no longer able to distinguish between neighboring pulses and error will occur at the detector. Thus, the dispersive properties of the fiber material determine the fundamental limit on the information carrying capacity of the fiber.

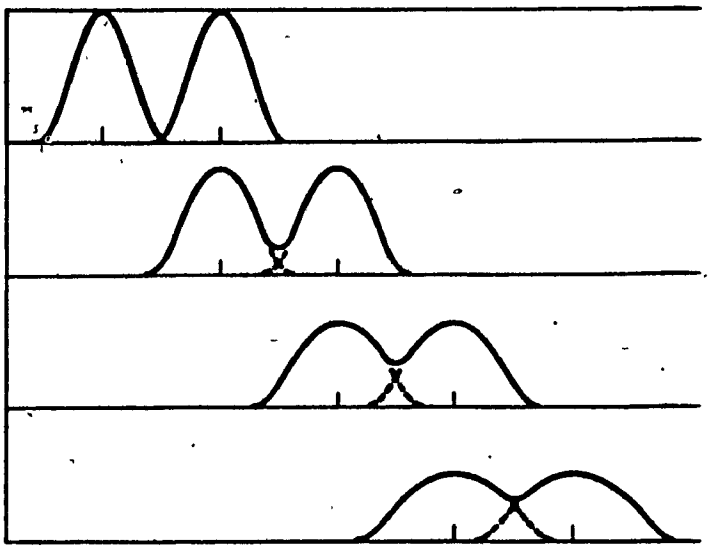

Figure 2.8 Optical pulses tend to overlap as they travel along the fiber.

In order to understand the dispersion on optical channel, the expression for the group delay (τ_g) is derived. As the signal propagates along the fiber, each spectral component of the source are assumed to be propagating independently and to undergo a time delay or group delay per unit length in the direction of the travel is given by [1],

$$\frac{t_g}{L} = \frac{1}{v_g} = \frac{1}{c}\frac{d\beta}{dk} \qquad (2.17)$$

$$= -\frac{\lambda^2}{2\pi c}\frac{d\beta}{dk}$$

where

L : distance traveled by a pulse

β: propagation constant along the fiber axis

The group velocity, V_g is given by

$$V_g = c\left[\frac{d\beta}{dk}\right]^{-1} \tag{2.18}$$

The group velocity is the speed at which the pulse travels along a fiber. As seen from Eq. (2.17), the group delay is a function of a wavelength. Each mode takes a different amount of time to travel a certain distance. Because of this difference in travel time of various modes the spectral components of the source, the optical pulse widens with time as it propagates along the fiber. The parameter of interest is how much the pulse spread (dispersion) is due to group delay variation.

If the spectral width ($\Delta\lambda$) of an optical source is characterized by its rms value σ_λ as shown in Fig. 2.9, then the pulse spreading can be approximated by [1].

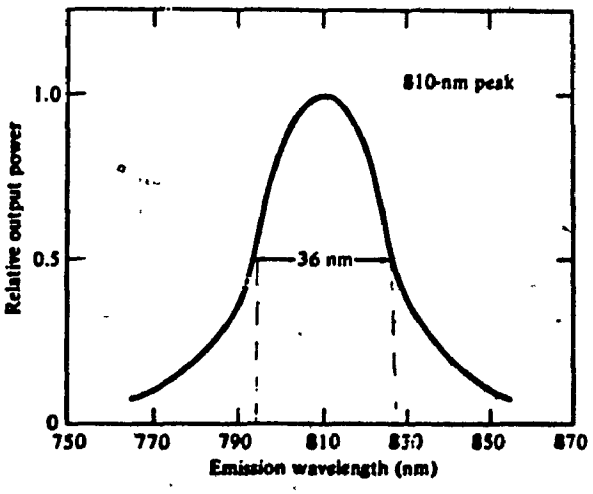

Figure 2.9 Spectral emission of a LED source [1].

$$\tau_g = \frac{dt_g}{d\lambda}\sigma_\lambda \tag{2.19}$$

Differentiating the expression t_g with respect to λ

$$\tau_g = \frac{-L\sigma_\lambda}{2\pi c}\left[2\lambda\frac{d\beta}{d\lambda} + \lambda^2\frac{d^2\beta}{d\lambda^2}\right] \tag{2.20}$$

The factor

$$D = \frac{1}{L}\frac{dt_g}{d\lambda}\sigma_\lambda$$

is termed as dispersion. It defines the pulse spread as a function λ (wavelength) and is measured in ns/nm-km.

The three primary causes for dispersion are :

(i) *material dispersion,*

(ii) *waveguide dispersion*

(iii) and *intermodal dispersion.*

These dispersions discussed in the following sections.

2.10.1 Material dispersion

This dispersion is due to variation of refractive index with respect to wavelength [1]. The variation is shown in Fig. 2.10. It is non-linear in nature.

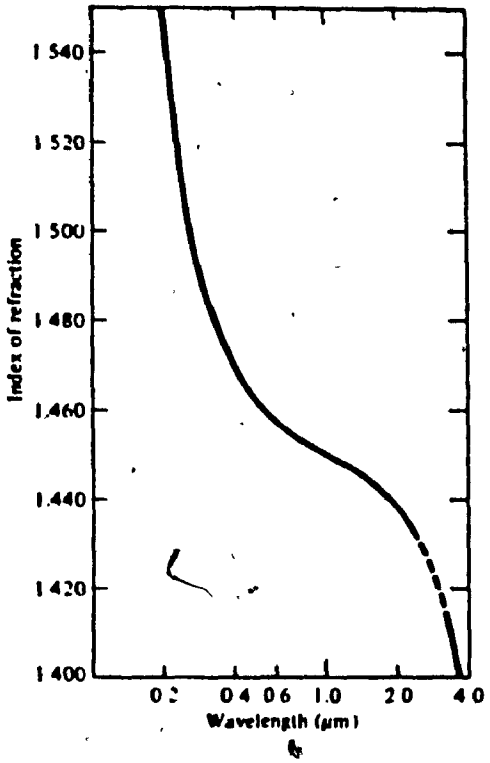

Figure 2.10 Variation of refractive index with respect to wavelength [1].

The mathematical expression for material induced dispersion is derived in the following section : assuming a plane wave propagating in an infinitely extended dielectric medium whose refractive index n(λ) is equal to that of fiber core. The propagation constant, β , is given by [1]

$$\beta = \frac{2\pi n(\lambda)}{\lambda} \tag{2.21}$$

Substituting β in the Eq. (2.17)

$$\frac{\tau_g}{L} = \frac{-\lambda^2}{2\pi c}\frac{d\beta}{d\lambda} \tag{2.22}$$

Differentiating β with respect to λ yields

$$\frac{d\beta}{d\lambda} = 2\pi\left[-\frac{n(\lambda)}{\lambda^2} + \frac{1}{\lambda}\frac{dn}{d\lambda}\right] \tag{2.23}$$

Substituting for $d\beta/d\lambda$ in Eq. (2.17), the group delay due to material dispersion (t_{mat}) is obtained.

$$t_{mat} = \frac{L}{C}\left[n(\lambda) - \lambda\frac{dn}{d\lambda}\right] \tag{2.24}$$

The pulse spread τ_{mat} for a source spectral width is given by differentiating the group delay with respect to wavelength ' λ ' and multiplying by source spectral width σ_λ . Performing above operations and simplifying, the pulse spread due to material dispersion is given by

$$\tau_{mat} = \frac{dt_{mat}}{d\lambda}\sigma_\lambda \tag{2.25}$$

$$\tau_{mat} = \frac{\sigma_\lambda L}{c}\left[-\lambda\frac{d^2n}{d\lambda^2}\right] \tag{2.26}$$

The plot of pulse spread variation with respect to wavelength λ is shown in Fig. 2.11.

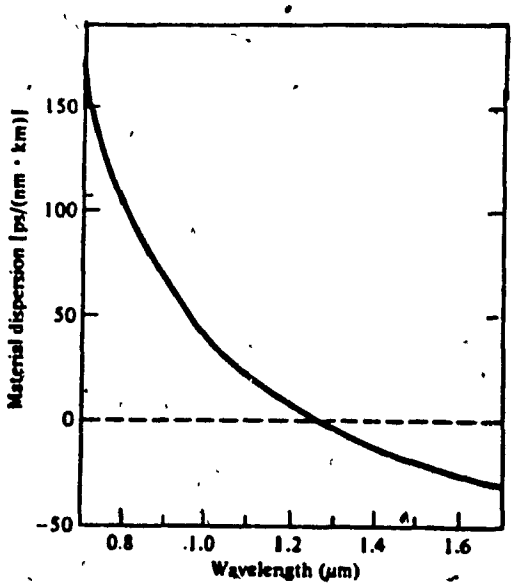

Figure 2.11 Material dispersion as a function of wavelength [1].

From the expression of material dispersion we can deduce the following :

(a) Material dispersion can be reduced by choosing sources that have narrower spectral widths ' σ_λ ' such as lasers or by operating the sources at longer wavelengths.

(b) The dispersion goes to zero at a wavelength 1.27 μ m for pure silica.

2.10.2 Waveguide dispersion

This is due to distribution of light between core and cladding [1]. The pulse spread τ_{wg} due to waveguide dispersion is obtained by differentiating the group delay with respect to wavelength [1].

$$\tau_{wg} = \sigma_\lambda \frac{dt_{wg}}{d\lambda} = -\frac{V}{\lambda}\sigma_\lambda \frac{dt_{wg}}{dv} \tag{2.27}$$

Where ' V ' is the number of modes an optical fiber can support. This expression is derived under the assumption that the refractive index of material is independent of wavelength [1].

2.10.3 Intermodal dispersion

This is due to variation in group velocities of the different modes [1]. This dispersion can be eliminated by choosing a single mode fiber as an optical channel for transmission. The pulse widening due to intermodal dispersion is the difference in travel time between the highest order mode and the fundamental mode this is given by the following expression [1],

$$\tau_{mod} = T_{\max} - T_{\min} = \frac{(n_2 - n_1)L}{c} \tag{2.28}$$

where

n_1 : is the refractive index of the core

L : is the length of the cable in km.

As seen from the Eq. (2.28), the intermodal dispersion is independent of source line width σ_λ . It is important to note that a pulse from a perfectly

coherent source i.e., $\sigma_\lambda = 0$, would still suffer from intermodal dispersion while the material and waveguide dispersion would be zero. The three dispersions that contribute to pulse spreading are shown in Figs. 2.12, 2.13 and 2.14.

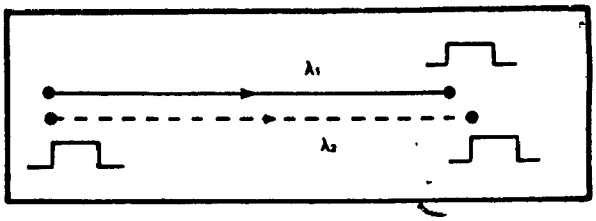

Figure 2.12 Pulses at different wavelengths have different velocities.

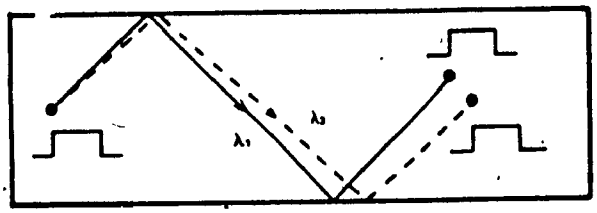

Figure 2.13 Pulses at different wavelength (but propagating in the same mode) must travel at slightly different angles, resulting in a difference in net axial velocities.

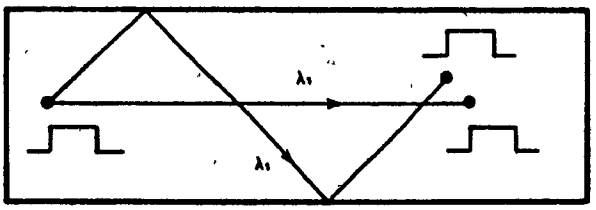

Figure 2.14 A pulse at single wavelength splits its power into modes that travel at different axial velocities because of path differences.

CHAPTER 3

OPTICAL SOURCES

3.1 Introduction

The block diagram shown in Fig. 3.1, contains the essential blocks of an optical transmitter. They are an information source, a modulator (driver) and an optical transducer.

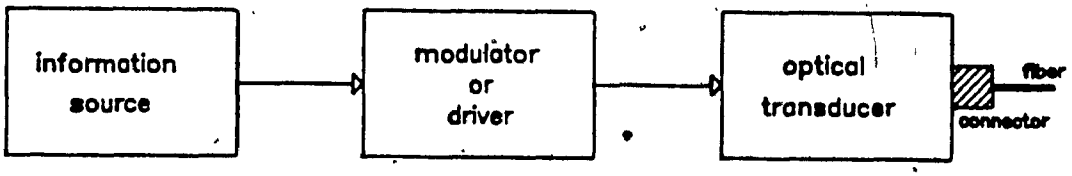

Figure 3.1 Optical transmitter block diagram.

The configuration before optical transducer is identical to electronic communication. The additional device added to the conventional subsystems is the optical transducer, to convert electrical signal to corresponding optical signal. In this chapter, the basic operating principles of these devices will be discussed and also various characterstics of these devices are summarized as a fiber optic communication system design aid.

The principal optical sources used in fiber optic communication systems are Laser diodes and Light Emitting Diodes (LED). The operation of these two sources are dealt in the following sections.

3.2 Light Emitting Diode (LED)

A LED consists of a semiconductor pn junction, which emits light when forward biased. The operation of this device can be explained by band theory. Referring to Fig. 3.2 , the two bands with energy gap E_g are the conduction

band and the valence band. In the conduction band, the electrons are loosely bounded to the atoms and are readily available for conduction. In the valence band, the holes (positively charged) are free to move. Holes exist locations at which an electron is taken away from neutral atom, as a result, the atom is positively charged. A free electron can recombine with a hole, returning the atom to its neutral state. Energy is released when this occurs. The amount of energy radiated out is given by [6,7].

$$E = hf$$

Where

E : is the difference in energy between conduction band and valence band.

f : is the frequency of radiation

h : is the Planck's constant

A p-type semiconductor has excess amount of holes and n-type semiconductor has excess amount of electrons. When a p-type and n-type materials are brought together an energy barrier is formed as shown in the Fig. 3.2.

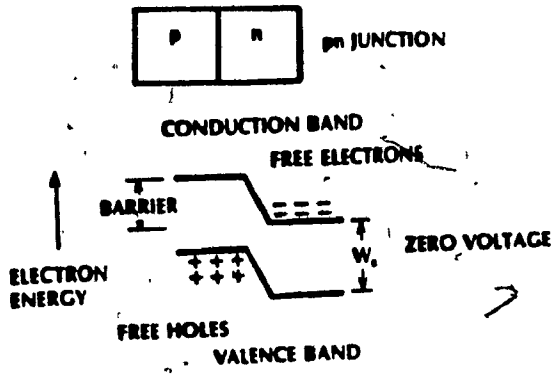

Figure 3.2 Band structure of pn junction.

Normally, the electrons in the conduction band do not have sufficient energy to cross the barrier and produce a photon. When the junction is forward biased, the barrier decreases, consequently, the electrons and holes have sufficient energy to

cross the barrier and recombine to produce a photon. In essence, radiation from LED is caused by recombination of holes and electrons under the influence of externally applied voltage[6,7].

As seen from the equation of the radiated energy, the frequency of radiation varies with the band gap energy (E_g), consequently, the material used for fabrication. Table 3.1 lists various types of LED's that are used in fiber optic communications.

Table 3.1 Various types of LED's used in fiber optic communications [4].

Material	Wavelength Range μ m	Bandgap Energy ev
GaAs	0.9	1.4
AlGaAs	0.8-0.9	1.4-1.55
InGaAs	1.0-1.3	0.95-1.24
InGaAsP	0.9-1.7	0.73-1.35

3.3 Laser

Laser is an abbreviation for *light amplification by stimulated emission of radiation.*

The medium for lasing can be a gas, liquid, a crystal or semiconductor [1]. For optical communications the Laser sources employed are semiconductor type. Laser action is the consequence of three processes [1]. They are photon absorption, spontaneous emission, and stimulated radiation. These are depicted by the energy level diagrams shown in Fig. 3.3

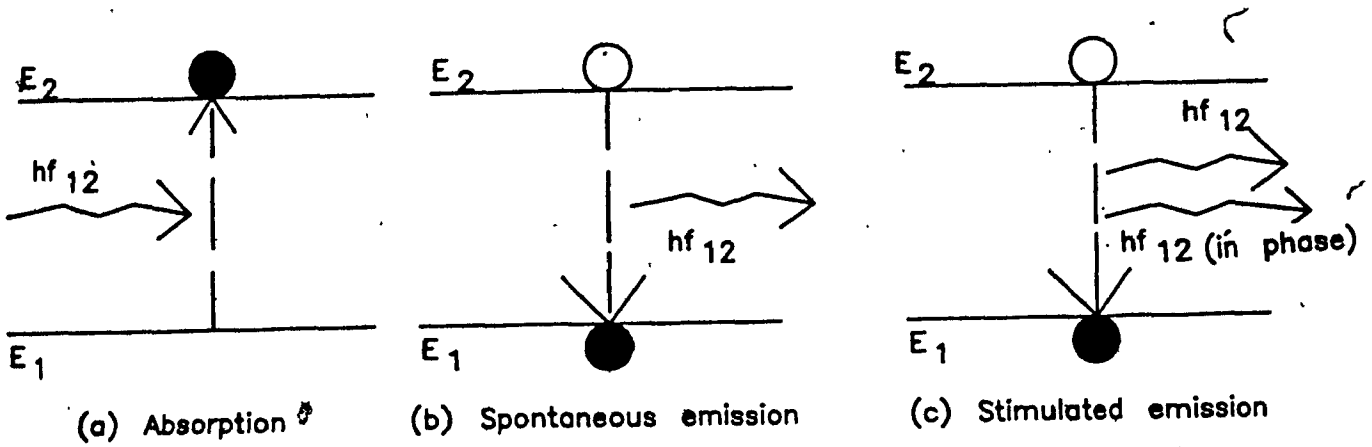

Figure 3.3 Energy level diagrams in Lasers.

E_1 is the ground level energy and E_2 is the excited state energy. In accordance with Plank's law, transition between these two states involves the absorption or emission of photon of energy, hf $= E_2 - E_1$ [1]. Usually the atom is at ground state, when a photon of energy $E_2 - E_1$ collides with the atom, an electron in state E_1 can absorb the photon energy and be excited to state E_2 as shown in Fig. 3.3. Since the electron is in an unstable state, it will eventually return to ground level emitting a photon of energy equal to the difference $E_2 - E_1$ [1]. This occurs without any external stimulation and is called spontaneous emission. It is possible for an electron to make downward transition from the state E_2 (the excited state) to E_1 (to the ground level) by an external stimulation as shown in Fig. 3.3c.

In selecting a LED or a Laser diode as a source there are certain advantages and disadvantages for each type of device. Some of the advantages of Laser over an LED are [1,2] :

(a) A faster response time. This implies faster data transmission rates are possible.

(b) The spectral width of a Laser is narrower, which implies less distortion due to dispersion.

(c) The optical power that can be coupled from a Laser is greater, consequently, greater transmission distances.

Some of the disadvantages of Lasers are :

(a) Fabrication of Lasers is more complicated.

(b) The optical output is strongly dependent on temperature. As a result, the transmitter circuitry is more complicated than the LED transmitter.

(c) The Lasers are very expensive compared to LEDs.

The major difference between LEDs and Lasers is that the power emitted from an LED is incoherent, whereas that from Laser is coherent. In a coherent source the optical power is generated in an optical resonant cavity. The optical power emanated from this cavity is highly chromatic and the output beam is very directional. In a incohrent source such as LED no optical cavity exists for wavelength selectivity consequently the output radiation has a broad spectral width. The coherent optical power from Laser can be coupled into a single-mode or multimode fibers. However, the optical power output from an LED because of its incoherency can only be coupled into a multimode fiber [1].

The choice of a particular optical source depends on many factors. As an aid in selecting a particular diode for fiber optic communications, the characteristics of optical sources are summarized in Table 3.2.

Table 3.2 Typical characteristics of diode light sources [4].

Property	LED	Laser Diode	Singlemode Laser Diode
Spectral width(nm)	20-30	1-5	< 0.2
Rise time(ns)	2-250	0.1-1	0.1-1
Modulation bandwidth(MHz)	< 300	< 2000	≈ 2000
Coupling efficiency	very low	moderate	moderate
Compatible fiber	multimode SI multimode GRIN	multimode GRIN single-mode	single-mode
Temperature sensitivity	low	high	high
Circuit complexity	simple	complex	complex
Lifetime(hours)	10^5	$10^4 - 10^5$	$10^4 - 10^5$
Costs	low	high	highest
Primary use	moderate paths moderate data rates	longpaths high data rates	very long paths very high data rates

3.4 Line Coding Schemes for Optical Fiber link

Optical fibers paved a significant path way for high speed communications. With light as a carrier it is possible to transfer large quantities of data at very high speeds through a fiber whose diameter is extremely small.

In the last decade or so the expansion of fiber optic technology has been tremendous. However, many unexpected problems were discovered. There are for example, some limiting factors especially in the performance of associated electronic circuitry [8,9,10,11,12].

The main advantages of optical fibers are high speed transmission and electrical isolation. Although optical medium can transmit large quantities of data at the speed of light the performance of the associated electronic circuitry is poor. This is because the response of the electronic circuitry has an inferior response when switching at extremely high speeds. In order to alleviate the problem the whole transmission process is AC coupled. Also the preamplifier in the optical receiver is very sensitive to high frequencies than low frequencies. The decision whether a binary '1' or binary '0' is transmitted is determined depending on the transition (low to high or high to low) at the sampling interval. The fact that the

preamplifier in the optical receiver module is sensitive to high frequencies than low frequencies implies that receiver may fail to detect when low data rates are transmitted. As a result, when a series of only 1's or 0's are transmitted, the output of an AC coupled preamplifier will remain in center level and not in positive or negative levels according to the data being transmitted. As a result, the decision logic cannot determine whether a binary 1 or binary 0 was transmitted. Above factors dictate the need for special line coding schemes (pulse formats) with zero DC content to be used in the optical fiber communications systems.

The data to be transmitted on optical link is first coded into a suitable pulse stream (line code) and transmitted as an optical signal. At the receiving end the pulse stream is first regenerated and then converted back to its original form. The optical link therefore acts as a conveying medium of light pulses. The line coding required is not always provided by the optical link or its associated circuitry such as drivers and detectors, leaving the line code to be selected by the user. The clock recovery and data phase synchronization, which are not always provided by the fiber optic link, are also effected by the choice of the line coding scheme. Certain formats can inherently provide the error monitoring capabilities without the need for parity bits.

In optical communications line coding is not only used to improve the performance of the communication system, but also to ensure successful transmission of the data itself. There is a possibility that when transmitting a signal through an optical channel employing an uncoded data stream, the signal received is so distorted that it is meaningless.

The requirement of line coding in an optical channel is as important as modulation of data over conventional facilities. In certain conditions (such as if the distance involved is not too great) modulation may not be necessary in con-

ventional facilities. The same also applies to optical fiber communications, in certain transmission conditions line coding may not be necessary, while in some other conditions coding may be indispensable to receive any kind of intelligence.

An optical communication system supports various line coding formats, since channel characteristics are independent of the line coding format. However, the proper transmission of data through the optical channel is dependent on the line coding scheme. Although, any code format is appropriate for optical fiber transmission, it does not necessarily mean that the utilization of the transmission facility is at optimum.

There are several problems tha affect the choice of a particular line coding scheme. Some of the requirements for selecting a particular line coding scheme are [8] :

(a) The fiber optic transmission systems operate at a very high data rates consequently, the receiver employed must have a sensitive decision logic to determine whether a binary 1 or 0 is transmitted. As a result, the eye opening (the technique used to evaluate the sensitivity of a digital communication systems to timing errors) of the detected signal at the sampling instant should be wide enough to be able to detect the data levels correctly. This can be achieved with a line coding scheme having only two distinct levels. It is generally known that the multilevel eye patterns have lower threshold tolerance of both horizontal and vertical eye openings. For this reason only ON-OFF pulses sometimes are preferred.

(b) The optical transmitter is electrically isolated from the receiver as a result, the receiver must be AC coupled to the transmission facility. This implies that the code format employed for transmission must allow AC coupling and not be vulnerable to any DC drift. Consequently, the code format must have

a zero DC component or a null at frequency (f=0) in its Power Spectral Density (PSD). This requirement excludes the possible use of formats such as RZ and NRZ.

(c) The transmitting source has a random pattern of 1's and 0's and it is the objective of the code format to prevent any base line wander (accumulation of pulse tails).

(d) In optical fiber communications, the transmission speeds are in hundreds of megabits. Consequently, in these systems, detection of the data only possible when the clock timing is fully synchronized with that of transmitter. Since, the only link between transmitter and receiver is the optical channel, the clock information must some how be embedded in the data stream. Consequently, each transition will indicate timing information. As a result, the restriction on the code format is to have as many transitions as possible. Line codes which enable receiver to extract clock information as well as data are termed as self clocking codes.

(e) The recovered timing information must be as stable as possible with no timing jitter in order to ensure sampling of the pulse is at the center of the eye opening with no wander.

(f) The optical communication system and its associated circuitry have wide bandwidths. However, the available bandwidth has an upper limit consequently, the transmission rates that will exceed the limit may result in Inter Symbol Interference (ISI). This implies the transmission spectrum of the coded stream must fit within the passband of the optical fiber system.

(g) One of the requirement on the choice of a certain line code is the simplicity of the encoder and decoder circuits.

Some of the popular line coding schemes in optical communication systems are RZ, NRZ, Manchester and Miller. For these line codes the bandwidth requirements are discussed in the following section.

3.5 Bandwidth Consideration for Optical Pulse Formats

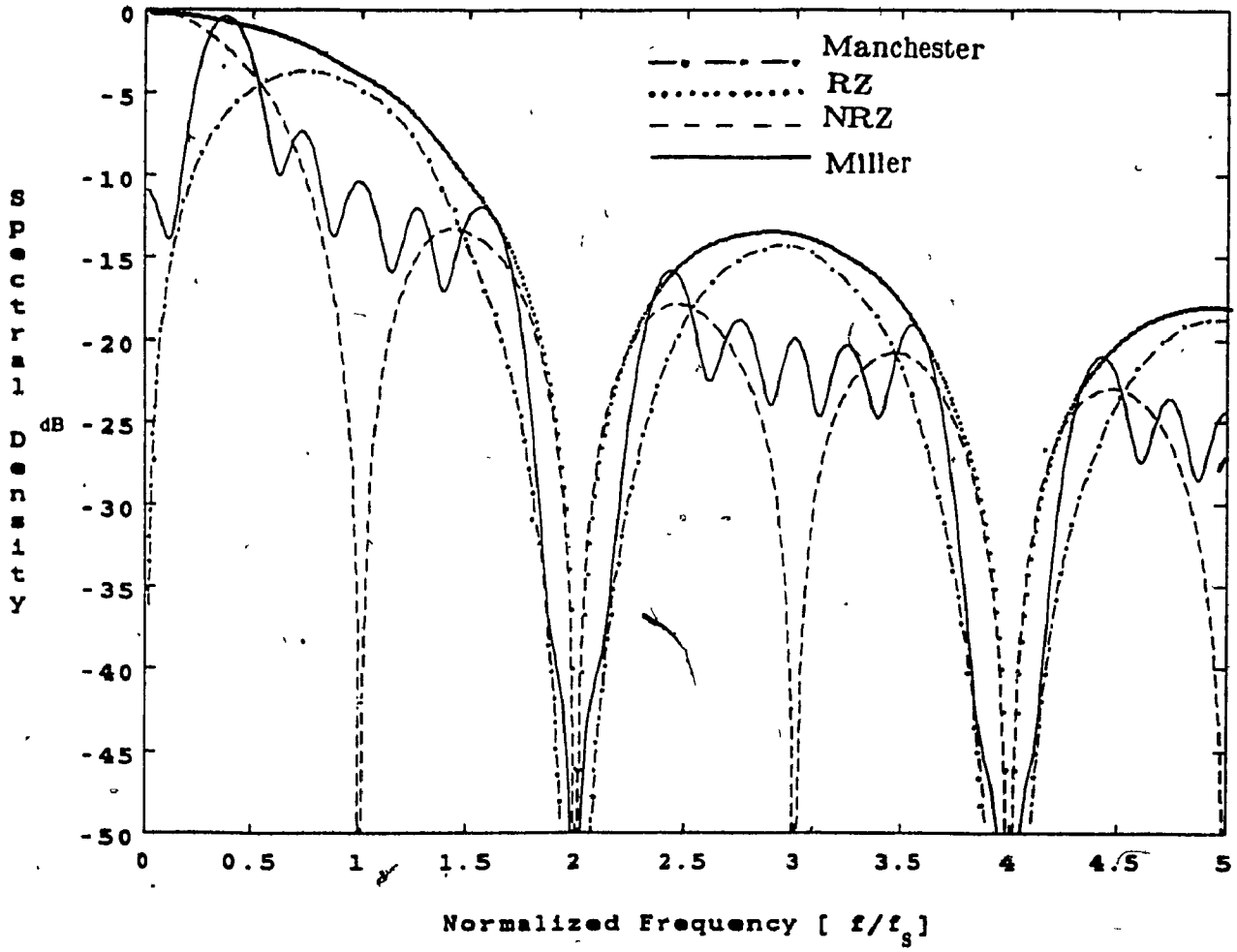

Figure 3.4 PSD of RZ, NRZ, Manchester and Miller formats.

Fig. 3.4 depicts the PSD of RZ, NRZ, Manchester and Miller formats. As seen from the Fig. 3.4 for RZ and NRZ pulse code formats the power is concentrated on the lower end of the spectrum. Consequently, the DC component is more predominant than other line codes such as Manchester and Miller. As a result, AC coupling may not possible or difficult to achieve. Also, for these codes the number of transitions are fewer compared to Manchester or Miller conse-

quently, the clock recovery may also be difficult.

The DC component for Manchester and Miller codes is almost nil, consequently the AC coupling may be possible between transmitter and receiver. In addition, these codes have at least one transition per bit, hence clock recovery is considerably easier than RZ and NRZ codes. However, for these codes the bandwidth required is significantly higher than RZ and NRZ codes.

CHAPTER 4

OPTICAL RECEIVER : STRUCTURE AND NOISE CHARACTERISTICS

4.1 Introduction

In this chapter the various components of an optical receiver are discussed, and the various noise sources that significantly affect the performance of an optical receiver are discussed along with a derivation of the required optical power to achieve a specified *Bit Error Rate* (BER).

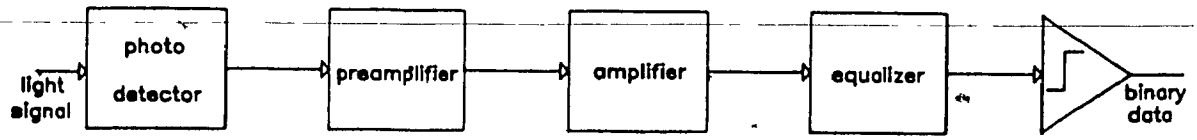

Figure 4.1 Optical receiver block diagram.

The building blocks of an optical receiver are shown in Fig. 4.1. It consists of a photodetector, preamplifier, main amplifier, equalizer, and threshold logic. In this chapter emphasis will be placed on photodetector, preamplifier and equalizer. The remainder of the signal processing from amplifier up to the threshold logic is identical to conventional electronic processing. One of the important blocks shown in Fig. 4.1 is the photodetector. In the following sections the characteristics and the operation of these photodetectors will be discussed.

4.2 Optical Detectors

The purpose of this device is to convert an optical signal to electrical signal. The signal is then amplified and processed further. If the chosen detector has good characteristics, such as linearity and responsivity, the requirements on the

rest of the signal processing circuitry are less stringent.

Some of the desirable characteristics of photodetectors are [2] :

(i) High fidelity: The output of the detector must be linear over a wide range.

(ii) High Quantum Efficiency: It implies large electrical response to corresponding optical signal.

(iii) Wide bandwidth: Response time of the device should be minimum in order to obtain a higher bandwidth.

(iv) Low noise figure: Noise introduced by the detector should be minimal.

4.2.1 Operation of an Optical Detector

The detection process in a photodiode is depicted in Fig. 4.2.

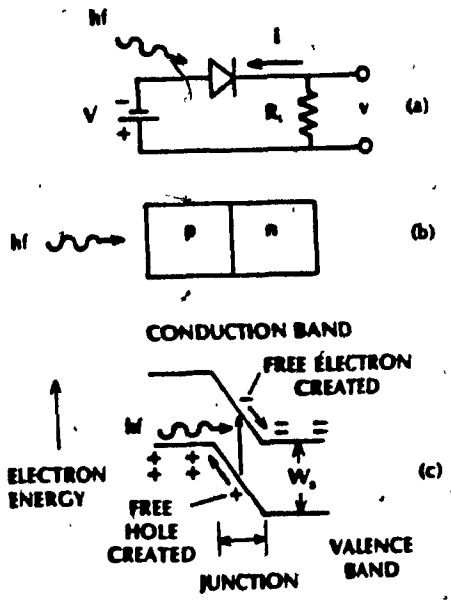

Figure 4.2 Detection process in a photodiode.

For normal operation the detector is reverse biased. When the device is reverse biased an electric field is developed across the pn junction. This field causes the depletion region to increase i.e. holes are attracted toward p side and the electrons are attracted toward n side. This barrier impedes the majority carriers in

either direction from crossing. However, the electrons on p side and holes on n side will cross the pn junction generating a leakage current in the detector [2].

When an incidence photon has energy greater than or equal to band gap energy E_g i.e., hf $> E_g$, the photon imparts its energy and will excite an electron from valence band to the conduction band. This process creates a free electron-hole pairs known as photocarriers [2]. The detectors are designed in such way that these carriers are produced mainly in the depletion region, where most of the detected power is absorbed [1]. The high reverse bias voltage causes the photocarriers to separate and be collected across the reversed biased junction. As a result, a current flow is established in an external circuit, this current is known as photocurrent.

For high photocurrent, it is apparent that the depletion region must be large. The performance of an optical detectors are measured in terms of *responsivity* and *quantum efficiency*.

Responsivity : is defined as the photocurrent generated per unit optical power. It is given by [2],

$$R_0 = \frac{I_p}{P_o} \quad amperes \ / \ watt \tag{4.1}$$

where

I_p : is the photocurrent in amperes (a)

P_o : is the incident optical power in watts (w)

Quantum Efficiency (η) : is defined as the number of electron-hole pairs generated per incident photon energy hf [2]. The responsivity and quantum efficiency are related by [2],

$$R_0 = \frac{I_p}{P_o} = \frac{\eta q}{hf} \tag{4.2}$$

where

q : is the electron charge

hf : is the photon energy

η : is the quantum efficiency

The two main photodetectors used in optical fiber communications are PIN and Avalanche photodiodes (APD).

4.2.2 PIN Photodetector

PIN photodetectors are the most common type of detectors employed in optical fiber systems. Its configuration and biasing arrangement is shown in Fig. 4.3.

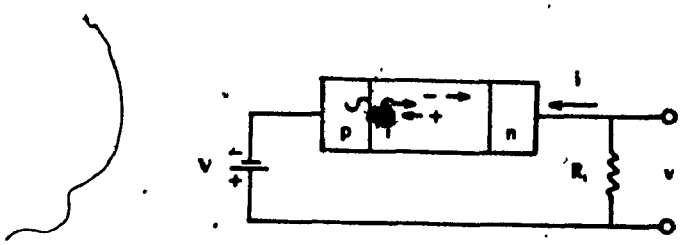

Figure 4.3 PIN Photodetector.

The device structure consists of p and n regions separated by lightly doped n-doped intrinsic (i) region. For normal operation the device is reverse biased. In the pn junction discussed earlier, the carriers drift randomly with relatively low velocities [7]. As a result, the displacement current produced by a hole-electron pair occurs as a pulse of short duration when the carriers are moving through the depletion region [7]. The response due to the optical power incident on the detector in the depletion region is immediate. However, the electron-hole pairs generated in diffusion region produce a delayed response [7]. To increase the speed of the device, it is necessary for the depletion region to enclose the absorption region

[2]. A method to increase the absorption region is to increase the reverse bias voltage or by decreasing the impurities (doping) in n-type material. However, the reverse bias cannot be indefinitely increased because of the practical limitations on the amount of reverse bias that can be applied to the device. The only option left is to increase the absorption region l. The resulting structure is shown in Fig. 4.3.

The area of l-region cannot be indefinitely increased either, because of the increase in transit time (the time taken by an electron to travel from n-side to p-side). Consequently, the response of the device is reduced. If the l-region is too narrow, then the useful photo current (quantum efficiency) is less. Therefore, a tradeoff exists between quantum efficiency and speed of response of the device [7].

4.2.3 Avalanche Photodetector (APD)

In an ideal situation, for PIN diode, if every incident photon produces a hole electron pair, then at wavelength of 1 μm, the responsivity is about 0.8 a/w [7]. Most of the receivers operate with input power levels as low as few nano watts. Thus, with PIN detectors, the photocurrent generated would be very small in the order few nano amperes. Such small currents would be severely corrupted by the amplifier noise. To increase the number of electron-hole pair generated for each incident photon an avalanche photodiode is used. The structure is shown in Fig. 4.4.

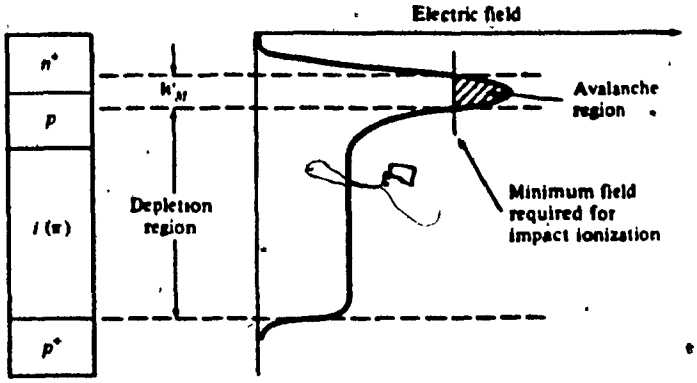

Figure 4.4 APD and its electric field profile [1].

Avalanche photodiode has high electric field region (avalanche region). In the avalanche region, carriers move randomly and occasionally collide with ions, thereby, producing new carriers. The newly created carriers gain sufficient velocity, thus producing some more carriers. This phenomena is called the avalanche effect [1]. This avalanche effect multiplies the primary photo current by a random gain factor, thereby, increasing the effective responsivity of the APD by a random gain factor 'G'. As a result, the receiver sensitivity is also increased.

The carrier multiplication achieved by this method causes noise, since the gain factor is random [7]. This randomness in the avalanche process produces an effective noise which limits the receiver sensitivity of the APD devices. However, at certain gain factors where in presence of amplifier noise, the APD offers significant benefits over the PIN detector [7]. The typical characteristics of PIN and APD's are shown in Table 4.1

Table 4.1 Typical characteristics of junction photodetectors.

Material	Structure	Risetime ns	Wavelength nm	Responsivity a/w	Dark Current na	Gain
Silicon	PIN	0.5	300-1100	0.5	1	1
Germanium	PIN	0.1	500-1800	0.7	200	1
InGaAs	PIN	0.3	1000-1700	0.6	10	1
Silicon	APD	0.5	400-1000	77	15	150
Germanium	APD	1	1000-1600	30	700	50

4.3 Noise in Photodetectors

The principal noise sources in photodetectors are :

(i) Quantum or shot noise due to random generation of photocurrent.

(ii) Dark current which is a small leakage current still flows in the external circuit, during the absence of the power transmission.

(iii) Thermal noise is due to interaction between free electrons and the ions in a conducting medium: this noise is generated by photodetectors load resistor (R_L).

The excess noise factor is the additional noise introduced by avalanche photodiode. The principal reason for the presence of this noise is due to the random nature of multiplication process. This noise factor depends on electron ionization factor 'k' and on the gain factor'G' [1]

$$F(k,G) = k\ G + (2 - \frac{1}{G})(1 - k) \qquad (4.3)$$

For PIN photodiodes the thermal noise due to the load resistor and the active elements of the remaining signal processing circuitry will dictate the performance of the receiver [1]. For avalanche photodiodes the multiplication noise usually dominates the thermal noise [1].

4.4 Optical Receiver Operation and Analysis

As shown in Fig. 4.1, an optical receiver consists of a photodetector, an amplifier, and other signal processing circuitry. The purpose of the receiver is to detect an optical signal, amplify it and then estimate the transmitted data with a minimum possible error.

During this process various types of noises are introduced by the photodetector and amplifiers. The receiver must estimate the transmitted message in the presence of various noise sources with least possible amount of error. The designer must take into account all the noises that occur along the fiber optic system for a proper detection of the signal.

One of the criteria for measuring the performance of a digital communication system is the average probability of error, whereas for analog systems, the criteria is usually specified in terms of signal to noise ratio (SNR).

In this section, sensitivity of the receiver is derived for binary signal transmission. The modulation technique is assumed to be direct modulation (on-off keying) and direct detection at the receiver.

Quantum Limit : When an optical power is incident on the photodiode, the electron-hole pairs are created. On the average, $\lambda(t)$, is the number of hole-electron pairs created in a time interval T, is directly proportional to the incident optical energy and is given by [1],

$$\lambda(t)=\frac{\eta}{hf}\int_0^{T_i} W(t)\,dt = \frac{\eta E}{hf} \qquad (4.4)$$

where

$\lambda(t)$: is the average number of electron-hole pairs generated

W(t) : is the incident optical power

η : is the detector quantum efficiency

E : is the energy received in time interval T_b

hf : is the photon energy

The exact number of electron-hole pairs created in a bit interval, T_b , deviates from the average according to the Poisson distribution given by [1],

$$p(n) = \frac{\lambda(t)^n}{n!} e^{-\lambda(t)} \tag{4.5}$$

where P (n) is the probability that n electrons are generated in bit interval T_b .

Assume an ideal receiver, i.e., which receives only 0 or E (joules) of energy. Thus, the receiver produces no dark current, so no electron-hole pairs are generated when binary signal '0' is transmitted. An error is made, if and only if the detector detects an optical pulse of energy E, when no electron-hole pairs are generated. The probability of such an occurrence is given by substituting zero for n in Poisson distribution, therefore

$$P_E = P(0) = e^{-\lambda(t)} \tag{4.6}$$

For example, if the desired Bit Error Rate (BER) is 10^{-9} the average number of electron-hole pairs required is 21. Therefore the required energy per bit is, E = 21 hf (assuming, $\eta = 1$). This is the ideal minimum energy required to maintain a given BER, for any optical receiver, and is called *quantum limit.*

4.5 Equivalent Circuit for an Optical Receiver

An equivalent circuit of three principal stages of an optical receiver is shown in Fig. 4.5. They are a photodetector, an amplifier, and an equalizer.

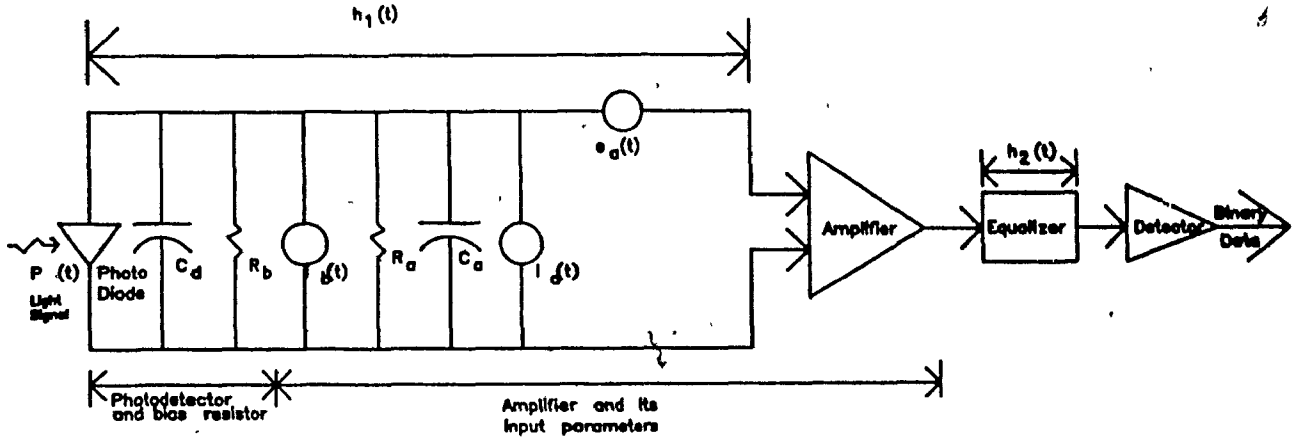

Figure 4.5 Equivalent circuit for an optical receiver.

The photodetector can be either an APD with a mean gain factor of $<G>$ or a PIN photodiode with G=1. The photodiode has a quantum efficiency η and capacitance C_d. The bias resistor of the photodiode has a resistance R_b which contributes to thermal noise represented by $i_b(t)$.

The amplifier has an input impedance, which is a parallel combination of amplifiers input resistance R_a and a shunt capacitance C_a. The $e_a(t)$ and $i_a(t)$ are the amplifier noise sources. The $i_a(t)$ and $e_a(t)$ represent the thermal noise sources caused by input-resistance of the amplifier R_a. These noise sources assumed to have a white Gaussian process characteristics. The equalizer immediately following the amplifier compensates for the distortion introduced by the fiber.

Assume that the digital signal is transmitted with a rectangular pulse shaping function $h_p(t)$. The optical power incident on the photodetector can be represented by

$$P(t) = \sum_{k=-\infty}^{\infty} b_k h_p(t - kT_b) \tag{4.7}$$

where

$h_p(t)$: is the pulse shaping function

b_k can assume one of two values 0 or 1

The average output current from detector at any time, t due to the received optical power can be represented by ,

$$<i(t)> = R_o\, GP(t) \tag{4.8}$$

substituting Eq. (4.7) for P(t) we have

$$<i(t)> = R_o\, G \sum_{k=-\infty}^{\infty} b_k\, h_p(t - kT_b) \tag{4.9}$$

where R_o is the responsivity of the photodiode. The output voltage of the equalizer is amplified and filtered. The mean output current resulting in a mean output voltage is given by the convolution of amplifier impulse response and equalizer impulse response, therefore the mean output voltage is given by

$$<V_{out}(t)> = AR_o\, GP(t) * h_1(t) * h_2(t) \tag{4.10}$$

where

A : is the amplifier gain

h_1 (t) : is the impulse response of biasing circuit detector and amplifier

h_2(t) : is the impulse response of the equalizer

The Fourier transform of $h_1(t)$ is the impedance function of the bias circuit given by

$$H_1(f) = \frac{1}{\frac{1}{R_T} + j2\pi f C_T} \tag{4.11}$$

where

$$R_T = R_e \,||\, R_b = \frac{R_e R_b}{R_e + R_b} \tag{4.12}$$

$$C_T = C_a + C_d \tag{4.13}$$

The mean output voltage at the equalizer output can be written in the form given by [14],

$$V_{out}(t) = \langle V_{out}(t) \rangle + V_n(t) \tag{4.14}$$

where $V_n(t)$ is the noise voltage associated with the signal.

Substituting Eq. (4.10) for $\langle V_{out}(t) \rangle$ and Eq. (4.7) for P(t) we obtain

$$V_{out}(t) = \sum_{k=-\infty}^{\infty} b_k \, h_{out}(t - kT_b) + V_n(t) \tag{4.15}$$

$$h_{out}(t) = A \;\; G \;\; R_o \;\; h_p(t) * h_1(t) * h_2(t) \tag{4.16}$$

The Fourier transform of the $h_{out}(t)$ is given by

$$H_{out}(f) = \int_{-\infty}^{\infty} h_{out}(t) \, e^{-j\,2\pi f t} \, dt \tag{4.17}$$

$$= A \;\; R_o \;\; H_p(f) \, H_1(f) \, H_2(f) \tag{4.18}$$

where $H_p(f)$ is the Fourier transform of transmitted pulse shape signal.

4.6 Receiver Noise

The receiver noise is given by Eq. (4.14). The noise voltage at the equalizer output can be broken down into four components which satisfy the following equation [9],

$$V_n^2(t) = V_S^2(t) + V_R^2(t) + V_I^2(t) + V_E^2(t) \tag{4.19}$$

where

$V_S(t)$: is the shot noise due to random gain factor G of the detector

$V_R(t)$: is the thermal noise (or Johnson Noise) associated with detectorbias resistor R_b

$V_I(t)$: is the noise due to amplifier input noise current $i_a(t)$

$V_E(t)$:is the noise due to amplifier input voltage source $e_a(t)$

Assuming the noise components are statistically independent the mean square noise variance $<V_n^2(t)>$ is given by [1],

$$\begin{aligned} <V_n^2(t)> &= <[V_{out}(t) - <V_{out}(t)>]^2> \\ &= <V_{out}^2(t)> - <V_{out}(t)>^2 \\ &= <V_S^2(t)> + <V_R^2(t)> + <V_I^2(t)> + <V_E^2(t)> \end{aligned} \tag{4.20}$$

The variance of the thermal noise voltage due to load resistor R_b is given by,

$$<V_R^2(t)> = \frac{4K\ T}{R_b} B_N\ R_T^2\ A^2 \tag{4.21}$$

where

KT : is the product of Boltzman's constant K and absolute temperature T

B_N : is the noise equivalent bandwidth of the bias circuit, amplifier and equalizer

B_N is defined as,

$$B_N = \frac{1}{|H(0)|^2} \int_0^\infty |H(f)|^2\, df \tag{4.22}$$

for the system under consideration, the B_N is given by,

$$2\,B_N = \frac{1}{|H_1(0)\,H_2(0)|^2} \int_{-\infty}^{\infty} |H_1(f)\,H_2(f)|^2\, df \tag{4.23}$$

in terms of $H_{out}(f)$ and $H_p(f)$ Eq. (4.23) can be written as

$$2\,B_N = \frac{1}{|H_{out}(0)/H_p(0)|^2} \int_{-\infty}^{\infty} \left| \frac{H_{out}(f)}{H_p(f)} \right|^2 df \tag{4.24}$$

The thermal noise due to amplifier input noise current $i_a(t)$ and amplifier input noise voltage source $e_a(t)$ are assumed to be Gaussian and statistically independent, therefore the noise sources can be completely characterized by their noise Power Spectral Densities (PSD). The PSDs of the noise voltage and current sources are given by [1],

$$< V_I^2(t) > = 2 S_I B_N R_T^2 A^2 \quad (4.25)$$

$$< V_E^2(t) > = 2 S_E B_N A^2 \quad (4.26)$$

where

S_I : is the PSD of amplifier input noise current source,

S_E : is the PSD of amplifier noise voltage source

The noise equivalent bandwidth of the equalizer is given by

$$2 B_{N_E} = \frac{1}{| H_2(0) |^2} \int_{-\infty}^{\infty} | H_2(f) |^2 \, df \quad (4.27)$$

In terms of $H_{out}(f)$ and $H_p(f)$ Eq. (4.27) can be written as

$$2 B_{N_E} = \frac{R_T^2}{| H_{out}(0)/H_p(0) |^2} \int_{-\infty}^{\infty} | \frac{H_{out}(f)}{H_p(f)} \left(\frac{1}{R_T} + j \, 2\pi f C_T \right) |^2 \, df \quad (4.28)$$

The only noise term to be derived in Eq. (4.19) is the shot-noise. The expression for shot noise voltage is given by [1],

$$< V_S^2(t) > = 2 q < i_{sn} > < G^2 > B_N R_T^2 A^2 \quad (4.29)$$

$< G^2 >$ is the mean square avalanche gain which is approximated to G^{2+x}, x varies between 0 and 1 depending on the photodiode material and structure [1].

The shot noise voltage is given by ,

$$< V_S^2(t) > = 2 q B_N < G^2 > R_T^2 A^2 [< i_{sn} >] \quad (4.30)$$

where $< i_{sn} >$ is the average shot noise current.

4.7 Derivation of Receiver Sensitivity

In digital systems the information is transmitted as series of binary 1 and 0 at f_b (in b/sec) . Since the channel is imperfect, it attenuates and corrupts the transmitted signal. The objective of the receiver is to determine whether a binary 1 or 0 was transmitted in a given bit time interval with a minimum probability

of error. The bit error rate (BER) is measured as the ratio of number of bits in error to the total number of bits transmitted. Typically the BER is in the range of 10^{-6} to 10^{-15} depending on the system applications

The sensitivity of the receiver is defined as the required optical power to achieve a desired BER [8]. To determine the sensitivity of an optical receiver, we need to guarantee the pulse stream has no ISI at the sampling instant KT_b [1]. This is illustrated in Fig. 4.6.

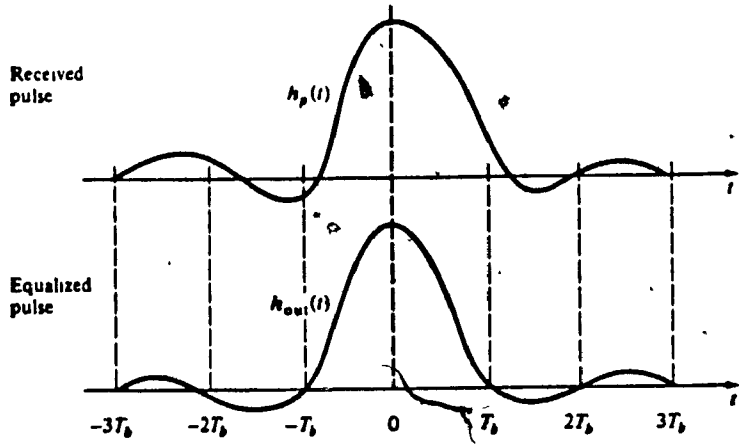

Figure 4.6 Equalized output pulse with no ISI at the sampling time.

This implies

$$h_{out}(t=0) = 1 \tag{4.31}$$

$$h_{out}(t=KT_b) = 0 \quad \text{for } n \neq 0. \tag{4.32}$$

substituting Eq. (4.31) in Eq. (4.15), we have

$$V_{out}(kT_b) = b_k + V_n(kT_b) \tag{4.33}$$

various components of the noise voltage are substituted in Eq. (4.33). To simplify the resulting Eq. (4.33) the following substitutions are made in Eq. (4.33). Let

$$I_1 = \int_{-\infty}^{\infty} \left| \frac{H_{out}(f)}{H_p(f)} \right|^2 df \tag{4.34}$$

$$I_2 = \int_{-\infty}^{\infty} \left| \frac{H_{out}(f)}{H_p(f)} \right|^2 f^2 \, df \tag{4.35}$$

and let

$$I_3 = |H_{out}(0)/H_p(0)|^2 \tag{4.36}$$

By substituting I_1, I_2 and I_3 in Eqs. (4.24) and (4.28), the expressions for noise equivalent bandwidth become

$$2B_N = \frac{I_1}{I_3} \tag{4.37}$$

$$2B_{N_E} = \frac{I_1}{I_3} + \frac{I_2}{I_3}(2\pi R_T C_T)^2 \tag{4.38}$$

substituting Eqs. (4.24), (4.25), (4.36), (4.37), in the expression for total mean square noise voltage and simplifying Eq. (4.19) we have,

$$\langle V_n^2(t)\rangle = \frac{I_1}{I_3}R_T^2 A^2\left\{q\langle i_{en}\rangle G^{2+z} + \frac{2KT}{R_B} + S_I + \frac{S_E}{R_T^2}\right\} + \frac{I_2}{I_3}S_E A^2\left(2\pi R_T C_T\right) \tag{4.39}$$

simplifying further we have

$$\langle V_n^2(t)\rangle = \frac{I_1}{I_3}R_T^2 A^2\left\{q\langle i_{en}\rangle\langle G^{2+z}\rangle + \delta\right\} \tag{4.40}$$

where δ

$$\delta = \frac{2KT}{R_B} + \frac{S_E}{R_T^2} + S_I + \frac{I_2}{I_1}S_E\left(2\pi C_T\right)^2$$

δ contains all the terms that contribute to thermal noise.

The objective is now to find minimum energy per pulse that is required to achieve a desired BER. In order to do this, the output voltage of the equalizer is assumed to be Gaussian distributed.

Let the mean and variance of the Gaussian output for binary 1 be b_1 and σ_1^2 and for binary 0 be b_0 and σ_0^2. The σ_1^2 and σ_0^2 represent the deviation from the $\langle V_n^2(t)\rangle$. If the decision threshold is set at V_{th} and assuming the transmission of binary 1 and 0 are equiprobable then the probability of error, P_e is,

$$P_e = \frac{1}{2}\frac{1}{\sqrt{2\pi\sigma_0}}\int_{V_{th}}^{\infty} \exp\left[-\frac{(v-b_0)^2}{2\sigma_0^2}\right] dv \qquad (4.41)$$

$$+ \frac{1}{2}\frac{1}{\sqrt{2\pi\sigma_1}}\int_{-\infty}^{V_{th}} \exp\left[-\frac{(-v+b_1)^2}{2\sigma_1^2}\right] dv$$

let the parameter Q be defined as,

$$Q = \frac{V_{th} - b_0}{\sigma_0} = \frac{b_1 - V_{th}}{\sigma_1} \qquad (4.43)$$

then Eq. (4.42) can be written as

$$P_e(Q) = \frac{1}{\sqrt{\pi}}\int_{Q/\sqrt{2}}^{\infty} \exp(-z^2)\, dz \qquad (4.44)$$

$$= \frac{1}{2}\left[1 - erf\ \left(\frac{Q}{\sqrt{2}}\right)\right]$$

using the equation for Q, the receiver sensitivity is given by

$$b_1 - b_0 = Q(\sigma_1 + \sigma_0) \qquad (4.45)$$

For ON-OFF systems the required energy per pulse needed to achieve a desired BER is obtained by substituting σ_1 and σ_0 . σ_1 and σ_0 are the worst case values of $<V_n^2>$ i.e., when shot noise voltage term is not neglected in the mean square voltage noise expression. If b_0 is zero, the required energy per pulse that is needed to achieve a desired BER is characterized by the parameter Q is

$$b_1 = Q\left\{\frac{I_1}{I_3} R_T^2 A^2 \left(q < i_{sn} > < G^{2+x} > + \delta\right)\right\}^{1/2} \qquad (4.46)$$

Since shot noise was taken into account Eq. (4.46) represents the minimum receiver sensitivity required to achieve a specified BER. A sub-optimum expression for the required sensitivity is obtained by neglecting shot noise term in Eq. (4.46).

4.8 A Practical System Design Example

The design of an optical fiber link involves several components such as fiber, source, and photodetector characteristics. Performance and cost constraints are some of the main factors in designing an optical fiber communication link. The system designer must carefully choose the components to ensure that the desired performance level can be maintained over the expected lifetime without over-specifying the component characteristics. The key system requirements needed in analyzing a link are :

(a) Transmission distance

(b) The data rate

(c) Threshold

(d) The bit error rate (BER)

To satisfy above requirements the designer has a choice of the following components and their associated parameters [1].

1. Multimode or single-mode optical fiber

    (a) Core size

    (b) Core refractive-index profile

    (c) Bandwidth

    (d) Attenuation

    (e) Numerical Aperture

2. LED or Laser optical source

    (a) Emission wavelength

(b) Spectral line width

(c) Output power

3. PIN or APD

(a) Responsivity

(b) Operating wavelength

(c) Speed

(d) Sensitivity

4.8.1 System Design Considerations

To determine the link power budget, the designer first decides at which wavelength to transmit. If the transmission distance is not too far, the designer may decide to operate in the 800 - 900 nm region (low cost components). However, for long distance communication, the designer may want to take advantage of lower attenuation and zero dispersion that occurs at wavelengths around 1300 nm.

Upon deciding on a wavelength to operate, we next consider the three major building blocks of an optical fiber link, that is, the transmitter, the optical fiber, and the receiver. The designer usually selects the parameters of two of these elements and then computes the requirement on the third component to check if the system performance requirements are met [1]. If the parameters of the components have been over or under specified, a design iteration may be needed. The normal procedure is first to select a photodetector and then choose an optical source and then estimate how far data can be transmitted over the fiber before a repeater is needed to boost up the power level of the optical signal.

In choosing a particular photodetector the designer need only to determine the minimum optical power level needed to achieve a specified BER requirement at the specified data rate. Usually this parameter is found on the data sheet provided by the manufacturer. As we noted in Section 4.2, there are two main photodiodes, PIN and APD photodiodes. A PIN photodiode receiver is simpler to operate, and more stable with changes in temperature and less expensive than an APD [1]. Also, the biasing voltages for PIN photodiodes are considerably lower than APDs. Typical biasing voltages for PIN photodiodes is less than 10 volts whereas for APDs several hundred volts [1]. However, the advantages of PIN receiver may be offset by the increased sensitivity of the APDs extremely low optical power levels are to be detected [1].

The important parameters involved in choosing between LED or a Laser diode are transmission distance, signal dispersion, and cost. As we noted in Chapter 3, the spectral width of a Laser source is much narrower than that of an LED. This is of prime importance in the 800 - 900 nm region, where the spectral width of an LED and the dispersion mechanism of optical fibers limit the data rate-distance product (performance measure of an optical communication system) to around 150 Mb/s [1]. To achieve a higher values of data rate-distance product a Laser diode must be used at these wavelengths. Since Laser diodes are coherent sources a greater optical power can be coupled into a fiber than an LED. Typically the Laser diode can couple 10 to 15 dB more optical power into fiber than an LED [1]. However, this advantage and narrower spectral width may be offset by the cost of a Laser diode. Not only a Laser diodes are expensive than an LED but the driving circuitry is much more complex because the lasing threshold has to be dynamically controlled as a function of temperature and device aging [1].

In choosing an optical fiber we have a choice between multimode and single-mode fiber, the refractive index profile of either fibers could be step or graded-index core. This choice depends on the type of transmitting source and the extent to which dispersion can be tolerated. Multimode fibers must be used with an LED source, since very little optical power can be coupled into a single-mode fiber from an LED. As noted in Chapter 3, the optical power that can be coupled into a fiber is a function of core-cladding index difference Δ, which is in turn is a function of NA (Numerical Aperture). As Δ increases, the optical power coupled into a fiber also increases, however, we also noted in Chapter 3, the dispersion is also a function of core-cladding index difference Δ. Consequently, a tradeoff must be made between the amount of optical power that can be coupled into a fiber and the amount of dispersion that can be tolerated.

A Laser diode can be used either with a single-mode or a multimode fibers. One of the problems associated with single-mode fibers is splicing (joint between fibers). Since the core size for single-mode fibers is typically around 5 to 16 μm, as a result, splicing is critical for single-mode fibers than multimode fibers having a core diameter of 50 μm [1].

Two analyses are usually carried out to guarantee that the desired system performance can be met; they are the *link power budget* and *risetime budget analysis* [1]. In the link power budget analysis the designer first determines the power margin needed between the optical transmitter output and the minimum receiver sensitivity needed to establish a specified BER [1]. The resulting margin can then be allocated to connectors, splices, and fiber losses plus any other additional margins required for expected component degradation or temperature effects. If the choice of components did not allow the desired transmission distance to be achieved, the components might have to changed or repeaters might have to be incorporated into the link. Once the link power budget analysis has

been carried out, the designer can perform system risetime analysis to ensure the dispersion limitation has been met.

The above two analyses are applied to the system to the example system. The following are the specifications of the designed system :

(a) The operating wavelength :1320 nm

(b) Data rate or channel bandwidth :50 Mb/s (NRZ)

(c) Type of fiber :Multimode

(d) Type of transmitter :LED

(e) Type of receiver :PIN receiver

(f) Bit error rate :10^{-9}

(g) Transmission distance :$\leq$ 1km

(h) Type of line coding :Manchester

4.8.2 Link Power Budget

The transmitter optical power, P_T, is 50 μW or -13 dBm at 200 nA. The required sensitivity, P_R, for 10^{-9} BER is -39 dBm (from PIN diode receiver module data sheet). The system gain G_s is defined as :

$$G_s = P_T - P_R \tag{4.47}$$

G_s can also be defined as :

$$G_s = \alpha d + L_m + FM$$

where

α: is the fiber loss coefficient in dB/km

d : is the distance in km between transmitter and receiver

FM : is the fade margin (expected component degradation due to aging,

temperature effects etc.)

L_m : is the connector losses, splice losses, NA losses etc.

substituting the transmitter optical power and the required sensitivity in Eq. (4.47) we obtain the numerical value for the system gain G_s

$$= -13dBm + 39dBm = 26dB$$

The system power budget is shown in Table 4.2

Table 4.2 System power budget.

Mean launch Power	- 13 dBm
1 km fiber (1 dB/km)	-1 dB
Connector Losses	-2 dB
Fade Margin	-6 dB
Received Power	-22 dB
Receiver Sensitivity	-39 dBm
Operating margin	17 dB

The system gain G_s is 26 dB is allocated to various losses shown in Table 4.2. The designed system has two connectors so the total loss is 2 dB. The fade margin, FM is added to the system gain to compensate for the expected component degradation due to aging, temperature effects. This margin is usually around 6 dB for LED based systems whereas for Laser based systems it is usually around 9 dB [2]. The high fade margin in Laser based systems is because the temperature effects in Laser based systems are more pronounced than compared to LED based systems. Assuming a fiber loss coeffient of 1 dB/km, the attenuation due to fiber is 1 dB (for a distance of 1 km). Therefore, the operating margin is 17 dB (26 -9). The power budget requirement are adequate enough to maintain the desired sensitivity for a bit error rate of 10^{-9} and also there is ample room for future upgrade of the system (in terms of distance and bit rate etc.).

4.8.3 Risetime Budget

The risetime budget analysis is a convenient method for determining the dispersion limitation of an optical fiber system. In this method the total risetime, t_{sys}, of the link is the root sum square of the risetimes from each contributor t_i [1].

$$t_{sys} = \sqrt{\sum_{i=1}^{N} t_i^2} \tag{4.48}$$

The four basic elements that may significantly limit system speed are the transmitter risetime, t_{tx}, the material dispersion risetime, t_{mat}, the modal dispersion risetime, t_{mod}, of the fiber, and the receiver risetime, t_{rx} [1]. As a rule of rule of thumb, the total system risetime of the link should not exceed 70% of NRZ bit period or 35% of RZ bit period.

For the system under consideration the transmitter the transmitter risetime is 10 nsec (worst case), receiver risetime is 4 nsec and neglecting the material dispersion risetime, t_{mat} and modal dispersion risetime, t_{mod} (since the length of the cable is less than 1km). Therefore, the total system risetime is obtained by substituting various risetimes in Eq. (4.49).

$$\begin{aligned} t_{sys} &= \sqrt{t_{tx}^2 + t_{rx}^2} \\ &= \sqrt{15^2 + 4^2} = 15.5 nsec \end{aligned}$$

This value falls below the maximum allowable 14 nsec risetime degradation for 50 Mb/s NRZ data stream. We next consider the design of individual blocks of an optical communication system.

4.8.4 Transmitter Design

The digital data to be transmitted is fed to the driver of LED. The driver in turn controls the driving current for LED corresponding to the data being transmitted. The driver is configured as shown in Fig. 4.7

The output of LED is a function of forward current I_F. As this forward current increases, the output power also increases. This forward current flowing through the LED generates heat P_D which causes the junction temperature θ_j of the diode to increase. As the junction temperature increases the output power decreases.

When the temperature of LED rises to a certain level, the temperature sensor (a transducer) converts the rise in temperature to a corresponding voltage signal which will reduce the driving current of LED in turn the temperature.

The digital data to be transmitted is fed to one of the inputs Q or $\overline{Q}$ of the driver. The resistors R_{intial} and R_{slope} resistors will prevent LED from going into saturation region by controlling the current through LED. For normnal operation the current is fixed at 200 ma for which the output power is $50\mu w$.

4.8.5 Receiver Design

In this section the purpose and design consideration of each block are dealt. In the block diagram shown in Fig. 4.7 the first stage is an optical detector which intercepts the optical pulses propagating in the fiber. Photodetector is essentially a current source whose magnitude is proportional to the incident optical power. The output current from the photodetector is very small. Consequently, it is rather difficult to interface an amplifier stage without introducing noise. For this reason the photodetector and amplifier are integrated. The preamplifier is essentially a current to voltage converter. This amplifier is a transimpedance amplifier built from an op-amp or other high gain amplifier with negative current feedback. The transimpedance amplifier does three things. First, it converts photocurrent to corresponding voltage and provides signal amplification. Second, because of high open loop gain and negative feedback, it provides a low output impedance. Third, it provides a virtual ground at its signal input.

4.8.5.1 Main Amplifier Design

The output signal from the photodetector and pre-amplifier is calculated as follows : The output from the photodiode and pre-amplifier is -39 dBm or 0.12 mw. A typical responsivity of photodiode (from the data sheet of C30986) is $5X10^5$ v/w therefore, the expected output voltage v_0 is

$$v_0 = R_0 P_R$$

substituting values for R_0 and P_R we have for v_0

$$v_0 = (5X10^5 v/w)(-0.12X10^{-3})w = 6v$$

Assume that the worst case signal-to-noise ratio at the detector output is 20 dB. The measured output noise voltage is 50 mv or 36 mv rms. Therefore, the output signal must be atleast 360 mv. The measured output voltage is 500 mv, which exceeds the minimum level. This voltage is amplified with SL560C (Plessy component). This amplifier was chosen because of its low noise and wide bandwidth. It was configured to give a gain of 13 dB. Amplifying further at this stage will only increase the noise level.

4.8.5.2 Comparator Design

This stage is used to convert analog voltage from the main amplifier to digital signal. The SP9680 from Plessy was chosen for this purpose. This is an ultrafast comparator. The optimum reference voltage for the comparator is chosen as the midpoint of the limits of the ECL output swing, that is

$$V_{ref} = \frac{(V_{OH} + V_{OL})}{2}$$

substituting for V_{OH} and V_{OL} (from ECL data manual)

$$= \frac{-0.8 - 1.85}{2} = -1.325v$$

this reference will guarantee equal swing on positive and negative peaks of the input signal. The schematics of the photodetector and pre-amplifier, main

amplifier, and comparator are shown in Fig. 4.10

4.8.5.3 Symbol Timing Recovery

Conventionally the clock is recovered by the signal through an appropriate non-linear circuit so that a discrete tone is generated at the symbol rate frequency [14]. The non-linear function may be implemented by differentiator, full wave rectifier, detector, squarer etc. [14].

This particular technique shown in Fig. 4.11 employs a digital technique to recover the clock information from the transmitted data. First, the clock to be transmitted is EX-ORed with data signal to generate a Manchester encoded signal (refer to Figure 4.12). The Manchester encoded signal converted to an optical signal and transmitted on an optical fiber.

At the receiving end the optical signal is converted back to an optical signal. The electrical signal is amplified and converted to binary signal by passing through a comparator.

The output still in Manchester form is EX-NORed with delayed replica of itself to generate a form of Return-to-Zero (RZ) signal (refer to Fig .4.12). The delay d_1 can be chosen arbitrarily, the delay d_2 can be adjusted for 50% duty cycle, but it is not important as long $d_2 > T_b/2$, where T_b is the bit period of the signal. Since the D input of the D-flip flop is always at high state, for every rising edge of the clock input signal the output toggles. The resulting output Q is the desired clock signal. This clock signal is used to recover the transmitted data. The schematic of symbol timing recovery circuit is shown in Fig. 4.11

In this chapter a sensitivity equation was derived for ON-OFF cases. In deriving this expression various approximations were made. This sensitivity equation is only valid for ON-OFF cases. If line code were to change then the complexity of the derivation increases enormously. To decode the optical information

a simple direct detection receiver was assumed which is not optimum. Consequently, the system is inferior in performance than the optimum receiver. Also, in this chapter a procedure to select various components associated with the design of an optical receiver was described. In Chapter 5, an optimum receiver is considered to detect various line codes in Gaussian as well as in Poisson regime. In both cases sensitivity is plotted as a function of BER. An optimum threshold is also derived in both of these cases.

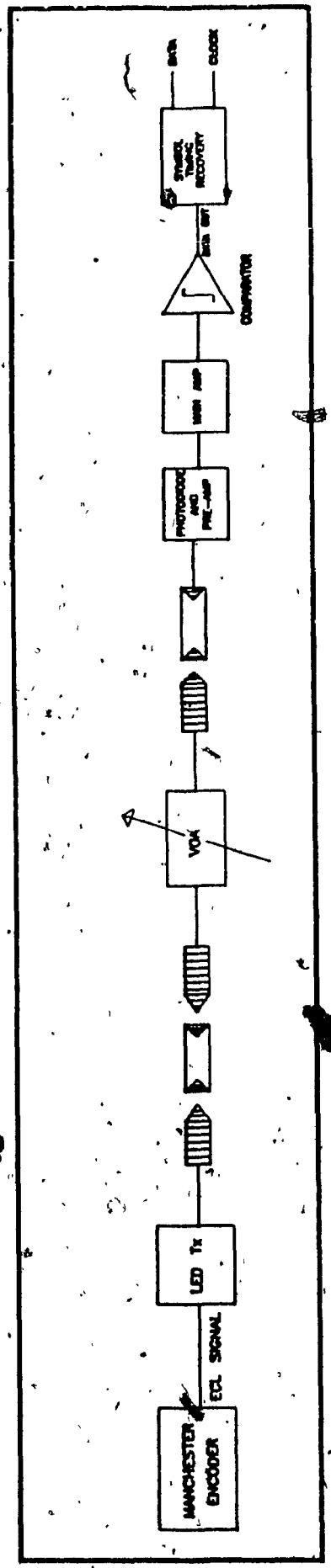

Figure 4.7 Block diagram of fiber optic communications system.

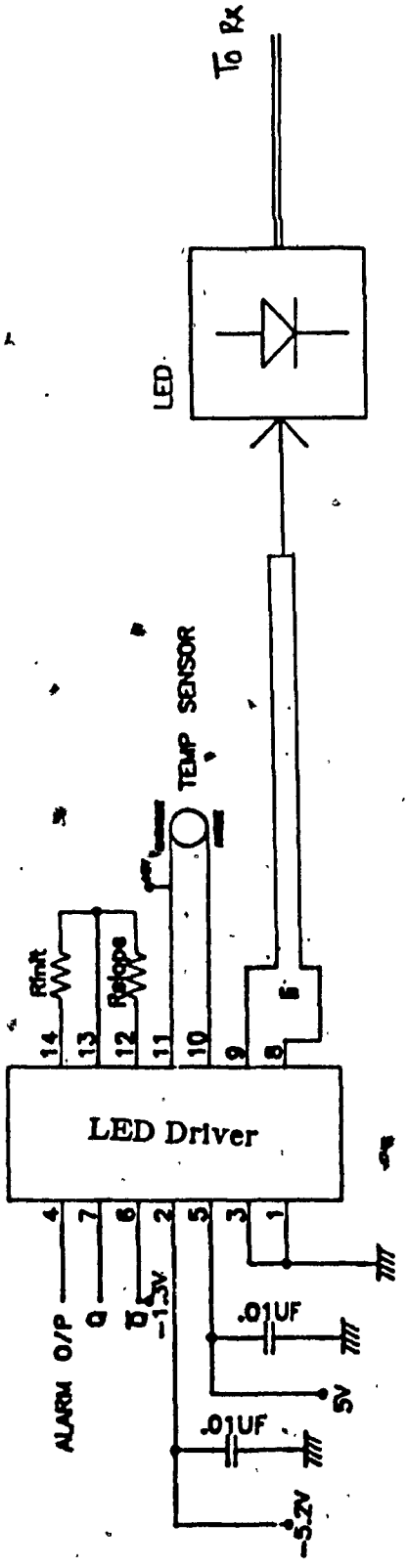

Figure 4.8 Transmitter schematic.

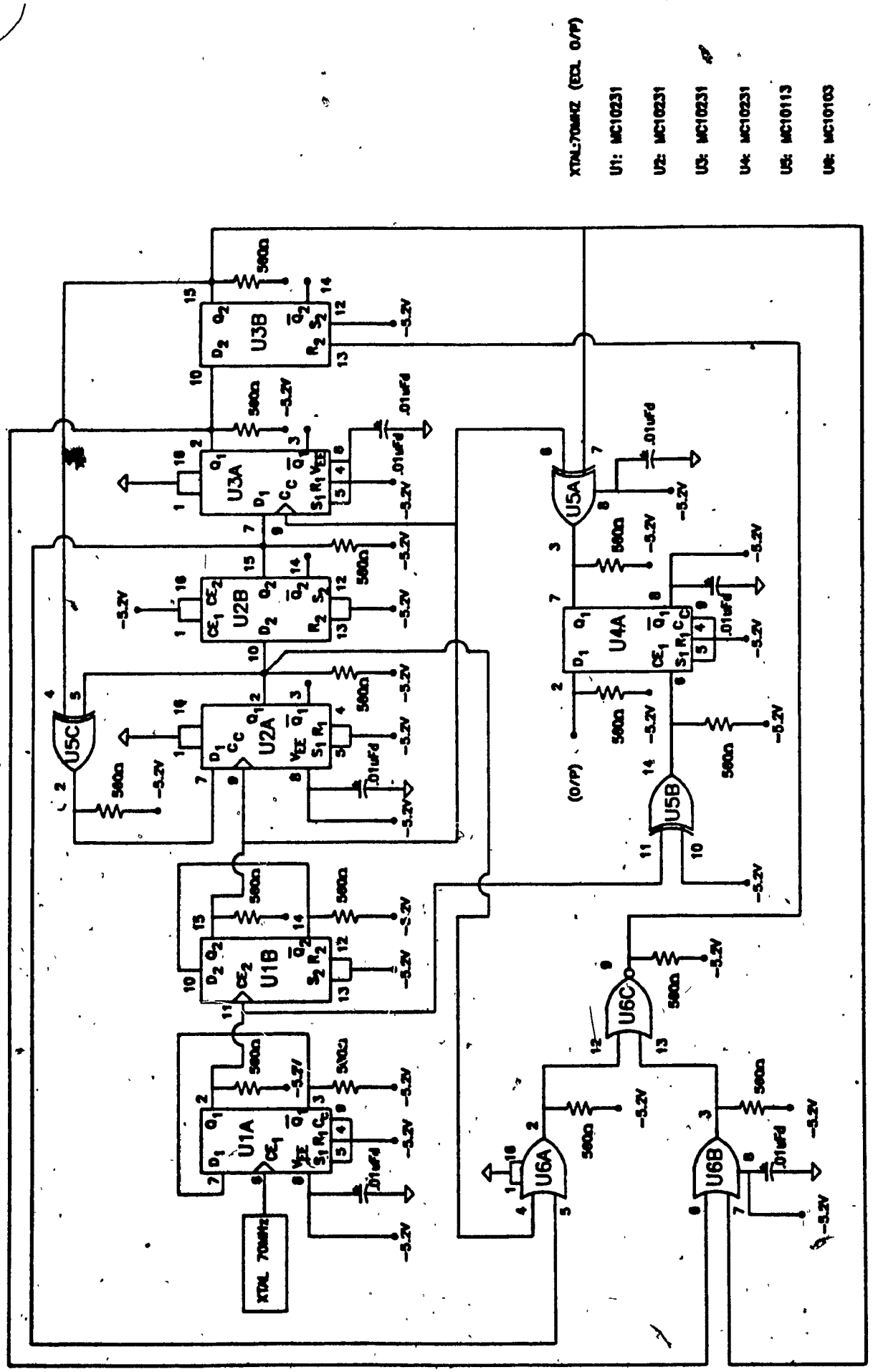

Figure 4.9 Manchester encoder.

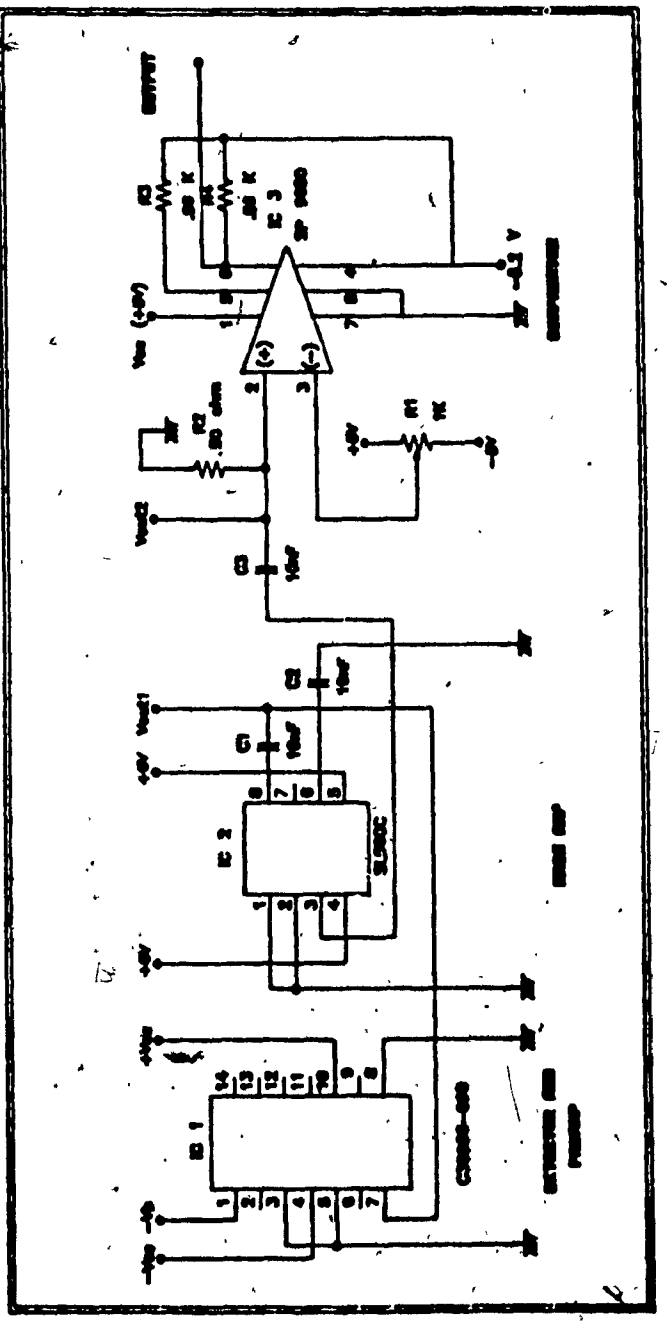

Figure 4.10 Fiber optic receiver schematic.

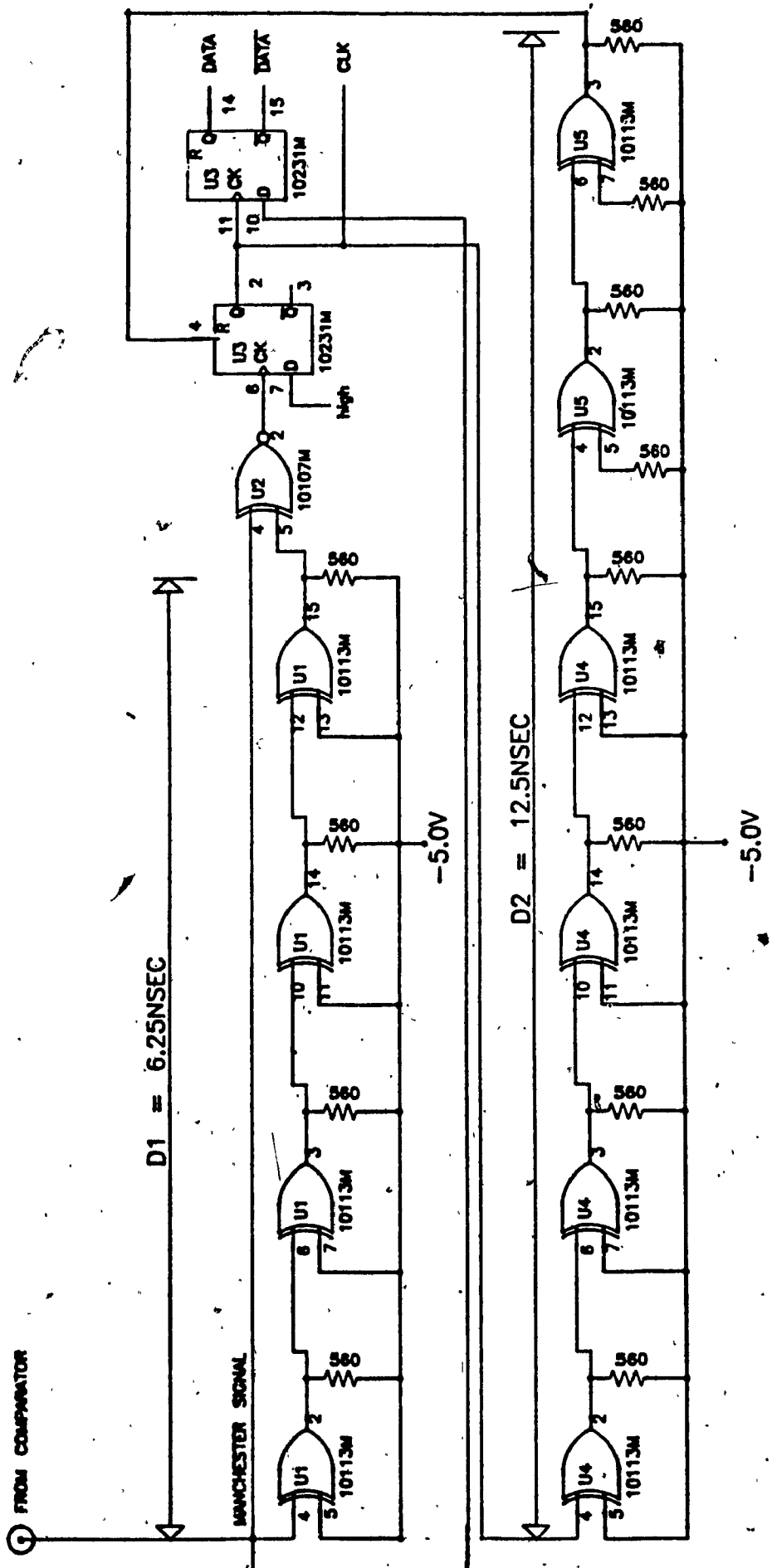

Figure 4.11 Symbol timing recovery.

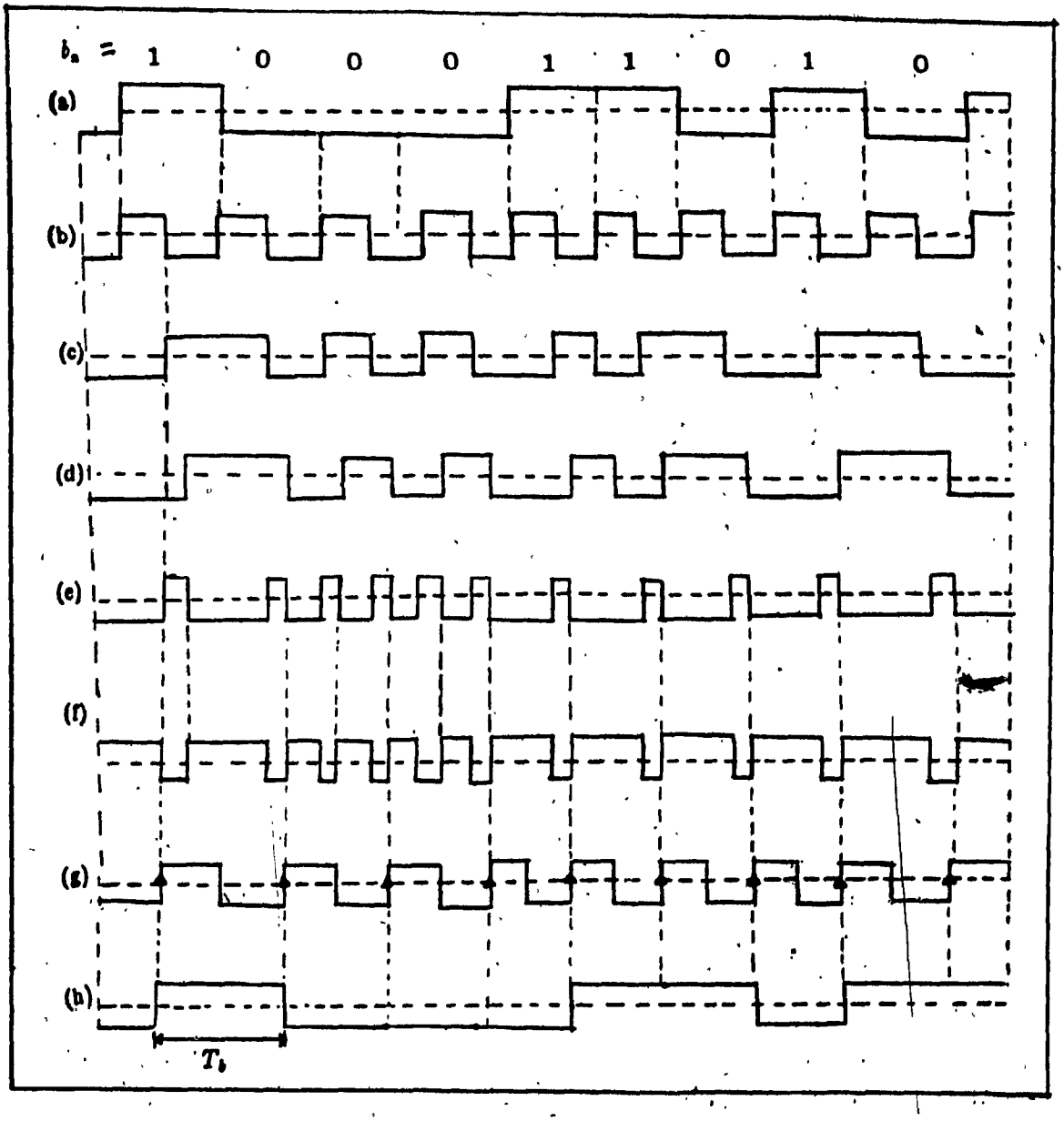

(a) NRZ data (b) The clock (c) Manchester code

(d) Signal after delay (D1) (e) EX-OR of clock & delayed clock (x)

(f) The inversion x ($\bar{x}$) (g) The recovered clock

(h) Recovered data (NRZ data)

Figure 4.12 Waveforms of symbol timing recovery.

CHAPTER 5

OPTICAL FIBER RECEIVER : PERFORMANCE ANALYSIS

5.1 Introduction

In this chapter an optimum receiver is considered for demodulating various line coding formats and probability of error equations are derived for different line coding schemes. Depending on the type of noise dominant at the front end of the receiver, such as thermal or Poisson, a particular probability of error equation is chosen to determine the required sensitivity for a desired BER.

5.2 The General Structure of an Optimum Receiver

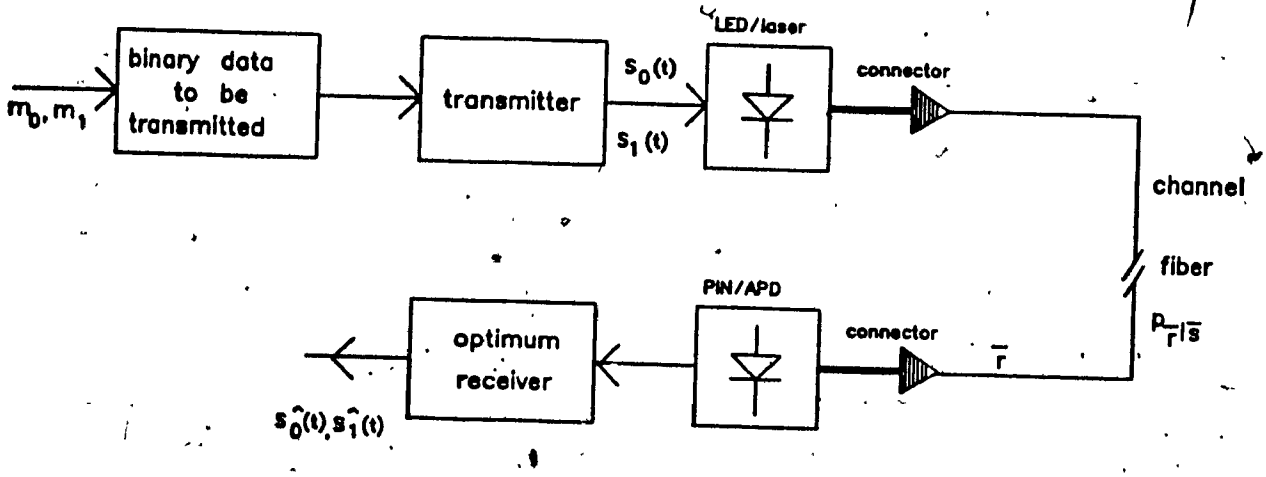

Figure 5.1 Optical fiber communication system.

The block diagram of fiber optic communication system is shown in Fig. 5.1. The transmitter emits a signal waveform $s_0(t)$, $s_1(t)$ for binary messages m_0 and m_1 respectively. Due to noise introduced by a photodiode a random vector is received. The objective of the optimum receiver is to determine which one of the possible messages m_0 and m_1 is received based on the knowledge of conditional probability density function and a priori probabilities of transmitted messages. Given that any particular vector say, $\bar{r}=\bar{\gamma}$, is received , the optimum receiver sets $\hat{m}=m_k$ whenever

$$p[m_k \mid \bar{r} = \bar{\gamma}] > p[m_i \mid \bar{r} = \bar{\gamma}]; \quad \text{for } i = 0,1, \quad i \neq k \tag{5.1}$$

where $\bar{r}$ is the received vector and m_k is the transmitted message. For binary case Eq. (5.1) reduces to

$$P(m_1 \mid \bar{r}) \underset{0}{\overset{1}{\gtrless}} P(m_0 \mid \bar{r}) \tag{5.2}$$

This particular receiver is known as *maximum a posteriori* probability (MAP) receiver [15]. This receiver is also called an optimum receiver, since whenever receiver sets $\hat{m} = m_k$, the conditional probability of a correct decision given that $\bar{r} = \bar{\gamma}$ is

$$P[C \mid \bar{r} = \bar{\gamma}] = P[m_k \mid \bar{r} = \bar{\gamma}] \tag{5.3}$$

removing the conditionality in Eq. (5.3), the probability of correct decision can be written as

$$P[C] = \int_{-\infty}^{\infty} P[C \mid \bar{r} = \bar{\gamma}] \; p_r(\bar{\gamma}) \; d\bar{\gamma} \tag{5.4}$$

Since $p_r(\bar{\gamma}) \geq 0$, P[C] is maximized by maximizing the factor $P[C \mid \bar{r} = \bar{\gamma}]$ in Eq. (5.4) for each received vector $\bar{\gamma}$.

The conditional a posteriori probabilities $P[m_i \mid \bar{r} = \bar{\gamma}]$ can be obtained by employing Bayes rule.

$$P[m_i \mid \bar{r} = \bar{\gamma}] = \frac{P[m_i] p_r[\bar{\gamma} \mid m_i]}{p_r(\bar{\gamma})} \tag{5.5}$$

since $p_r(\bar{\gamma})$ is independent of the index i, the optimum receiver on observing $\bar{r} = \bar{\gamma}$, sets $\hat{m} = m_k$ whenever the decision function

$$P[m_i] p_r[\bar{\gamma} \mid \bar{s} = \bar{s}_i] \quad ; i = 0,1 \tag{5.6}$$

is maximum for i = k.

A receiver that determines $\hat{m}$ by maximizing only the factor $p_r(\bar{\gamma} \mid \bar{s} = \bar{s}_i)$ without regard to the factor $P[m_i]$ is called *maximum likelihood receiver* (MLR). This receiver yields minimum probability of error when the transmitter inputs

are equally likely [15]. The MLR receiver can equivalently compute the conditional probability $P(\overline{r} \mid \overline{s}=\overline{s}_i)$. Let Z_i be defined as $P(\overline{r} \mid \overline{s}=\overline{s}_i)$. The transmitted signal is determined by the test

$$Z_1 \underset{0}{\overset{1}{\gtrless}} Z_0 \tag{5.7}$$

this test is also equivalent to

$$\log Z_1 \underset{0}{\overset{1}{\gtrless}} \log Z_0 \tag{5.8}$$

since, logarithmic function is monotonic increasing in its argument. The optimum receiver just described is employed for processing optical signals.

The threshold of the detector for the optimum receiver is based on two effects, thermal noise and shot noise. Depending on which noise is dominant, a threshold is chosen for optimum detection. These two noises are dealt in the following sections and probability of error expressions are derived for various binary formats for the above noise effects.

5.2.1 Thermal Noise

This noise is due to the photodetector load resistor R_l and also due to the biasing resistors of the amplifier. This noise arises due to random motion of electrons within the resistor. The mean noise power generated within the resistor is $R_l \overline{i_{th}^2}$, where $\overline{i_{th}^2}$ is the mean square value of the thermal noise current. The signal current due to the incident optic power, is added to the thermal noise current. The average signal current due to incident optic power is [5]

$$\overline{i_s} = \frac{\eta q P_{in}}{hf} \tag{5.9}$$

where

η: is the quantum efficiency

q: is the electron charge

P_{in}: is the incident optical power

hf: is the incident photon energy

When thermal noise current is superimposed on this signal current the load current fluctuates randomly around $\bar{i}_s$. When the incident power is small the signal current may be masked by the thermal noise current causing errors at the decision point.

The thermal noise can be modeled by an equivalent circuit shown in Fig. 5.2. In Fig. 5.2, the R_l is the ideal noiseless load resistor.

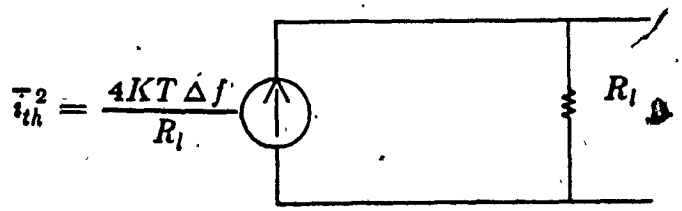

Figure 5.2 Thermal noise equivalent circuit.

The mean square current $\bar{i}_{th}^2$ produced by the load resistor R_l is given by

$$\bar{i}_{th}^2 = \frac{4KTB}{R_l} \tag{5.10}$$

where

K: is the Boltzman constant ($1.38 * 10^{-23}$)

T: is the absolute temperature in degree Kelvin

B: is the bandwidth of the receiver

5.2.2 Shot Noise

This noise is due to random and quantum detection process. Shot noise can be represented by an equivalent circuit consisting of a current source as shown in Fig. 5.3.

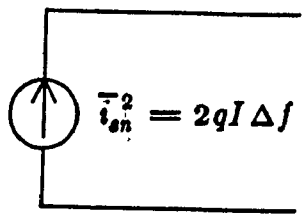

Figure 5.3 Shot noise current model.

The average shot noise current is given by [4,16]

$$\overline{i_{sn}^2} = 2qIB \tag{5.11}$$

where

q: is the magnitude of the electron charge

I: is the average detector current

B: is the receiver bandwidth

The detector average current I, is the superposition of the average signal current $\overline{i_s}$ and the dark current I_D, therefore substituting for I in the mean square shot noise current ($\overline{i_{sn}^2}$) we have shot noise current,

$$\overline{i_{sn}^2} = 2q(\overline{i_s} + I_D)B \tag{5.12}$$

5.2.3 Signal-to-Noise Ratio (SNR)

The equivalent circuit of a photodiode is shown in Fig. 5.4.

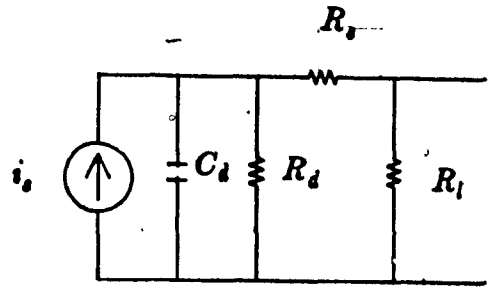

Figure 5.4 Photodiode equivalent circuit.

When a constant power is illuminated on a photodiode, the average value of the photocurrent is given by Eq. (5.9). The average signal power delivered to the load resistor R_l is given by,

$$\begin{aligned}\bar{P}_l &= \bar{i}_s^2 R_l \\ &= \left[\frac{\eta q P}{hf}\right]^2 R_l\end{aligned} \tag{5.13}$$

The average shot noise power delivered to the load is $\bar{i}_{sn}^2 R_l$. Substituting (5.9) in (5.12) the shot noise power is obtained. The resulting equation is given by,

$$\bar{P}_{sn} = 2qB\left\{\frac{\eta q P_{in}}{hf} + I_D\right\} R_l \tag{5.14}$$

The thermal noise power delivered to the load resistor is given by, $\bar{i}_{th}^2 R_l$ is given by,

$$\bar{P}_{th} = 4KTB \tag{5.15}$$

The signal to noise ratio (SNR), is the signal power delivered to the load divided by the noise power due to all noise sources. Substituting for signal power and noise power the expression for SNR is obtained.

$$\frac{S}{N} = \frac{Signal\ \ power}{Noise\ \ power} \tag{5.16a}$$

$$\frac{S}{N_0} = \frac{\left[\frac{\eta q P_{in}}{hf}\right]^2 R_l}{2qR_l B\left[I_D + \frac{\eta q P_{in}}{hf}\right] + 4KTB} \tag{5.16b}$$

Eq. (5.16 a) can be written in terms of bit energy and noise power (E_b / N_0, by noting the bit energy, E_b, is related to signal power, S, by the relation $E_b = ST_b$.

Therefore, Eq. (5.16) in terms of bit energy and noise power is given by

$$\frac{E_b}{N_0} = \frac{\left[\frac{\eta q P_{in}}{hf}\right]^2 R_l T_b}{2qR_l B\left[I_D + \frac{\eta q P_{in}}{hf}\right] + 4KTB} \tag{5.17}$$

Important Cases :

If the signal current, $\bar{i}_s = \eta q P_{in} / hf >>$ dark current, I_D, then I_D can be neglected from SNR equation. Above situation occurs for large values of optical powers and low values of dark current. Also, if shot noise power exceeds the thermal noise power, then the thermal noise power can be neglected from SNR equation. The SNR equation then simplifies to

$$\frac{S}{N} = \frac{\eta P_{in}}{2hfB} \tag{5.18}$$

In this case, the SNR is shot noise limited also called *quantum limited.* The effects due to dark current and thermal noise are eliminated by increasing the optical power levels.

When the optical power is limited, the thermal noise power usually dominates over shot noise power [5]. Thus neglecting the effects due to shot noise current the SNR reduces to

$$\frac{S}{N} = \frac{\left[\frac{\eta q P_{in}}{hf}\right]^2 R_l}{4KTB} \tag{5.19}$$

This case is the *thermal noise limited case.* The SNR can be increased significantly by increasing the value of load resistance R_l. However, this may

reduce receiver bandwidth and dynamic range, since bandwidth is inversely proportional to R_l (B = 1 / (2 πR_l C)). The SNR is proportional to the square of the incident optic power level thus producing significant increase in SNR for relatively small change in optical power levels.

The SNR equation can be modified easily to accommodate for photodetectors having an internal gain, G, such as photomultipliers. For these devices the signal power increases by G^2. The mean square shot noise power also increases by G^2. The thermal noise power remains constant, since this power is not generated within the photodetector. With the above modifications the SNR equation can be written as

$$\frac{S}{N} = \frac{\left[\frac{G\eta q P_{in}}{hf}\right]^2 R_l}{G^2 2qR_l B\left(I_D + \eta q P/hf\right) + 4KTB} \qquad (5.20)$$

If the internal gain of the photodetector is large enough, the shot noise power can exceed the thermal noise power even for moderately low optic power levels. For the above situation and assuming negligible dark current the SNR expression is reduced to the following expression.

$$\frac{S}{N} = \frac{\eta P_{in}}{2hfB} \qquad (5.21)$$

Which is the shot noise limited expression (5.18) obtained earlier.

5.2.4 The Excess Noise Factor

The expression derived for shot noise limited case is valid for photomultiplier, It can be modified to accommodate for APDs. In APD the shot noise power rather than increasing as G^2 it increases as G^n, where n lies between 2 and 3 [5]. The shot noise power is also increased relative to the signal power by the excess noise factor which is defined as $G^n / G^2 = G^{n-2}$) [5]. Therefore, the SNR

equation is modified as

$$\frac{S}{N} = \frac{\left[\frac{G\,\eta q P_{in}}{hf}\right]^2 R_l}{G^n q R_l B\left(I_D + \frac{\eta q P_{in}}{hf}\right) + 4KTB} \tag{5.22}$$

The SNR can be improved significantly by choosing detectors having gain beyond unity. These detectors improve the SNR by making the thermal noise negligible at low optic power levels. However, for detectors having a large gain such that the shot noise power is dominant, consequently, neglecting dark current, I_D in Eq. (5.21), the SNR expression reduces to

$$\frac{S}{N} = \frac{1}{G^{n-2}} \frac{\eta P_{in}}{2hf\,B} \tag{5.23}$$

which is equal to

$$\frac{S}{N} = \frac{Quantun\ limited\ SNR}{Excess\ noise\ factor} \tag{5.24}$$

In Eq. (5.23), as G increases the quantum limited SNR is decreased by the excess noise factor. As a result, the quality of the signal is degraded.

5.3 The Probability of Error Expression for Thermal Noise Limited Case

When thermal noise is dominant at the front end of the receiver the probability density function is assumed to be of Gaussian type. The probability of error expressions for various binary formats such as RZ, NRZ, Manchester, Miller are derived in this section.

The function of a communication receiver is to distinguish between 'm' transmitted signals $\{ s_1(t), \ldots\ldots, s_m(t) \}$ in the presence of noise. In this section the structure of an optimum receiver is derived for Gaussian approximation. A general probability of error equation and an optimum threshold is derived. It will

be shown that the structure of an optimum receiver takes the form of a correlator -integrator type (matched filter) receiver when the noise at the receiver input is white noise.

The analysis is carried out for binary communication system transmitting $\{ s_i , i=0,1 \}$. In Fig. 5.5,

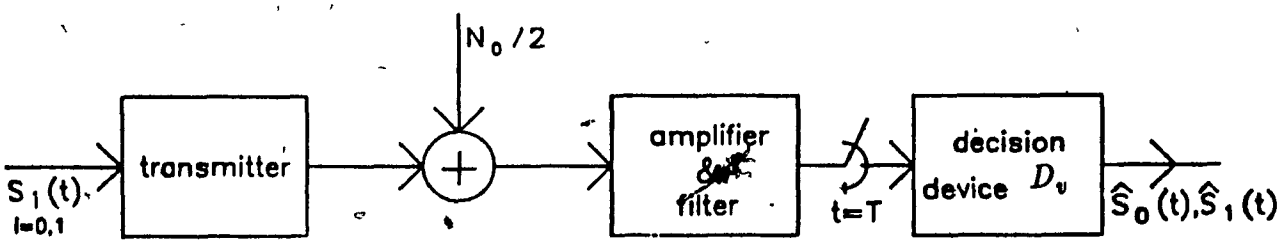

Figure 5.5 Binary communication system in additive noisy environment.

At the decision point if the "signal + noise" exceeds the threshold D_v a binary 1 is assumed to be sent and if "signal + noise" is less than the threshold D_v a binary 0 is assumed to be sent. There are two possibilities in which an error can occur (a) if $s_1(t)$ is transmitted and "signal + noise " does not exceed the threshold (b) if $s_0(t)$ is transmitted i.e., if background noise alone exceeds the threshold D_v. Symbolically, the decision can be expressed as follows :

$$V_T \underset{0}{\overset{1}{\gtrless}} D_v \tag{5.25}$$

Let S_0 (T) and S_1(T) be the outputs of $s_0(t)$ and $s_1(t)$ respectively at the sampling instant (t=T) and also let V_T be the voltage at the sampling instant. A correct decision is made if $V_T > D_v$, when $s_1(t)$ is transmitted. A correct decision is also made if $V_T < D_v$, when $s_0(t)$ is transmitted. If $s_i(t)$ is transmitted where i= 0, 1, the sampling voltage at the decision point is

$$V_T = s_i(T) + n(T) \tag{5.26}$$

Since the noise is Gaussian type the sampler output V_T is also of Gaussian type with mean equal to $s_1(T)$ and $s_0(T)$ for binary 1 and 0 respectively and variance equal to σ_0^2. The conditional probability density function of V given $s_1(t)$ transmitted is $f_V(v \mid s_1(t))$ and the conditional probability density function V given $s_0(t)$ is transmitted is $f_V(v \mid s_0(t))$. These conditional probability densities are sketched in Fig. 5.6 assuming $S_0(T) < S_1(T)$.

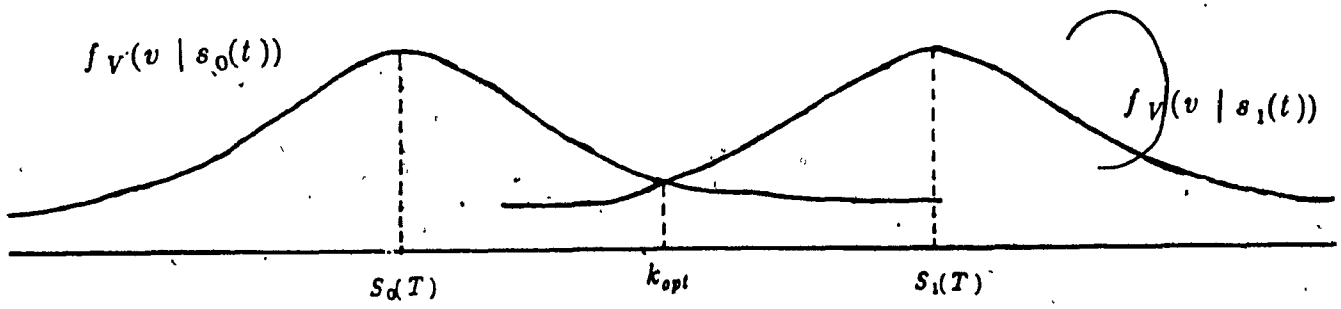

Figure 5.6 The conditional probability density functions.

The total probability of error is

$$P(e) = \frac{1}{2}\left[P(e \mid s_1(t)) + P(e \mid s_0(t))\right] \tag{5.27a}$$

substituting the appropriate conditional densities and simplifying the Eq. (5.27a) the probability of error can be written as [Appendix-I].

$$P(e) = \frac{1}{2}\, erfc\, \frac{1}{2}\sqrt{\frac{[E_0 + E_1 - 2\rho_{12}\sqrt{E_0 E_1}]}{N_0}} \tag{5.27b}$$

where E_0 and E_1 are the energy contents in signals $s_0(t)$ and $s_1(t)$ and ρ_{12} is the correlation coefficient between signals $s_0(t)$ and $s_1(t)$ which is defined as [23]

$$\rho_{12} = \frac{1}{\sqrt{E_1 E_0}} \int_0^{T_i} s_1(t) s_0(t)\, dt \tag{5.28}$$

For antipodal signals $\rho_{12} = -1$, in which case, P(E) is at minimum value.

The probability of error equation given by Eq.(5.28) can be used to derive the probability of error expressions for various line coding schemes that can be represented by two level signaling schemes such as RZ, NRZ, and Manchester encoded signals. However, for Miller encoding scheme the probability of error must be derived from first principles, since four levels are needed to represent a Miller encoded signal.

5.3.1 Nonreturn-to-Zero (NRZ)

In this type of signaling the voltage level is constant during a bit interval. This type of encoding is generated by turning the optical transmitter (Laser or LED) ON - OFF via a driver, according to the data being transmitted. The required bandwidth for this code is minimum compared to other coding schemes such as RZ, Manchester and Miller. However, this code suffers from a DC component (refer to Figure 3.4) and synchronization problem.

Probability of Error for NRZ Binary Format

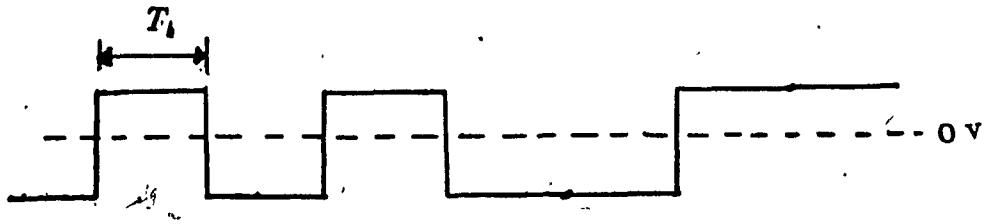

Figure 5.7 Representation of NRZ signal.

$$s_1(t) = A, \quad 0 < t < T_b \tag{5.29}$$

$$s_0(t) = -A, \quad 0 < t < T_b \tag{5.30}$$

$$E_i = \int_0^{T_b} s_i^2 dt, i = 0,1 \tag{5.31}$$

Substituting the signal and performing the integration the expression for energy is obtained.

$$E_1 = A^2 T_b = E_0; \tag{5.32}$$

therefore the average bit energy, $E_b = E_1 = E_0$. Substituting various expressions in the correlation coefficient equation, Eq. (5.28), and integrating the expression we obtain - 1 for ρ_{12} (since signals are antipodal), substituting for E_1 and E_0 in the probability of error expression (5.27b) we obtain,

$$P(e) = \frac{1}{2} erfc \sqrt{\left[\frac{E_b}{N_o}\right]} \tag{5.33}$$

5.3.2 Return to Zero (RZ)

In this type of signaling the signal is represented only half the bit period. As a result, the bandwidth of the signal is larger compared to NRZ scheme. This encoding scheme is also generated in the same way as the NRZ scheme except that the optical transmitter is ON only half the bit period compared to complete bit period as in the case of NRZ encoding scheme. This type of signaling also suffers from dc component and lack of synchronization. However, this representation is also used in practise because of simplicity in generating the signal.

Probability of Error for RZ Binary Format

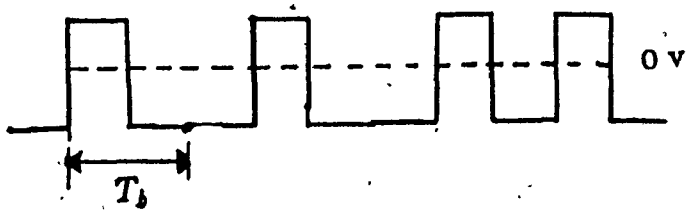

Figure 5.8 Representation of RZ signal.

$$s_1(t) = \begin{cases} A, & 0 < t < T_b/2 \\ -A, & T_b/2 < t < T_b \end{cases} \tag{5.34}$$

$$s_0(t) = -A, \quad 0 < t < T_b \tag{5.35}$$

The energy in the signal is given by

$$E_i = \int_0^{T_b/2} s_i^2 dt, \quad \text{for } i = 0,1 \tag{5.36}$$

$$E_1 = E_0 = E_b = A^2 T_b \tag{5.37}$$

and substituting various values in the correlation coefficient expression Eq. (5.28) we obtain zero for ρ_{12}. Substituting in the general probability of error Eq. (5.27b) we obtain,

$$P(E) = \frac{1}{2} erfc \sqrt{\left[\frac{E_b}{2N_o}\right]} \tag{5.38}$$

5.3.3 Manchester

This scheme is intended to overcome the disadvantages of NRZ and RZ (such as DC component in the spectrum and lack of synchronization) signal encoding techniques. In this scheme, at least one transition is guaranteed for every bit. Although this will increase the bandwidth to twice that of NRZ there are several advantages.

(i) *Synchronization* : Since there is at least one transition per bit the clock recovery is easier to accomplish than compared to other schemes.

(ii) This scheme has no DC component.

Probability of Error for Manchester coded signal

The representation of Manchester encoded signal is shown in Fig. 5.9.

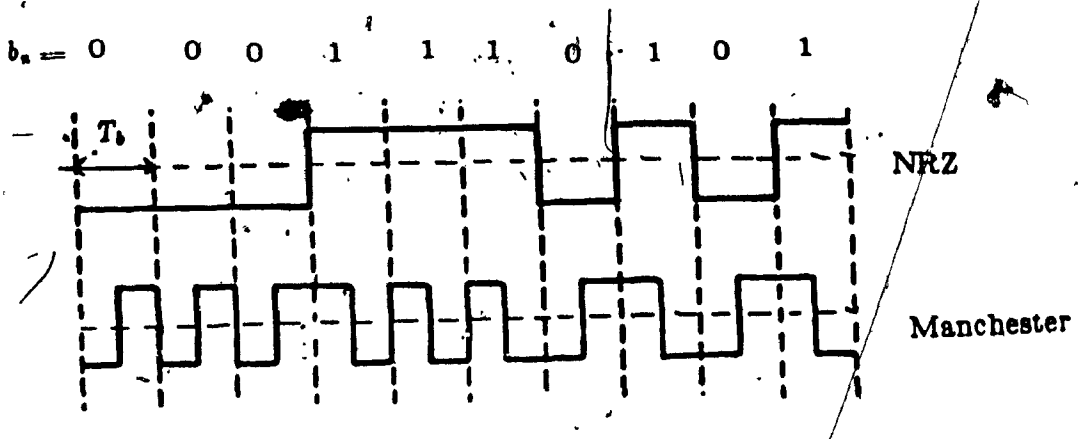

Figure 5.9 Manchester encoded signal.

The signals are defined as follows :

$$s_1(t) = \begin{cases} A & 0 < t < T_b/2 \\ -A & T_b/2 < t < T_b \end{cases} \tag{5.39a}$$

$$s_0(t) = \begin{cases} -A & 0 < t < T_b/2 \\ A & T_b/2 < t < T_b \end{cases} \tag{5.39b}$$

The energy in each signal is given by,

$$E_0 = E_1 = \int_0^{T_b/2} A^2 dt + \int_{T_b/2}^{T_b} A^2 dt \tag{5.39c}$$

$$E_0 = E_1 = A^2 T_b \tag{5.40}$$

The average bit energy $E_b = A^2 T_b$, and ρ_{12} (the correlation coefficient) = - 1, since signals are antipodal. Substituting the above values in the general probability of error equation and simplifying we obtain,

$$P(e) = \frac{1}{2} erfc \sqrt{\left[\frac{E_b}{N_o}\right]} \tag{5.41}$$

5.3.4 Miller Encoded Signal

Miller encoding also known as Delay Modulation code. This particular encoding scheme requires less bandwidth than Manchester encoding scheme. However, this encoding scheme has a larger DC component than Manchester encoding scheme and also this code requires less bandwidth than Manchester encoding

scheme (refer to Chapter 3). Miller encoding is very popular encoding method in magnetic recording because of its reduced DC component [13]. The Miller encoding scheme also has some sync capability.

Probability of Error for Miller Encoded Signal

The state diagram representation of Miller encoded signal is shown in Figure 5.10.

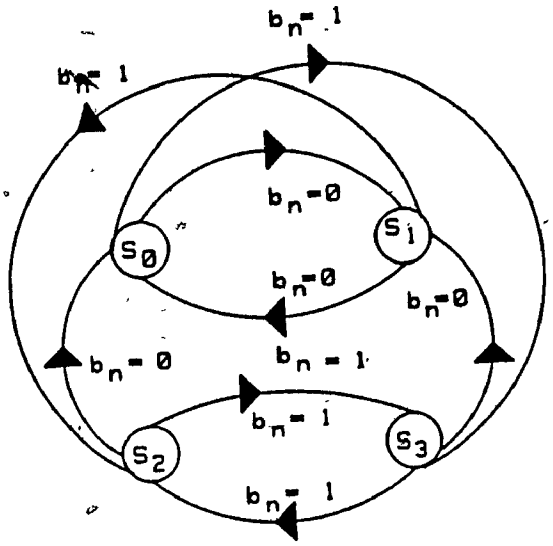

Figure 5.10 State diagram representation of Miller encoded signal.

The signals $s_0(t)$, $s_1(t)$, $s_2(t)$ and $s_3(t)$ are defined as follows (Fig. 5.22) :

$$s_0(t) = A \quad 0 < t < T_b = -s_1(t) \tag{5.42}$$

$$s_3(t) = -s_2(t) = \begin{cases} A & T_b/2 < t < T_b \\ -A & 0 < t < T_b/2 \end{cases} \tag{5.43}$$

The encoding rule for this format is as follows: a one is represented by a signal transition at the mid point of the symbol period and a zero is represented by a no transition unless it is followed by an another zero. The representation of Miller encoded signal is shown by a state diagram in Figure 5.10. As shown in Figure 5.10 the Miller code requires 4 levels (states) to represent the signal transitions. The example for Miller encoded signal is shown in Figure 5.11

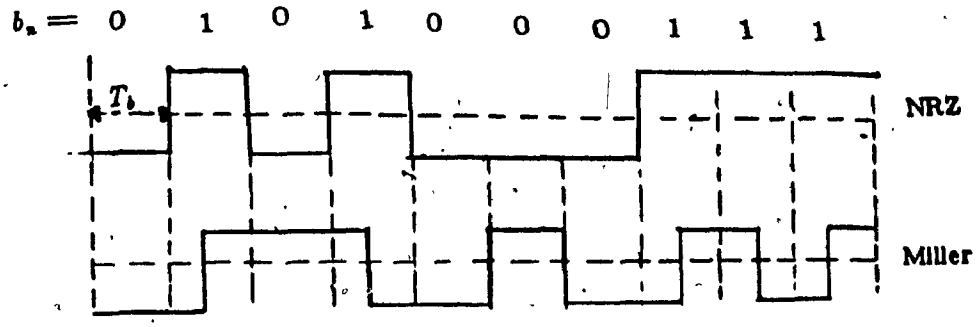

Figure 5.11 Example of a Miller encoded signal.

In order to detect a Miller encoded signal following matched filter receiver is proposed. The receiver structure is shown in Fig. 5.12. The operation of this receiver is as follows : assume a signal $s_0(t)$ is transmitted, the incoming signal is correlated with the difference of signals $s_0(t)$ and $s_2(t)$. The correlation yields two terms the product term $s_0(t)s_2(t)$ and the squared term $s_0^2(t)$. The product term is nothing but a zero (because signals are uncorrelated) and the second term which is the squared term when integrated or low pass filtered and sampled and fed to a comparator yields the desired output. The desired output in this case is nothing but $s_0(t)$.

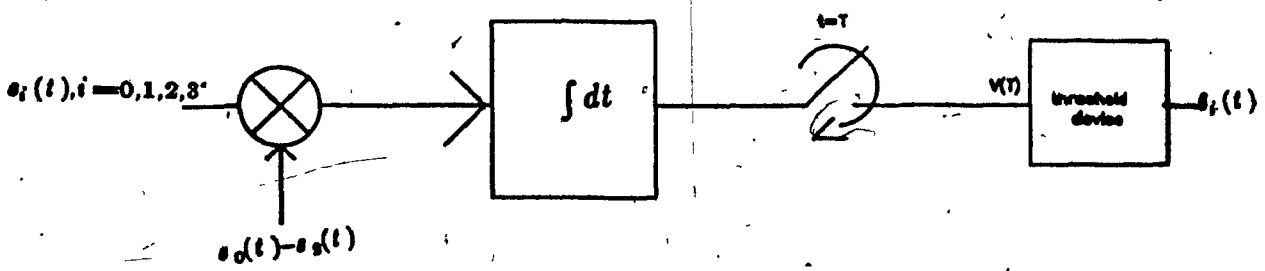

Figure 5.12 Receiver to demodulate the Miller encoded signal.

The decision region for the Miller encoded NRZ signal is shown in Fig. 5.13.

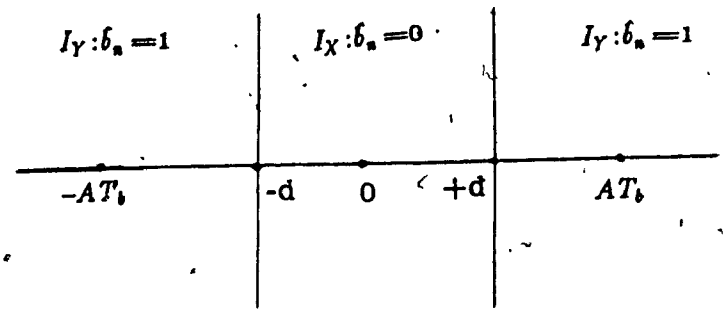

Figure 5.13 The decision region for Miller encoded NRZ signal.

In the Figure 5.11 there are two decision regions, $I_X : \{ \mid s(t) \mid < d \}$ and $I_Y : \{ \mid s(t) \mid > d \}$. If the receiver detects a signal in region I_X or I_Y, the estimated NRZ data, δ_n is 0 or 1 respectively. The probability of error given that binary '1' is transmitted is given by

$$P[e \mid 1] = \int_{-\infty}^{-d} f_V(v)dv + \int_{d}^{+\infty} f_V(v)dv \tag{5.44}$$

where $d = \frac{AT_b}{2}$ and $f_V(v)$ is a Gaussian distribution function.

$$= 2 \int_{d}^{+\infty} f_V(v)dv$$

$$= 2Q\left\{\frac{2d}{\sqrt{2N_0T_b}}\right\} \tag{5.45}$$

the probability of error given that binary '0' is transmitted is given by

$$P[e \mid 0] = \frac{1}{2}\int_{d}^{2d} f_V(v)dv + \frac{1}{2}\int_{-2d}^{d} f_V(v)dv \tag{5.46}$$

$$= \int_{d}^{2d} f_V(v)dv = \int_{d}^{+\infty} f_V(v)dv - \int_{2d}^{+\infty} f_V(v)dv$$

$$= Q\left\{\frac{2d}{\sqrt{2N_0T_b}}\right\} - Q\left\{\frac{4d}{\sqrt{2N_0T_b}}\right\} \tag{5.47}$$

The total probability of error, assuming the a priori probabilities $p_1 = p_2 = 1/2$ is

given by

$$P[e] = \frac{3}{2}Q\left\{\frac{2d}{\sqrt{2N_0T_b}}\right\} - \frac{1}{2}Q\left\{\frac{4d}{\sqrt{2N_0T_b}}\right\} \tag{5.48}$$

substituting for d the probability of error can be written as

$$= \frac{3}{2}Q\left\{\sqrt{\frac{A^2T_b^2}{2N_0T_b}}\right\} - \frac{1}{2}Q\left\{\sqrt{\frac{2A^2T_b^2}{N_0T_b}}\right\} \tag{5.49}$$

simplifying Eq. (5.49) we obtain

$$= \frac{3}{2}Q\left\{\sqrt{\frac{A^2T_b}{2N_0}}\right\} - \frac{1}{2}Q\left\{\sqrt{\frac{2A^2T_b}{N_0}}\right\} \tag{5.50}$$

For Miller code $E_1 = A^2T_b = E_0$, therefore, $E_b = 1/2(E_1+E_0) = A^2T_b$ substituting the bit energy in the probability of error equation we obtain

$$P[e] = \frac{3}{2}Q\left\{\sqrt{\frac{E_b}{2N_0}}\right\} - \frac{1}{2}Q\left\{\sqrt{\frac{2E_b}{2N_0}}\right\} \tag{5.51}$$

employing the relation between Q function and erfc we obtain,

$$= \frac{3}{4}\,erfc\left\{\sqrt{\frac{E_b}{4N_0}}\right\} - \frac{1}{4}\,erfc\left\{\sqrt{\frac{E_b}{N_0}}\right\} \tag{5.52}$$

the probability of error expressions Eqs. (5.33), (5.38), (5.41),and (5.52) are computed and plotted as a function of E_b/N_0 in Fig. 5.14. The performance of various line codes is shown in Fig. 5.14. As can be seen from the Fig. 5.14 Manchester and NRZ have identical performance, which is approximately 3 dB better than RZ and approximately 6 dB better than Miller. This can be explained as follows : In the case of NRZ and Manchester, there are only two signals to choose from. However, Miller code uses four signals thus making the decision at the receiver even more difficult than other line codes. In RZ case even though the receiver needs two levels to detect presence of binary '1' or binary '0', but RZ line code format under utilizes the bit period compared to NRZ or Manchester (either

half-pulse or no pulse) consequently, the performance of RZ is also inferior to NRZ or Manchester.

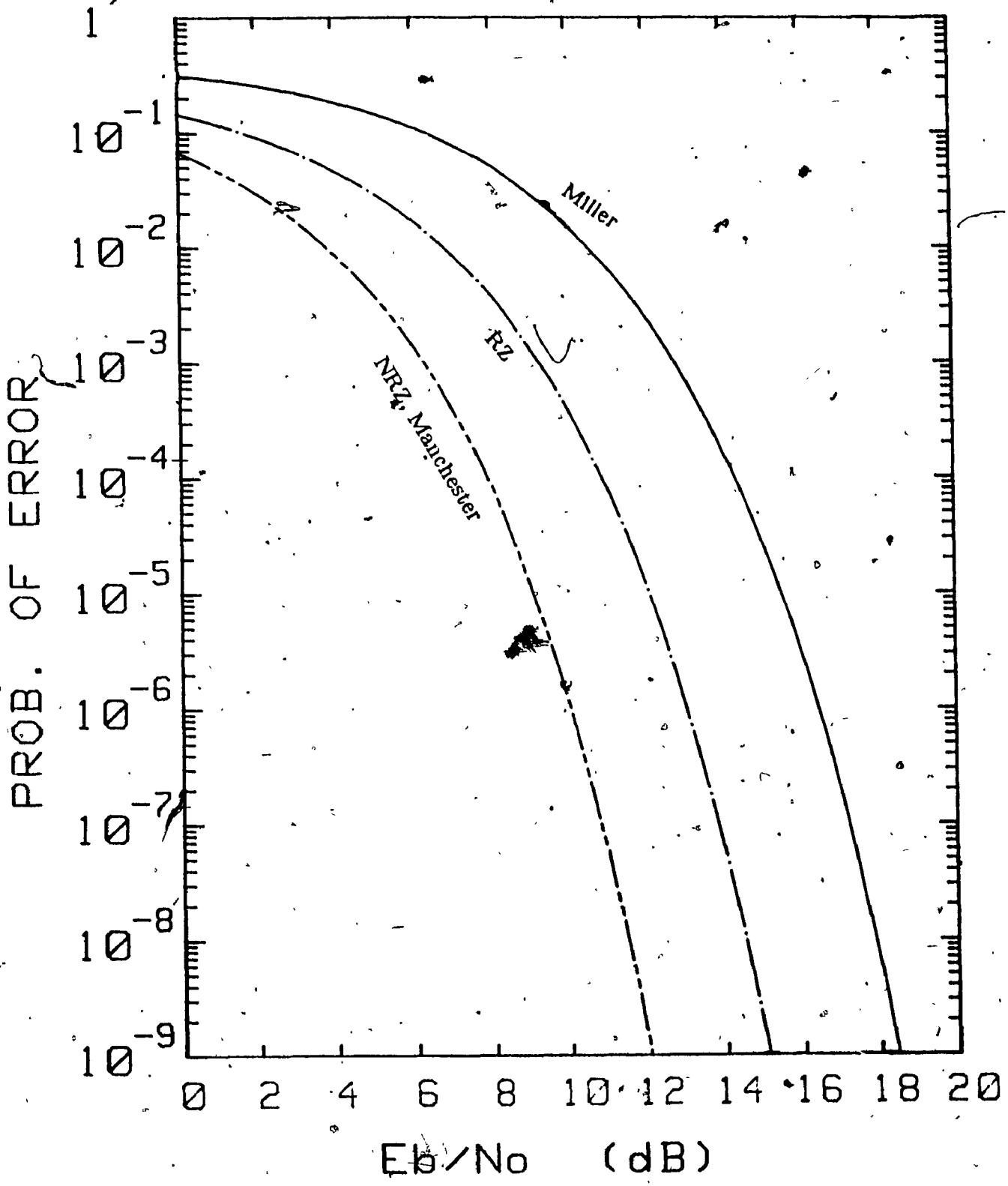

Figure 5.14 Probability of error for RZ, NRZ, Manchester, and Miller Formats.

5.4 Probability of Error Expression for Shot Noise Limited Case

To derive the probability of error expression for shot noise limited case the mathematical model for noise must be derived.

5.4.1 Noise Model

The noise encountered in optical detection is shot noise. This noise is introduced by the photodiode. The shot noise arises mainly due to random and quantum detection process. This noise can be modeled as a Poisson process [17,18].

When light having an energy (hf) greater than or equal to bandgap energy of the semiconductor material is incident on a photodiode, the photons can impart their energy and stimulate electrons from the valence band to the conduction band. As a result, free electron-hole pairs are created. When a reverse bias voltage is applied across the diode, the resultant electric field in the device causes the carriers to separate. This gives rise to a current flow in the external circuit, which is termed as a photocurrent. The current flow without avalanche effect can be represented by Eq. (5.53) [19],

$$I(t) = \sum_{j=1}^{M(t)} h(t - Z_j) \tag{5.53}$$

where h(t) is the current response due to an individual electron, Z_j is the time response of the jth electron and M(t) is the number of electrons released in a bit time interval. This number is a count variable and random in nature. The current flow at the output of the detector stage is a function of count variable M (t) as well as the function of occurrence time of an electron Z_j.

In deriving the noise model during a given time interval say, $(-T_1, +T_1)$ a Poisson process realization with time-varying expectation $\lambda(t)$ is observed [20]. Given a Poisson process with time-varying expectation $\lambda(t)$, the probability that k electrons (i.e., M (t) = k) will occur in a time interval $(-T_1, +T_1)$ is given by Poisson distribution which can represented by the following equation.

$$P\left[M(t)=k,(-T_1,T_1)\right]=\frac{\left\{\int_{-T_1}^{T_1}\lambda(t)dt\right\}^k}{k!}e^{\left\{-\int_{-T_1}^{T_1}\lambda(t)dt\right\}} \tag{5.54}$$

The joint probability density function of the shot noise process over the interval $(-T_1,+T_1)$ is obtained by considering all possible intervals, $t_1.....t_m$ and observing the total occurrences in each of the intervals. To cover all possibilities the observation time would tend to infinite. An alternative approach is to use the intervals, $t_1....t_m$ as the observables [17]. The advantage to this approach being the observation time would not tend to infinite since the number of intervals are finite. Consider Fig. 5.15, in which the time interval (- T_1 to T_1) is divided into infinitesimal intervals of length Δt [18]. Following conditions are assumed in deriving the probability density function [18].

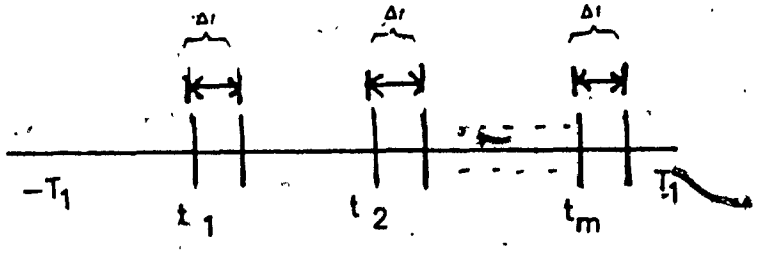

Figure 5.15 Time axis model.

(a) The probability of one occurrence in an infinitesimal interval Δt i.e., P [1, Δt] is given by P [1, Δt] = λ (t) Δt , $\Delta t \rightarrow 0$

(b) The probability of more than one occurrence in Δ t is zero for $\Delta t \rightarrow 0$.

(c) The number of occurrences in any interval are statistically independent.

(d) The probability of no occurrence in an interval (a,b) is given by

$$P\left[0,(a,b)\right]=\exp\left(-\int_a^b\lambda(t)dt\right) \tag{5.55}$$

Consider Fig. 5.13 again. Let $\{ t_i , i=1,2,3,....m\}$ be the set of disjoint intervals. The 'm' dimensional joint probability density function $p\{ t_m \}$ of such a system (shown in Figure 5.3) can be evaluated by first segmenting the interval $(- T_1 , T_1)$ to infinitesimal intervals of width $\pm (\Delta t_i) / 2$ about t_i, $(i=1,2,....m)$. The probability that one and only one electron would occur within each of these intervals and none outside the interval is $p \{ t_m \} \Delta t_1 \Delta t_2 ....$ Δt_m which can be written as [18]

$$p(t_m)\Delta t_1 \Delta t_2 ..... \Delta t_m = \tag{5.56}$$

$$P\left[0,(-T_1, t_1 - \frac{\Delta t_1}{2})\right]\lambda(t_1)\Delta t_1 \cdot$$

$$P\left[0,(t_1+\frac{\Delta t_1}{2}, t_2 - \frac{\Delta t_2}{2})\right]\lambda(t_2)\Delta t_2 \cdot \cdot \cdot \cdot \cdot \cdot$$

$$\lambda(t_m)\Delta t_m P\left[0,(t_m + \frac{\Delta t_m}{2}, T_1)\right]$$

As $\Delta t_i \rightarrow 0$ (for all i) $p\{ t_m \}$ reduces to

$$p(t_m) = P\left[0,(-T_1, t_1 - \frac{\Delta t_1}{2})\right] \prod_{i=1}^{m} \lambda(t_i) \tag{5.57}$$

$$p(t_m) = e^{\left\{ \int_{-T_1}^{t_1 - \frac{\Delta t_1}{2}} \lambda(t)dt \right\}} \prod_{i=1}^{m} \lambda(t_i) \tag{5.58}$$

Eq. (5.58) provides a statistical model for the noise of Poisson nature. The above derivation assumes the filtering effects (the response of the filter is small compared to the signal) and the random delay between samples do not affect the nature of the process. The density of shot noise can also be found by the method suggested in [19]. However, the derivation in [19] assumes the density of shot noise is low i.e., when $\lambda T'$ (where T' is the interval in which the observation is being done) is of the order of 1. The Eq. (5.58) does not assume such a process.

5.4.2 The Optimum Receiver Structure for Shot Noise Case

For analysis purposes the output of the detector is expressed as a vector. One of the methods used for vectorizing the detector output is to model the output process of a photodetector as a counting process [10] and this is represented by time samples taken every $t_s \approx 1/2\ B_d$ apart. Where ' B_d ' is the approximate bandwidth needed to represent the data being modulated [21]. This implies the detectors shot noise is also band limited to bandwidth B_d of the data. In order to represent accurately the field intensity we must sample at least $r_{2B_d T_b}$. These time samples can be used to estimate the transmitted signal at the photodetector output. The received vector $\bar{r} = (r_1, r_2, \ldots, r_{2B_d T_b})$, where $2\ B_d\ T_b$ is the number of t_s counting intervals occurring in the observation time T_b. These samples are assumed to be statistically independent [18].

5.4.3 Additive Poisson Noise

The received signal after photodetection is signal plus a random noise. The noise can be represented by, $\bar{n} = (n_1, n_2, \ldots, n_{2B_d T})$. The received signal vector $\bar{r}$ and transmitted vector, $\bar{s}$, are related by the following expression.

$$\bar{r} = \bar{s} + \bar{n} = (s_1 + n_1,\ s_2 + n_2,\ \ldots\ s_{2B_d T_b} + n_{2B_d T_b}) \qquad (5.59)$$

Eq. (5.59) states that $\bar{r} = \bar{\gamma}$ when $\bar{s} = \bar{s}_i$ if and only if $\bar{n} = \bar{\gamma} - \bar{s}_i$. The conditional density functions ($p_r(r \mid s)$), are given by

$$p_r(\bar{\gamma} \mid \bar{s} = \bar{s}_i) = P_n(\bar{\gamma} - \bar{s}_i \mid \bar{s} = \bar{s}_i) \qquad (5.60)$$

since noise vector, $\bar{n}$, and transmitted signal vector, $\bar{s}$, are statistically independent therefore, $p_{(n \mid s)} = p_n$.

$$p_n(\bar{\gamma} - \bar{s}_i \mid \bar{s} = s_i) = p_n(\bar{\gamma} - \bar{s}_i); \qquad i = 0,1 \qquad (5.61)$$

In optical detection the received vector $\bar{r}$ is a count vector and the bit interval is the observation time. The vector, $\bar{r}$ consists of 'J ' components which are

mutually exclusive time intervals. These time intervals represent disjoint random count variables. The probability of count r_j occurring in any particular interval t_j, when signal s_i is transmitted, the resulting distribution of signal plus noise is Poisson (since shot noise is Poisson distributed as shown earlier, therefore signal + noise is also Poisson distributed).

$$P(r_j \mid s_i) = \frac{(E_{s_{ij}} + \mu_n)^{r_j}}{(r_j)!} e^{-(E_i + \mu_n)} \tag{5.62}$$

Where $E_{s_{ij}}$ is the signal count energy and μ_n is the average noise count energy and E_i is the average signal count energy over the bit interval T_b. Since the count vector $\bar{r}$ has 'j' components ($j = 1, \ldots, 2B_d T_b$) and each component is Poisson distributed and mutually exclusive [18] the total count vector $\bar{r}$ has a probability given by

$$P(\bar{r} \mid s_i) = \prod_{j=1}^{2B_d T_b} \frac{\left\{E_{s_{ij}} + \mu_n\right\}^{r_j}}{(r_j)!} e^{-(E_{si} + \mu_n)} \tag{5.63}$$

$Z_i = P_r(\bar{\gamma} \mid \bar{s} = \bar{s}_i)$ then the MAP criterion is given by

$$\log Z_i = \sum_{j=1}^{2B_d T_b} \left[r_j \log\left\{E_{s_{ij}} + \mu_n\right\} - \log\ (r_j)! \right] - (E_i + \mu_n) \tag{5.64}$$

Eq. (5.64) can be simplified to

$$\log Z_i = \sum_{j=1}^{2B_d T_b} \left[r_j \log\left\{\mu_n (1 + \frac{E_{s_{ij}}}{\mu_n})\right\} \right] - E_i + \sum_{j=1}^{2B_d T_b} - \left(\log\ (r_j)! - \mu_n\right) \tag{5.65}$$

The first two terms of the Eq. (5.65) are dependent on the transmitted signal s_0 and s_1 and the remaining terms are independent of s_0 and s_1, therefore, remains same for both bits. Therefore, the receiver need to compute only, $\log Z_i = Z_i'$

$$Z_i' = r_j \sum_{j=1}^{2B_d T_b} \left[\log\left\{1 + \frac{E_{s_{ij}}}{\mu_n}\right\} \right] - E_{s_i} \tag{5.66}$$

Above summation is equivalent to discrete correlation of vector $\bar{F}$ and log function of signal and noise counts. The subtraction of E_i is bias adjustment to account for energy differences in the bit transmissions [15]. The discrete version of the model is shown in Fig. 5.16.

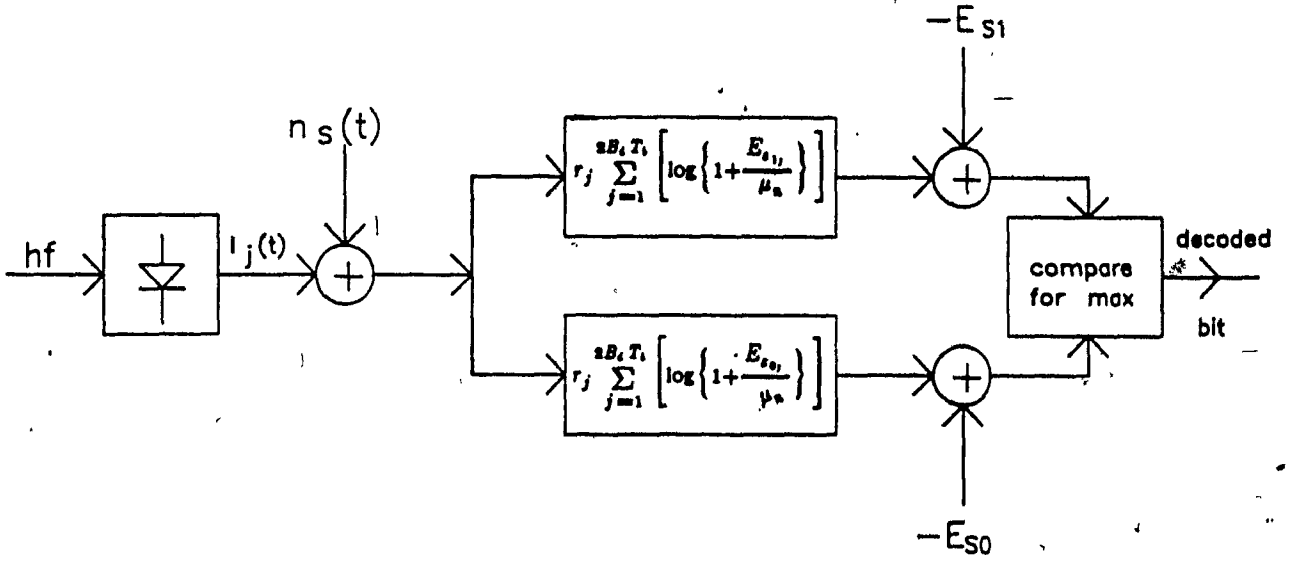

Figure 5.16 Discrete version of an optimum receiver.

Where

I_j (t): is the photocurrent

n_s (t): is the shot noise

E_{s_1}: is the bias adjustment for binary 1

E_{s_0}: is the bias adjustment for binary 0

The integral version of optimum receiver structure can be obtained by replacing the discrete summation by an equivalent integral. This can be achieved by assuming the number of samples and signal bandwidth are band limited to a bandwidth less than $B_d = 1/2T_s$, where T_s is the sampling interval therefore, the integral version is given by [18]

$$\int_0^{T_b} r(t) \log\left[\mu_n\left(1 + \frac{s_i(t)}{\mu_n}\right)\right] dt - E_i \qquad (5.67)$$

This is equivalent to time integral of the discrete version of the MAP decoder, which is correlation between photodiode output and log function of the transmitted signal. The block diagram for the integral model is shown in Fig. 5.17.

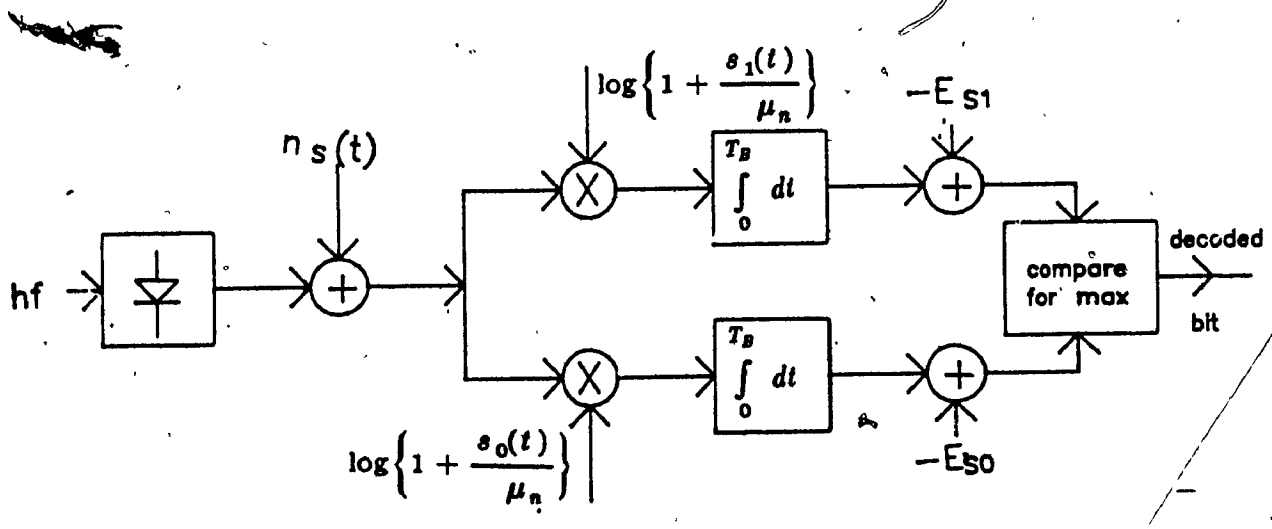

Figure 5.17 MAP decoder for continuous version.

5.4.4 Derivation of Decision Threshold and Probability of Error Expression for Shot Noise Limited case

The probability of detecting 'k' electrons during a bit interval (0, T_b) as shown earlier is governed by a Poisson process.

$$P_k = \frac{\left[\int_0^{T_b} \lambda(t)dt\right]^k}{k!} e^{\left(-\int_0^{T_b} \lambda(t)dt\right)} \tag{5.68}$$

To derive the probability of error and decision threshold the maximum likelihood ratio test is utilized [22].

$$L(Z) = \frac{f_z(Z \mid s_0)}{f_z(Z \mid s_1)} \underset{s_0}{\overset{s_1}{\gtrless}} \frac{(C_{21} - C_{11})p_1}{(C_{12} - C_{22})p_2} \tag{5.69}$$

where

$f_z(Z \mid s_i)$: is the conditional Probability density function of the data given that s_i was true.

Z : is the data on which decision is based.

C_{ij} : is the cost of deciding hypothesis s_i was true when s_j was in actuality true.

p_i : is the a priori probability that hypothesis s_i is true.

Using the special cost assignment $C_{11} = C_{22} = 0$ (right decisions cost zero) $C_{21} = C_{12}$ (either type of wrong decision is equally costly) Eq. (5.69) can be simplified to

$$\frac{f_z(Z \mid s_0)}{f_z(Z \mid s_1)} \underset{s_1}{\overset{s_0}{\gtrless}} \frac{p_1}{p_2} \Delta \frac{P(s_1)}{P(s_2)} \tag{5.70}$$

for ON-OFF cases such as NRZ and RZ the probability density function on Z when binary 1 is transmitted is given by

$$f_z(Z \mid 1) = \sum_{j=0}^{\infty} \frac{(E_{s1} + \mu_n)^j}{j!} e^{-(E_{s1} + \mu_n)} \delta(z - j) \tag{5.71}$$

The probability density function on Z when binary 0 is transmitted i.e., only background radiation is present is given by

$$f_z(Z \mid 0) = \sum_{j=0}^{\infty} \frac{(\mu_n)^j}{j!} e^{(-\mu_n)} \delta(z-j) \tag{5.72}$$

The optimum threshold 'k' which leads to minimum probability of error is given by

$$L(Z) = \frac{f_z(Z \mid 1)}{f_z(Z \mid 0)} \geq \frac{p_0}{p_1} \tag{5.73}$$

and if no signal is present $L(Z) < p_0 / p_1$. Where p_0 is the a priori probability that no signal is present, p_1 is the a priori probability that a signal is present and L (Z) is the likelihood decision function. Substituting for f_z (Z | 1) and f_z (Z | 0) and simplifying we have

$$L(Z) = \sum_{j=0}^{\infty} \left[1 + \frac{E_{s1}}{\mu_n}\right]^j e^{(-E_{s1})} \delta(z-j) \tag{5.74}$$

For some value of $Z = j = Z_0$, the function L (Z) will equal to or greater than p_0 / p_1. This value will occur at Z_0, when the $L(Z) \geq p_0 / p_1$ i.e., for p_0 and $p_1 = 1/2$

$$\left[1 + \frac{E_{s1}}{\mu_n}\right]^{Z_0} = \frac{p_0}{p_1} = 1 \tag{5.75}$$

solving for Z_0, we have

$$Z_0 = \frac{E_{s1}}{\log(1 + E_{s1}/\mu_n)} \tag{5.76}$$

The minimum probability of error P_e can be obtained using the threshold derived. The total probability of error is given by

$$P_e = \frac{1}{2} P(e \mid 1) + \frac{1}{2} P(e \mid 0) \tag{5.77}$$

$$P_e = \frac{1}{2}\left[\sum_{j=0}^{Z_0}\frac{(E_{s1}+\mu_n)}{j!}e^{-(E_{s1}+\mu_n)}\right] + \frac{1}{2}\left[\sum_{j=Z_0}^{\infty}\frac{\mu_n{}^j}{j!}e^{-\mu_n}\right] \quad (5.78)$$

Simplifying Eq.(6.47) we have,

$$P_e = \frac{1}{2}\left[\sum_{j=0}^{Z_0}\frac{(E_{s1}+\mu_n)}{j!}e^{-(E_{s1}+\mu_n)}\right] + \frac{1}{2}\left[1-\sum_{j=0}^{Z_0-1}\frac{\mu_n{}^j}{j!}e^{-\mu_n}\right] \quad (5.79)$$

$$P_e = \frac{1}{2}\left[\sum_{j=0}^{Z_0}\frac{\mu_n^j\left(1+\frac{E_{s1}}{\mu_n}\right)^j}{j!}e^{-(E_{s1}+\mu_n)}\right] + \frac{1}{2}\left[1-\sum_{j=0}^{Z_0-1}\frac{\mu_n{}^j}{j!}e^{-\mu_n}\right] \quad (5.80)$$

The Eq. (5.76) is the required threshold Z_0 to calculate the probability of error. As seen from Eq. (5.76) the threshold Z_0 is a function of received signal energy E_{S1} and noise energy this the main drawback of RZ and NRZ schemes, this implies that the received signal signal energy and noise energy must be known precisely in order to appropriately set the threshold for MAP detection. The typical plots of probability of error for RZ and NRZ line codes are plotted as function of various noise powers in Figs. 5.18 and 5.19 respectively. These plots assume an optimum threshold derived in Eq. (5.76). This threshold will yield a minimum probability of error for a given signal to noise ratio.

The error probability depends on the average signal energy E_{s1} collected over the bit interval T_b. The error rate also depends on the average number of electrons (μ_n) produced by the dark current I_D. The curves shown in Figs. 5.18 and 5.19 are optimized for detection threshold given by Eq. (5.76).

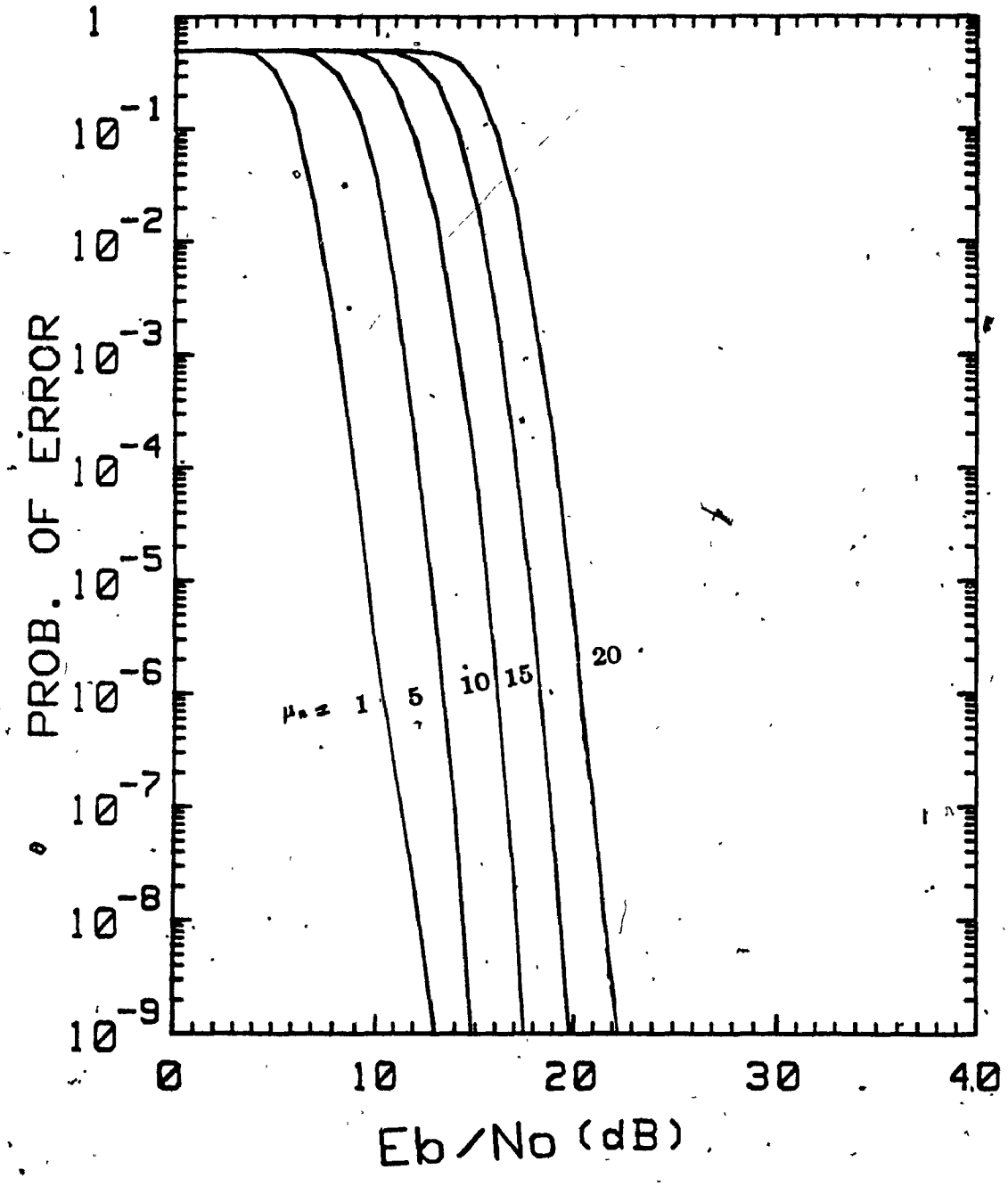

Figure 5.18 Probability of error for RZ.

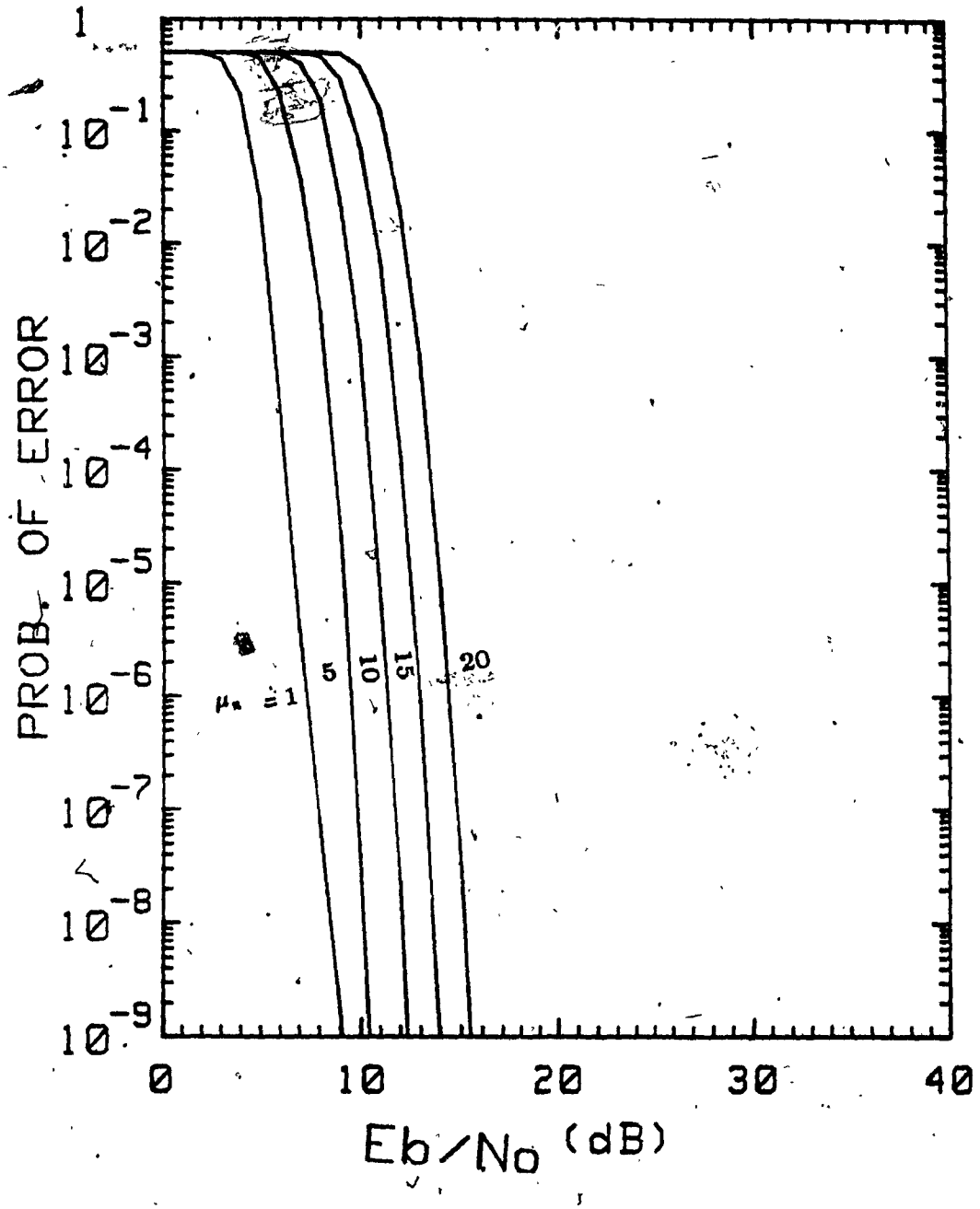

Figure 5.19 Probability of error for NRZ.

Probability of Error for Manchester Encoded Signals

In the case of Manchester encoded signal unlike RZ, NRZ cases the signal is transmitted at all times. To derive the probability of error in this case it is only necessary to compare the energy in one bit interval to the other. The transmitted bit is decoded by the largest count in a bit. The advantage in this case is that the threshold is not dependent on the transmitted power levels as in the case of RZ and NRZ.

Manchester encoded signals can be represented by following set of signals :

$$s_1(t) = \begin{cases} A & 0 < t < T_b/2 \\ -A & T_b/2 \leq t \leq T_b \end{cases} \tag{5.81}$$

and

$$s_0(t) = \begin{cases} -A & 0 < t \leq T_b/2 \\ A & T_b/2 < t \leq T_b \end{cases} \tag{5.82}$$

These signals are antipodal. They can be represented by a vector diagram shown in Fig. 5.20.

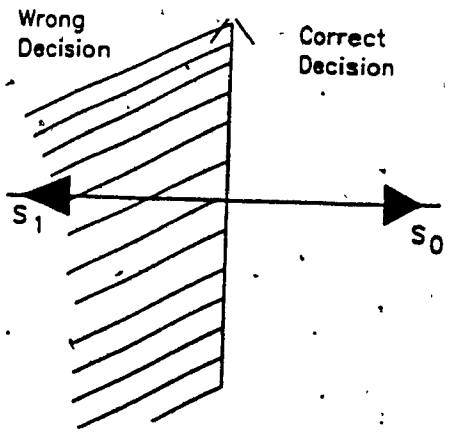

Figure 5.20 Vector representation of antipodal signals.

The optimum decision regions for Fig. 5.15 are obtained by the Eq. (5.83).

$$\min\left\{ \left| \bar{r} - s_i \right|^2 - N_0 \ln P[m_i] \right\} \tag{5.83}$$

Where

$\bar{r}$: is the received vector

s_i [2]: is the transmitted vector

N_0: is the power spectral density of the noise

$P[m_i]$: is the a priori probability of message i

For equal a priori probabilities, the decision rule simplifies to min $|\bar{r}-s_i|^2$. Assuming $s_0(t)$ is transmitted, the probability that an error occurs is the probability that the noise vector causes the received vector $\bar{r}$ to leave the decision region (I_1) associated with the transmitted vector i.e.,

$$P[e \mid s_0]=P[\bar{r}=\bar{\gamma} \text{ in } I_1 \mid s_0]=P[n>\gamma] \tag{5.84}$$

The probability of error is given by

$$P[e \mid s_0]=\int_{-\infty}^{k} f_X(x)dx \tag{5.85}$$

where $f_X(x)$ is the probability density function of noise and k is the threshold level, substituting the discrete Poisson probability density function in Eq. (5.85) the probability of error given that s_0 transmitted is given by

$$P[e \mid s_0] = \sum_{j_1=0}^{k} \frac{\mu_n^{j_1}\left\{1+\frac{E_{s1}}{\mu_n}\right\}^{j_1}}{(j_1)!} e^{-\mu_n\left\{1+\frac{E_{s1}}{\mu_n}\right\}} \tag{5.86}$$

by symmetry the conditional probability of error is same for either signal, $P[e \mid s_0]=P[e \mid s_1]=P[e]$

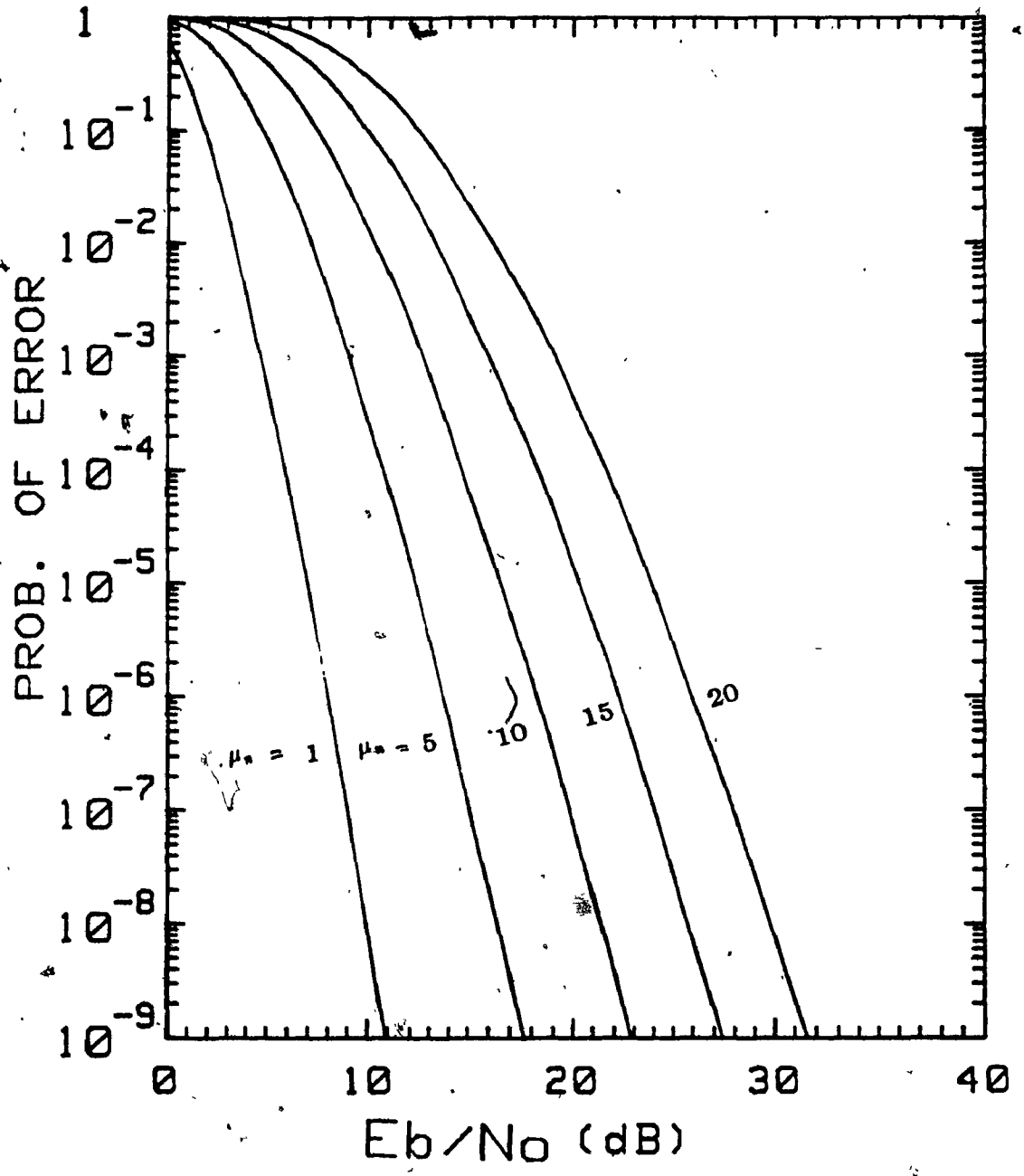

Figure 5.21 Probability of error for Manchester.

The probability of error equation (Eq. 5.86) is plotted in Fig. 5.21 as a function of probability of error and E_b/N_0 for various $\mu_n s$ (the average noise due to dark current). Unlike RZ and NRZ schemes the threshold for Manchester code is not dependent on the received signal energy. This is one of the advantages of Manchester coding scheme. In the case of Manchester code the error probability Eq. (5.86) is simply the probability that one Poisson variate containing signal plus noise energy does not exceed another Poisson variate containing noise energy alone. In Manchester case also the error probability is a function of average signal energy collected over the bit interval T_b. The error rate is also depends on the average number of electrons μ_n produced by the dark current I_D.

Probability of Error for Miller Encoded Signals

There are four types of signals that are used to represent the Miller encoded signal as shown in Fig. 5.22.

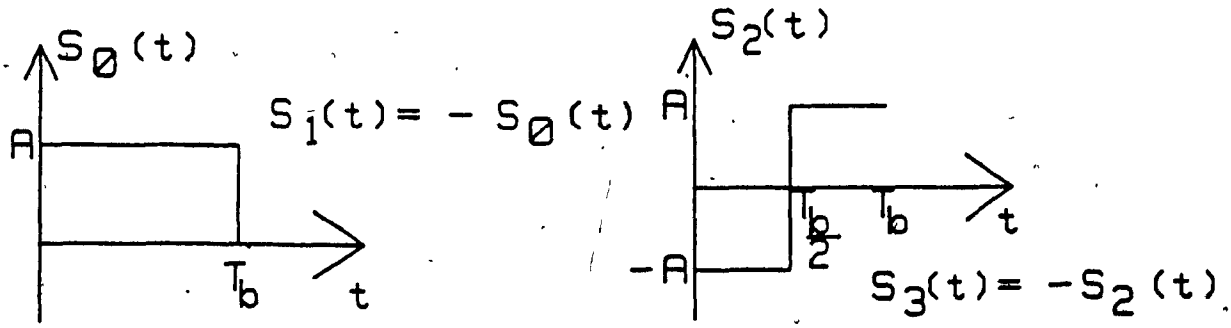

Figure 5.22 Representation of Miller encoded signal.

$s_1(t)=-s_0(t)$ and $s_3(t)=-s_2(t)$. The signal vectors can be represented by $\bar{s}_0=(\sqrt{E},0)$, $\bar{s}_1=(-\sqrt{E},0)$, $\bar{s}_2=(0,\sqrt{E})$, $\bar{s}_3=(0,-\sqrt{E})$, where $\sqrt{E}$ is the energy in each signal. For equally likely signals the a priori probability, $P(m_i)=1/4$, for $i = 1, 2, 3, 4$. Since the signals are orthogonal to each other the Miller encoded signals can be represented by as shown in Figure 5.23.

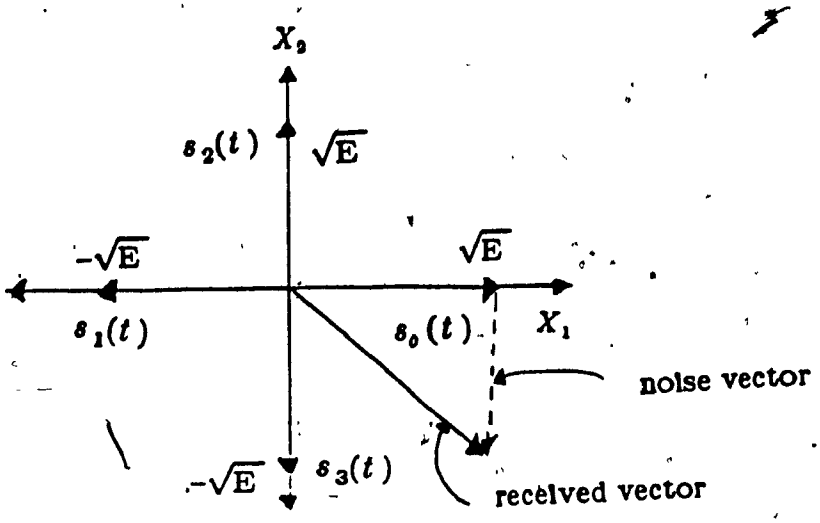

Figure 5.23 The vector representation of Miller encoded signals.

The conditional probability of correct decision given s_0 is transmitted is given by,

$$P(C \mid s_0) = \int_{-\sqrt{E}}^{\infty} \int_{-\sqrt{E}}^{\infty} f_X(x_1) f_X(x_2) dx_1 dx_2 \tag{5.87}$$

Where $f_X(x_1)$ is the probability distribution function of signal + noise and $f_X(x_2)$ is the distribution of noise alone. For noise of Poisson nature the distribution function is also of Poisson type. Substituting the discrete Poisson distribution function in Eq. (5.87) the probability of correct decision given that s_0 is transmitted is given by

$$P(C \mid s_0) = \sum_{j_1=0}^{\infty} \sum_{j_1=0}^{\infty} \frac{\mu_n^{j_1} \left[1 + \frac{E_{s0}}{\mu_n}\right]^{j_1}}{(j_1)!} e^{-\mu_n\left(1 + \frac{E_{s0}}{\mu_n}\right)} \frac{\mu_n^{j_1}}{(j_1)!} e^{-\mu_n} \tag{5.88}$$

By the symmetry of the decision regions the quantities $P(C \mid s_i)$ are all equal for $i = 1, 2, 3, 4$ therefore the probability of correct decision is

$$P(C) = \sum_{i=1}^{4} P(m_i) P(C \mid s_i) \tag{5.89}$$

$$= P(C \mid m_1) \tag{5.90}$$

Therefore the probability of error is,

$$P[e]=1-P(C) \tag{5.91}$$

The probability of error Equation (Eq. 5.91) is plotted in Fig. 5.24 as a function of E_b/N_0 for various μ_n s (the average noise produced by the dark current). As seen from the plots the performance of Miller encoding scheme is inferior to all other encoding schemes. This implies for the same probability of error the Miller encoding scheme requires more SNR than compared to other encoding schemes such as RZ, NRZ, and Manchester. The reason being in Miller case the receiver must be able to distinguish between four levels that are required to represent the basic signals $s_0(t)$ and $s_1(t)$.

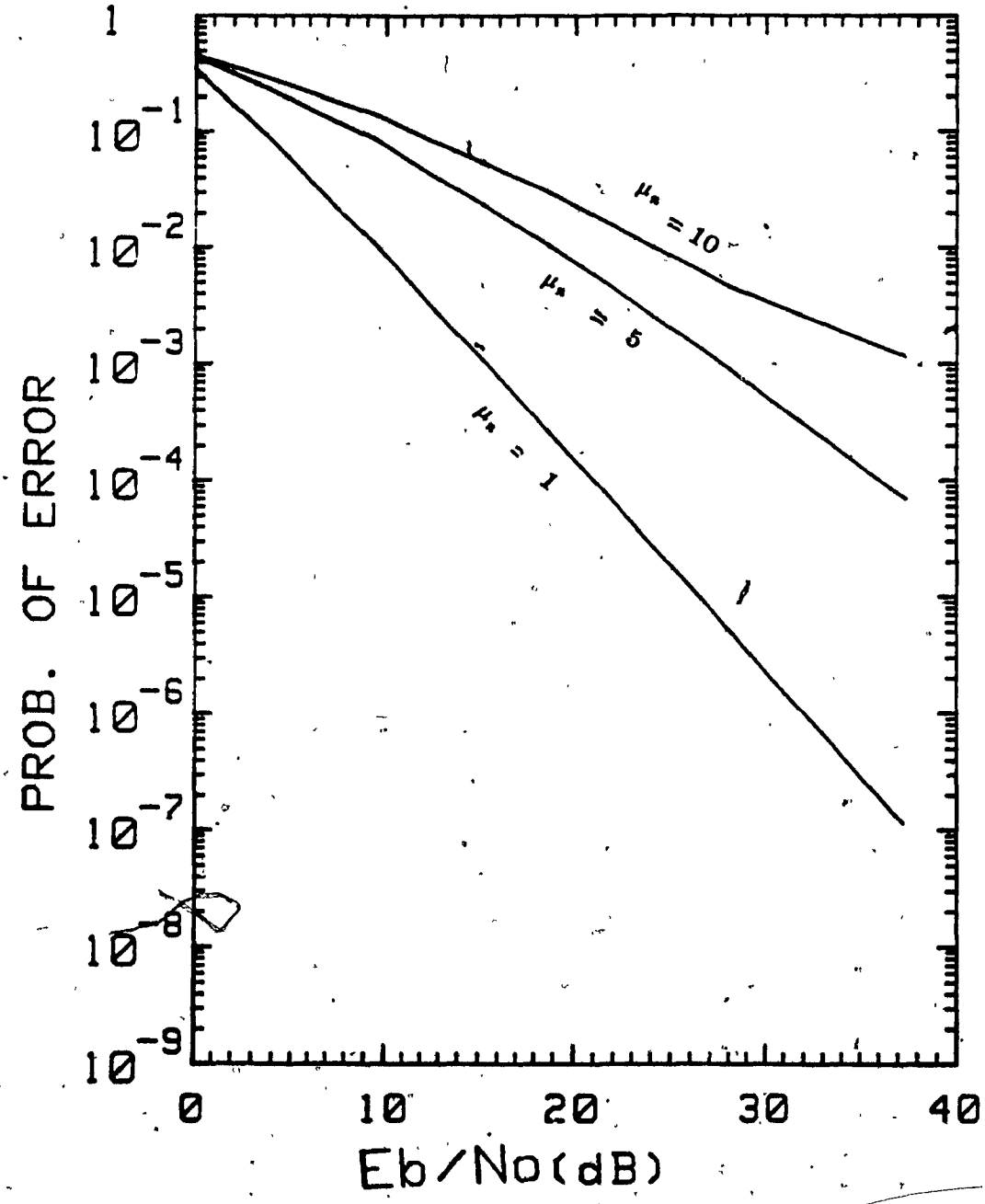

Figure 5.24 Probability of error for Miller.

5.5 Performance Comparison of Various Coding Schemes

In this section the performance comparison of various coding schemes in Gaussian as well as Poisson regime will be discussed.

In Gaussian case, (see Fig. 5.14) the performance of Manchester and NRZ is superior to RZ and Miller encoding schemes. The inferior performance of Miller encoding scheme is mainly due to the number of levels needed to represent the basic signals $s_0(t)$ and $s_1(t)$. In Miller case, the receiver must be able to distinguish between four levels that are needed to represent the basic digital signals. The performance of Miller encoding scheme is also inferior in Poisson case (see Fig. 5.24). The same reason given for Gaussian case also holds for Poisson case. The advantage in Gaussian approximation of noise is that the simplicity in deriving and evaluating the probability of error equations. The receiver employed in Gaussian case is a simple matched filter receiver which is extremely easy to implement practically.

In Poisson case, because of infinite summations in all of the probability of error equations, the accuracy is dependent on the number of iterations performed. The receiver employed for the decoding the transmitted bit sequence is practically is difficult to implement because of the need to generate logarithmic signals for correlation.

The error probability for various line codes can also be obtained for shot noise case by using Gauss Quadrature Analysis [25].

CHAPTER 6

CONCLUSIONS AND SUGGESTIONS FOR FURTHER STUDY

6.1 Conclusions

Following the introductory Chapter, in Chapter 2, the principle of propagation of optical energy and transmission characteristics of optical fibers were discussed. Chapter 3, mainly dealt with the principle and operation of light sources that are commonly used in optical communication systems. This Chapter also dealt with various line codes that are commonly employed in optical communication systems. In Chapter 4, a typical receiver was considered and the minimum optical power needed to achieve a desired BER was derived. This Chapter also discussed the design of an optical communication system and the various parameters associated in selecting optical components. In Chapter 5, performance of various pulse formats have been investigated in Gaussian as well as Poisson regime. For each of the formats probability of error equations were derived. In deriving these equations an optimum receiver was assumed to achieve a minimum probability of error.

The analysis shows that the error probability for RZ, and NRZ depends on the average signal energy collected over the bit interval T_b. The dependence of threshold on the received signal energy and noise energy implies the received signal energy must be known in order to appropriately set the threshold of the comparator. Unlike RZ, and NRZ schemes the threshold for Manchester code is not dependent on the received energy. This is one of the advantages of Manchester encoding scheme. In the case of Manchester code the error probability is simply the probability that one Poisson distribution containing signal plus noise does not exceed another Poisson distribution containing noise alone.

The performance of Miller encoding scheme as seen from the Gaussian as well as Poisson environment (see Figs. 5.14 and 5.24) is inferior than other line coding schemes. This is because four levels are needed to represent the basic binary signals in Miller encoded scheme. Consequently, the detection of the transmitted data that employs Miller encoding scheme is more difficult for the receiver to detect than other line coding that use two level signalling schemes.

In designing an optical link the important considerations the designer must consider are : (a) the data rate (b) transmission distance (c) the bit error rate. Depending on these parameters the designer selects the optical components for the design of an optical link. If the transmission distance is less than 1 km such as in the case of LANs and the data rate is few tens of mega bits then the designer can select a LED as an optical source and multimode fiber for transmission and PIN diode for detecting the optical pulses. However, if the transmission distance and data rate were to be increased the above choice of components will severely deteriorate the performance of an optical link. The deterioration is mainly due to ISI which occurs due to modal and material dispersions. This dispersion is predominant in multimode fibers than in sigle-mode fibers. Higher data rate-distance products can be achieved with choice of Laser as an optical source, single-mode fiber as transmission medium and APD as the photodetector. Although, these components are quite, expensive a considerable amount of economic savings can be realized in repeater costs.

6.2 Suggestions for Further Study

Although the considered line codes for optical systems in this thesis are RZ, NRZ, Manchester and Miller there are several other formts such as mBnB line codes (where n is greater than m) and AMI (Alternate Mark Inversion) same type of anlaysis can be used to investigate the performance in Gaussian as well as Poisson environments.

For data rates less than 100 Mb/s and distances less than 1 km usually the dispersion on the optical link can be neglected for LED and multimode fiber systems. However, for data rates greater than 100 Mb/s and distances greater than 1 km the affect due to dispersion must taken into account. The consequence of the dispersion is the limitation in the information carrying capacity of the channel. One way to solve this problem is to characterize the response of an optical fiber in time or frequency domain. Once the characterization is done an inverse operation can be done at the receiver i.e., equalization. By this method we can control the affects of ISI on the transmission channel.

REFERENCES

[1] G. Kelser, *Optical Fiber Communications,* Ist ed., McGraw Hill Book Company, 1983.

[2] J.M. Senior, *Optical Fiber Communications Principles and Practice,* Prentice Hall, 1985.

[3] Technical Staff of CSELT, *Optical Fiber Communications,* McGraw Hill Book Company, 1980.

[4] Motorola Inc., *Optoelectronics Device Data,* 1983.

[5] J.C. Palais, *Fiber Optic Communications,* Prentice Hall, Inc., 1984.

[6] S.D. Personic, *Optical Fiber Transmission Systems,* Plenum Press, 1981.

[7] H. Kressel, *Semiconductor Devices for Optical Communication,* Springer-Verlag, Vol. 39, 1980.

[8] D. J. Morris, *Pulse Code Formats for Fiber Optical Data Communications,* Mercel Dekker, Inc., 1983.

[9] Y. Takasaki et al, "Optical Pulse Formats for Fiber Optic Digital Communications," *IEEE Trans. on Comm.,* Vol. Com-24, No. 4, April 1976, pp. 404 - 412.

[10] R. M. Brooks and A. Jessop, "Line Coding for Optical Fiber Systems," *Int. J. Electronics,* Vol. 55, No. 1, 1983, pp. 81 - 120.

[11] S. Murakami et al, "Pulse Format for Bandlimited Multimode Fiber Transmission," *Int. J. Electronics,* Vol. 55, No. 1, 1983,

[12] K.W. Cattermole, "Principles of Digital Line Coding," *Int. J. Electronics,* Vol. 55, No. 1, 1983, pp. 3 - 33.

[13] F. G. Stremler, *Introduction to Communication Systems,* Addison-Wesley, 1982.

[14] T. Le-Ngoc and K. Feher, "A Digital Approach to Symbol Timing Recovery Systems," *IEEE Tran. Commun.*, Vol. COM - 28, No. 12 Dec. 1980, pp. 1993 - 1999.

[15] S.D. Personic, "Receiver Design for Digital Fiber Optic Communication Systems," *Bell Systems Technical Journal*, Vol. 52, No. 6, Aug. 1973, pp. 843 - 873.

[16] J. M. Wozencroft and I. M. Jacobs, *Principles of Communication Engineering*, John Wiley & Sons, 1965.

[17] J.R. Pierce and E. C. Posner, *Introduction to Communication Science and Systems*, Plenum Press, 1980.

[18] I. B. David, "Communication Under the Poisson Regime," *IEEE Trans. on Information Theory*, Vol. 11-15, No. 1, Jan. 1969, pp. 31 - 37.

[19] A. Papoulis, *Probability, Random Variables, and Stochastic Processes* McGraw - Hill Book Company, 1984.

[20] G.F. Hermann, "Optimum Versus Suboptimum Detection Under the Poisson Regime - Application to Optical Communication and Quadriphase Modulated Subcarrier," *IEEE Trans. Commun.*, Vol. Com-21, No. 7, July 1973, pp. 800 - 809.

[21] R. M. Gagliardi and S. Karp, *Optical Communications*, John Wiley & Sons, 1976.

[22] R. E. Ziemer and R. L. Peterson, *Digital Communications and Spread Spectrum Systems*, Macmillan Publishing Co. 1985.

[23] R. W. Lucky, J. Salz, and E. J. Weldon, Jr., *Principles of Data Communications*, McGraw-Hill Inc., 1968.

[24] J. G. Proakis, *Digital Communications*, McGraw-Hill Inc., 1983.

[25] W. Hauk etal, " The Calculation of Error Rates for Optical Fiber Systems," *IEEE Trans. Commun.*, Vol. Com-26,No.7, July 1978, pp. 1119 - 1126.

APPENDIX-I

DERIVATION OF PROBABILITY OF ERROR EQUATION FOR BINARY SIGNALS IN GAUSSIAN ENVIRONMENT

A.1 Introduction

The function of a communication receiver is to distinguish between 'm' transmitted signals $\{ s_1(t),.....s_m(t) \}$ in the presence of noise. In this appendix the structure of an optimum receiver is derived for Gaussian approximation. This model is used to demodulate various line coding schemes. A general probability of error equation and an optimum threshold is derived. It will be shown that the structure of an optimum receiver takes the form of a matched filter receiver when the noise at the receiver input is white.

A.2 Derivation of Probability of Error and Optimum Threshold

The analysis is carried out for binary communication system transmitting sss $\{ s_i , i=0,1 \}$. Consider Fig. A.1, for demodulating ON-OFF signals.

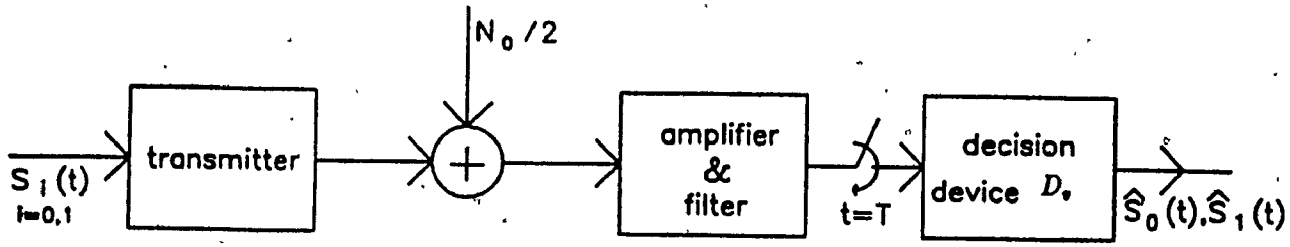

Figure A.1 Binary communication system in additive noisy environment.

At the decision point if the "signal + noise" exceeds the threshold D_v a binary 1 is assumed to be sent and if "signal + noise" is less than the threshold D_v a binary 0 is assumed to be sent. There are two possibilities in which an error

can occur (a) if s_1 (t) is transmitted and "signal + noise " does not exceed the threshold (b) if s_0 (t) is transmitted i.e., background noise alone exceeds the threshold D_v. Symbolically, the decision can be expressed as follows :

$$V_T \underset{0}{\overset{1}{\gtrless}} D_v \tag{A1}$$

Let $S_0(T)$ and $S_1(T)$ be the outputs of signals s_0 and s_1 respectively at the sampling instant (t=T) and also let V_T be the voltage at the sampling instant. A correct decision is made if $V_T > D_v$, when s_1 (t) is transmitted. A correct decision is also made if $V_T < D_v$, when s_0 is transmitted. The sampling voltage at the decision point when s_i is transmitted where i = 0, 1 is given by

$$V_T = S_i(T) + N(T) \text{ for } i = 0,1 \tag{A2}$$

Since the thermal noise is assumed to be dominating at the front end of the receiver the noise at the sampling instant can be characterized by a Gaussian distribution function with a zero mean and variance of σ_0^2. Its Probability Density Function (PDF) is given by [15],

$$f_N(x) = \frac{e^{-x^2/2\sigma_0^2}}{\sqrt{2\pi\sigma_0^2}} \tag{A5}$$

Since the noise is Gaussian type the sampler output V_T is also of Gaussian type with a mean equal to $S_1(T)$ and $S_0(T)$ for binary 1 and 0 respectively, and the variance is equal to σ_0^2 .

The conditional probability density function of 'V' given s_1 (t) is transmitted is f (v | s_1(t)) and the conditional probability density function 'V' given $s_0(t)$ is transmitted is f (v | s_0(t)). They are sketched in Fig. A.2, assuming $S_0(T) < S_1(T)$

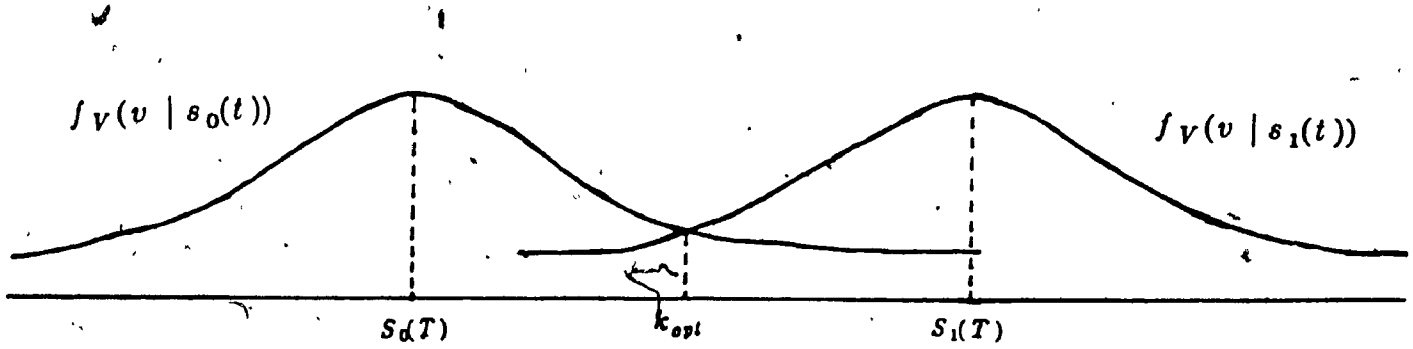

Figure A.2 The conditional probability density functions.

From Fig. A.2, the probability of error given s_1 (t) transmitted is

$$P(E \mid s_1(t)) = \int_{v=-\infty}^{k} f_V(v \mid s_1(t))\ dv \tag{A6}$$

$$= \int_{v=-\infty}^{k} \frac{e^{\frac{-\left[v - S_1(T)\right]^2}{(2\sigma_o^2)}}}{\sqrt{2\pi\sigma_o^2}}\ dv \tag{A7}$$

which is the area under $f_V(v \mid s_1(t))$ to the right of v=k. Similarly, the probability of error given s_0 (t) transmitted is

$$P(E \mid s_0(t)) = \int_{v=k}^{\infty} f_V(v \mid s_0(t))\ dv \tag{A8}$$

$$= \int_{v=k}^{\infty} \frac{e^{\frac{-\left[-v - S_0(T)\right]^2}{(2\sigma_o^2)}}}{\sqrt{2\pi\sigma_o^2}}\ dv \tag{A9}$$

The total probability of error is given by

$$P(E) = p_1 P(E \mid s_1(t)) + p_2 P(E \mid s_0(t)) \tag{A10}$$

where p_1 and p_2 are the a priori probabilities. If $p_1 = p_2 = 1/2$ i.e., the transmission of signals s_1 (t) or s_0 (t) are equally likely then

$$P(E) = \frac{1}{2}\left[P(E \mid s_1(t)) + P(E \mid s_0(t))\right] \qquad \text{(A11)}$$

The objective now is to minimize the probability of error expression by choosing the threshold and the filter transfer function, H(f) appropriately. By observing the symmetry of the PDF's of $f_V(v \mid s_1(t))$ and $f_V(v \mid s_0(t))$, intuitively, the optimum choice for k is the intersection of PDF's which is

$$K_{opt} = \frac{1}{2}\left[S_1(T) + S_0(T)\right] \qquad \text{(A12)}$$

However, this can be proved in a following manner. Substituting for PDF's in the expression for average probability of error we have,

$$P(E) = p_1 \int_{v=-\infty}^{k} \frac{e^{\frac{-\left[v - S_1(T)\right]^2}{2\sigma_0^2}}}{\sqrt{2\pi\sigma_0^2}}\, dv + p_0 \int_{v=k}^{\infty} \frac{e^{\frac{-\left[v - S_0(T)\right]^2}{2\sigma_0^2}}}{\sqrt{2\pi\sigma_0^2}}\, dv \qquad \text{(A13)}$$

differentiating Eq. (A13) with respect to 'k' and equating it to zero we obtain the optimum threshold, k_{opt}

$$k_{opt} = \frac{S_1(T) + S_0(T)}{2} + \frac{2\sigma_0^2 \ln(p_1/p_2)}{2(S_1(T) - S_0(T))} \qquad \text{(A14)}$$

If $p_1 = p_2$ then k_{opt} reduces to

$$k_{opt} = \frac{S_1(T) + S_0(T)}{2} \qquad \text{(A15)}$$

which is equivalent to the expression obtained intuitively. Since the integral is symmetric, the P(E) can be written as.

$$P(E) = \frac{1}{2} \int_{v=k}^{\infty} \frac{e^{\frac{-(v + S_0(T))^2}{2\sigma_0^2}}}{\sqrt{2\pi\sigma_0^2}} dv \qquad \text{(A16)}$$

changing variables in the above integral the P(E) can be written as

$$P(E) = \frac{1}{2} \int_{z=\frac{k - S_1(T)}{\sqrt{(2)\sigma_0^2}}}^{\infty} \frac{e^{-(z^2)}}{\sqrt{2\pi}} dz \qquad \text{(A17)}$$

The above integral can be identified as an erf function, consequently, the proba-

bility of error can be written as

$$= \frac{1}{2} \, erfc \left[\frac{k - S_1(T)}{\sqrt{2\sigma_o^2}} \right] \tag{A18}$$

Substituting for k = k_{opt} in Eq. (A18) P(E) can be written as,

$$P(E) = \frac{1}{2} \, erfc \left[\frac{\frac{S_1(T) + S_0(T)}{2} - S_1(T)}{\sqrt{2\,\sigma_0^2}} \right] \tag{A19}$$

$$= \frac{1}{2} \, erfc \left[\frac{S_1(T) - S_0(T)}{2\sqrt{2\sigma_0^2}} \right] \tag{A20}$$

Now we need to know the filter transfer function H(f) or h (t) that maximizes

$$\rho = \frac{S_1(T) - S_0(T)}{\sigma_0} \tag{A21}$$

The optimum filter then is the filter that maximizes above ratio or the square of the ratio ρ^2.

Let $g(t) = S_0(t) - S_1(t)$, the objective is now is to find the the H (f) that maximizes $\rho = \frac{g_{(T)}}{\sigma_0}$, where g(T) is the output of the filter due to input function, g(t), at the sampling instant t = T

$$\rho^2 = \frac{g^2(T)}{\sigma_0^2} \tag{A22}$$

$$= \frac{g^2(t)}{E\left\{ n^2(t) \right\}} \Big|_{t = T} \tag{A23}$$

Since the noise is stationary i.e., mean is constant and autocorrelation is a function of time difference. Output noise power from the filter is given by,

$$E\left\{ n^2(t) \right\} = \int_{-\infty}^{\infty} S_n(f) \, |H(f)|^2 df \tag{A24}$$

Where $S_n(f)$ is the input Power Spectral Density (PSD) of the white noise, which is equal to $N_0 / 2$. Substituting the PSD of the white noise in Eq. (A24), the filter output noise power can be written as

$$E\left\{n^2(t)\right\} = \frac{N_o}{2} \int_{-\infty}^{\infty} |H(f)|^2 df \tag{A25}$$

g(T) can be written terms of the inverse Fourier transform

$$g(T) = F^{-1}\left\{G(f)H(f)\right\} \tag{A26}$$

$$= \int_{-\infty}^{\infty} H(f)G(f)\, e^{(j2\pi fT)}\, df \tag{A27}$$

Where G (f) is the Fourier transform of g(t), substituting in Eq. (A22) for $g^2(t)$ we have

$$\rho^2 = \frac{\left| \int_{-\infty}^{\infty} G(f)H(f)\, e^{(j2\pi fT)} df \right|^2}{\frac{N_0}{2} \int_{-\infty}^{\infty} |H(f)|^2 df} \tag{A28}$$

using Schwartz's inequality Eq. (A28) can be reduced to

$$\rho^2 \leq \frac{2}{N_o} \int_{-\infty}^{\infty} |G(f)|^2 df \tag{A29}$$

Schwartz's inequality holds if and only if

$$H(f) = kG^*(f)e^{(-j2\pi fT)} \tag{A30}$$

The optimum choice for H(f) is $kG^*(f)e^{(-j2\pi fT)}$. The impulse response corresponding to H (f) is h(t) which is given by

$$h(t) = F^{-1}\left[H(f)\right] \tag{A31}$$

$$= \int_{-\infty}^{\infty} kG^*(f)e^{(+j2\pi fT)} e^{(-j2\pi fT)} df \tag{A32}$$

$$= \int_{-\infty}^{\infty} kG(-f)e^{(+j2\pi fT)} e^{(-j2\pi fT)}\, df \tag{A33}$$

$$= \int_{-\infty}^{\infty} kG(f')e^{(-j2\pi f'(T-t)}\, df' \tag{A34}$$

$$= g(T - t) \tag{A35}$$

Therefore, $h(t) = S_1(T-t) - S_0(T-t)$

Thus the optimum receiver consists of parallel filters which pass "signal + noise" whose impulse responses are time inverses of s_1 and s_0. The difference in impulse responses are compared against a threshold at each sampling interval t = T. The receiver structure is shown in Fig. A.3.

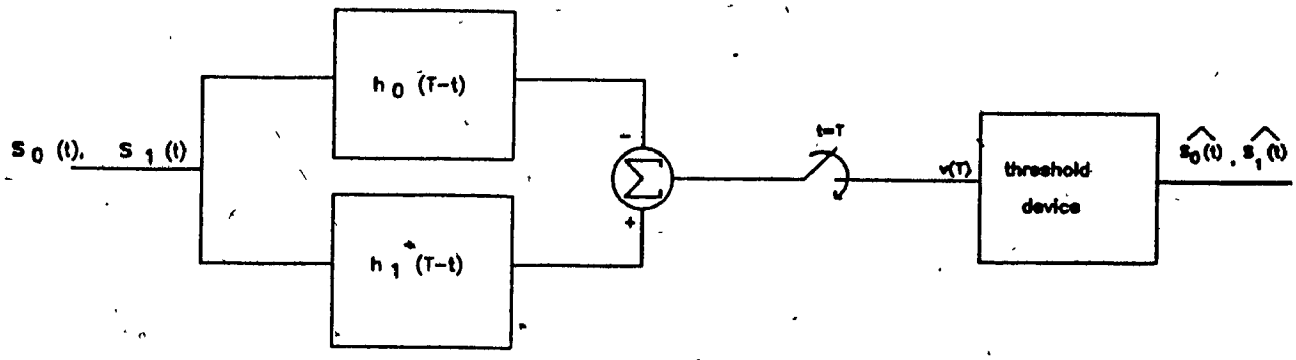

Figure A.3 The optimum receiver for decoding binary signals.

The probability of error for matched filter receiver is given by

$$P(E) = \frac{1}{2}\, erfc\, \left\{\frac{\rho}{2\sqrt{(2)}}\right\} \tag{A36}$$

ρ was derived earlier as

$$\rho \leq \sqrt{\frac{2}{N_o}\int_{-\infty}^{\infty} |G(f)|^2 df} \tag{A37}$$

In time domain $g(t) = s_0(t) - s_1(t)$, substituting for g(t) in Eq. (A38), for ρ we have,

$$\rho^2 = \frac{2}{N_o}\int_{-\infty}^{\infty}\left[s_0(t) - s_1(t)\right]^2 dt \tag{A38}$$

expanding the bracketed term and using Parseval's theorem we have,

$$\rho^2 = \frac{2}{N_o}\left[E_0 - E_1 - 2\rho_{12}\sqrt{E_1 E_0}\right] \tag{A39}$$

Where ρ_{12} is the cross correlation between signals s_0 and s_1, which is defined as [24]

$$\rho_{12} = \frac{1}{\sqrt{E_0 E_1}} \int_0^{T_i} s_1(t) s_0(t)\, dt \qquad \text{(A40)}$$

where E_0, and E_1 are energy contents in signals s_0 and s_1 respectively. Substituting for ρ in the probability of error expression and simplifying we have,

$$P(E) = \frac{1}{2}\, erfc\, \frac{1}{2} \sqrt{\frac{[E_0 + E_1 - 2\rho_{12}\sqrt{E_0 E_1}]}{N_0}} \qquad \text{(A41)}$$

For antipodal signals $\rho_{12} = -1$, in which case, P(E) is at minimum value. The probability of error Eq. (A41) derived can be used to derive the probability of error expression for line coding schemes that can be represented by two level signaling schemes such as RZ, NRZ, and Manchester encoded signals. However, for Miller encoding scheme the probability of error must be derived from first principles since four levels are needed to represent a Miller encoded signal.